Spring 5-2012

# CRETACEOUS UNROOFING HISTORY FROM APATITE FISSION-TRACK AGES, COG RAILROAD, MT. WASHINGTON, NEW HAMPSHIRE

Brigit Anderson
*Bates College*, banders2@bates.edu

# CRETACEOUS UNROOFING HISTORY FROM APATITE FISSION-TRACK AGES, COG RAILROAD, MT. WASHINGTON, NEW HAMPSHIRE

Presented to

the Faculty of the Department of Geology

Bates College

In partial fulfillment of the requirements for the

Degree of Bachelor Arts

By

Brigit Anderson

Lewiston, ME

April 6, 2012

## Table of Contents

## Table of Figures

## Table of Tables

## Abstract

The unroofing rate of Mt. Washington, NH is being calculated using apatite fission-track ages (AFT) of thirteen samples along the Cog Railroad on Mt. Washington's western slope using the relief method. Samples were collected approximately every 500 vertical feet from the summit (6280') to the base (1770') of Mt. Washington. The AFT ages determined thus far are: 148.0 ± 15 Ma at 1914 m, 147.2 ± 15 Ma at 1886.7 m, 114.5 +/- 18 Ma at 1743.5 m, 114.4 +/- 12 Ma at 1624.6 m, 119.3 +/- 13 Ma at 1482.2 m, 126.6 +/- 14 Ma at 1392.0 m, 114.4 +/- 16 Ma at 1325.9 m, 118.4 +/- 12 Ma at 1190.6 m, 110.1 +/-13 Ma at 1089.7 m, 102.9 ± 11 at 930.6 m, 96.4 +/- 9 Ma at 842.8 m, 86.4 +/- 8 Ma at 647.1 m and 89.2 ± 10 at 539.5 m. These ages are analogous to ages determined along Mt. Washington's Auto Road at similar elevations. These values yield an exhumation rate of 0.022 mm/yr between approximately 150 Ma and 80 Ma, which is comparable to the exhumation rate of 0.027 mm/yr calculated for the eastern slope of Mt. Washington along the Auto Road (Roden-Tice et. al., 2011) during this time. Trends in exhumation correlate with with late Cretaceous regional magmatic events associated with local asthenospheric upwelling that reactivated zones of crustal weakness.

## Acknowledgments

First of all, I need to thank the Bates Faculty Development Fund and the Bates Student Research Fund for providing the (as is implied by their names) funding for this project. I would also like to thank Mary Roden-Tice for not only teaching me the sometimes tedious ways of fission track counting, but also for, along with her husband Steve, housing and feeding me during my two trips to SUNY Plattsburgh. Thanks to Marty Yates for always making free time for me and walking me through the electron microprobe up at UMO. Above all, I would like to thank Dyk Eusden for generally being a motivating and influential advisor, but perhaps more importantly for being wonderfully understanding throughout the past few years. Also thanks to the entire NPR crew for keeping me wildly entertained during a year a much driving.

# Introduction

## 1.1 Purpose

The purpose of this study is to obtain cooling ages from samples along the western edge of Mt. Washington, New Hampshire using apatite fission-track (AFT) dating. The results from the age dating can be used to constrain the unroofing history of Mt. Washington through the Mesozoic and Cenozoic. This study completes an AFT project for Mt. Washington and contributes to the understanding of Mesozoic and Cenozoic low-temperature cooling in the Northern Appalachians. It also illuminates the North Atlantic margin's cooling history and path to the current topographic setting.

This study is based on data from 13 samples along the Cog Railroad on the western slope of Mt. Washington; seven are from the Littleton Formation, five from the Rangeley Formation and two from the Bretton Woods Granite. The summit sample is at 1914 m elevation and the base sample is at 540 m in elevation, thus the study covers a 1374 m change in elevation.

Given this elevation change, the relief method is employed to determine the exhumation rate. Mt. Washington is among the few sites in the Northern Appalachian range that provide enough topographic variation that allow for the comparison of age v. elevation that is used to interpret exhumation rates.



## 1.2 Apatite Fission Track Dating

Apatite Fission-Track (AFT) dating is used to determine the low-temperature history of a sample. Apatite is a commonly occurring mineral that has significant amounts of Uranium. When $^{238}U$ spontaneously decays in apatite minerals, it creates a trail of damage, or fission-track, in the crystal lattice (Figure 1.1) that anneal at or above apatite's closure temperature, approximately 100°C (Roden-Tice and Wintsch, 2002). If the apatite is reintroduced to these high temperatures, the AFT clock essentially resets itself and, therefore, starts above the 100 °C isotherm. Because the spontaneous decay half-life for $^{238}U$ is a known constant, the total number of fission tracks relative to initial abundance is proportional to the cooling age, or time at which the sample passed through the 100°C isotherm.

Between the temperatures of 60°C and 100°C, the partial annealing zone (PAZ) (Roden-Tice and Wintsch, 2002), the tracks will shorten in length based on the duration of time spent at a certain temperature within this range (Figure 1.2). A frequency distribution of track lengths informs the low temperature-time path of the sample through the PAZ. This time-temperature path is constrained by the AFT age, thus a comprehensive reconstruction of the low-temperature history can be created.

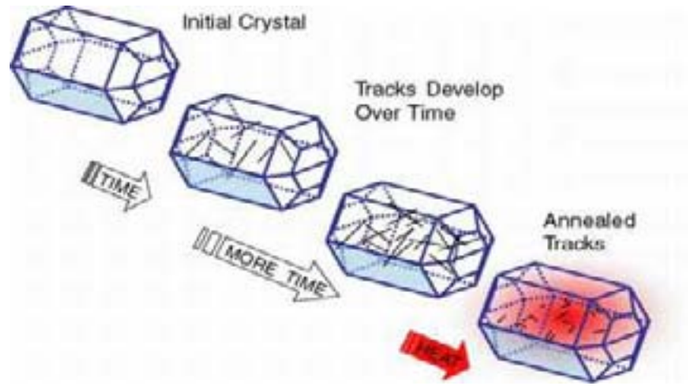


Figure 1.1: Apatite Fission Track development over time. Over times, tracks develop as $^{238}U$ decays over time. When tracks get exposed to temperatures above 100 °C, tracks anneal; between temperatures 60 °C and 100 °C tracks partially anneal. (d'Alessio et. al, 2003)

Apatite is a commonly occurring mineral that can be produced under various conditions. It is frequently found in the metamorphic formations and igneous intrusions throughout New England. The general equation for apatite is $Ca_5(PO_4)_3(F,Cl,OH)$; the variations in F, Cl and OH concentrations have a significant impact on the minerals' exact closure temperature. Fission tracks in Cl-rich apatites (chloroapatite) anneal at higher temperatures than F-rich apatites (fluoroapatite) (Warnock, et. al, 1996).

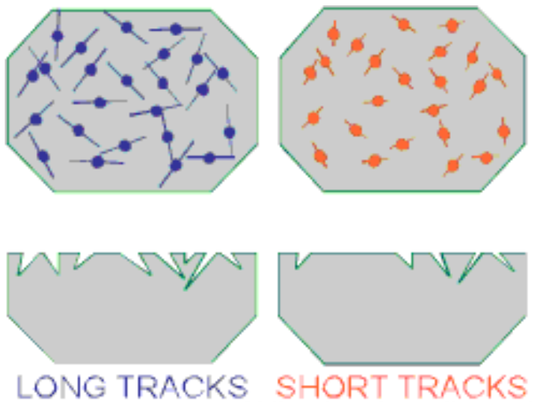


Figure 1.2: Comparison of full tracks and partially annealed tracks after time in the PAZ (Geotrack, 1987)

## 1.3 Geologic Setting

*1.3.a Regional Geologic Setting*

The Presidential Range sits in the Central Maine Terrane (CMT) which stretches from Maine to Connecticut and is bounded to the northwest by the Bronson Hill Anticlinorium (BHA) and to the southeast by the Campbell Hill-Nonesuch River Fault (Figure 1.3). BHA is composed of two Ordovician volcanic sequences with Silurian and Devonian marine sediments overlying the volcanics (Eusden et al., 1996, Bennett et al., 2006).

The southern bound is the Massabesic Gneiss Complex; the eastern bound is comprised of Ordovician belts of metavolcanic and metasedimentary units that were deposited on the Laurentia-Gondwarna boundary (West et. al, 2007). From west to east the subregions of the CMT are the Bronson Hill Anticlinorium, Kearsage Central Maine Synclonorium (KCMS),



Central New Hampshire Anticlinorium (CNHA) and the Lebanon Antiformal Syncliorium (LAS) (Eusden, et.al., 1996).

The CMT and neighboring terranes are naturally linked to a series of orogenies eventually forming Pangea. In the middle Silurian, the Iapetus Ocean began to close after a series of mountain-building events during the Taconic Orogeny (Figure 1.4). Land masses included in the Taconic Orogeny were Gander, Avalon and Laurentia. The closing of the Iapetus Ocean accounts for the sedimentation of marine turbidites that now partially make up the CMT. In the early Silurian, the Salinic orogeny began as back-arc basins from the Ordovician subducted beneath Laurentia.

In the early Devonian, the now Laurentia/Gander landmass created in the first stages of the Salinic Orogeny collided with Avalon (Figure 1.4). This was the beginning of the Acadian Orogeny and the final closing of the Iapetus Ocean basin. During this time, ocean crust was subducting beneath the Laurentia/Gander landmass resulting in a long period of Presidential Range deformation through 355 Ma (Hibbard et. al, 2007, Van Staal et. al, 2009).

The central Appalachians were deformed further in the late Mississippian when Gondwanaland collided with Laurentia, closing the pre-existing Rheic Ocean. This end of this orogeny, the Alleghenian Orogeny, was the final stage in the creation of the supercontinent Pangea, which lasted for approximately 75 my. Pangea eventually broke up during a series of rifting events starting 210 Ma (Figure 1.5). During the period of intraplate rifting, deformation and normal faulting occurred within plates (Faure et al., 2006), including reactivation of previously existing thrust faults originated during the initial mountain building events (McHone and Butler, 1984).

Some of these reactivated faults are particularly relevant to the Mt. Washington setting. The Presidential Range is in a region bounded between the Norumbega Fault to the southeast and the Amonoosuc Fault to the west (Figure 1.3). The Norumbega Fault extends from northeast southwest coastal Maine. It is a system of orogen-parallel faults and shear zones 400 km in length and up to 40 km in width activated in the middle Devonian during the Acadian Orogeny. and

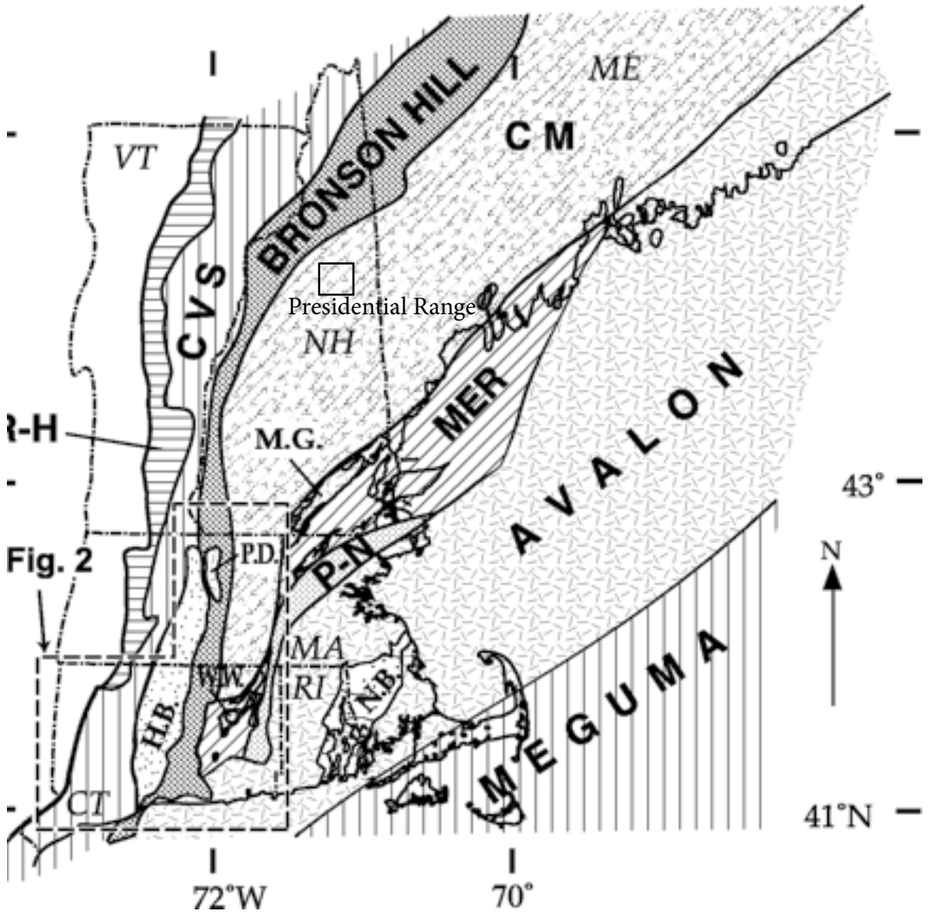


Figure 1.3: Generalized map of New Hampshire terranes, including Presidential Range location relative to regional setting (Wintsch et. al, 2003)



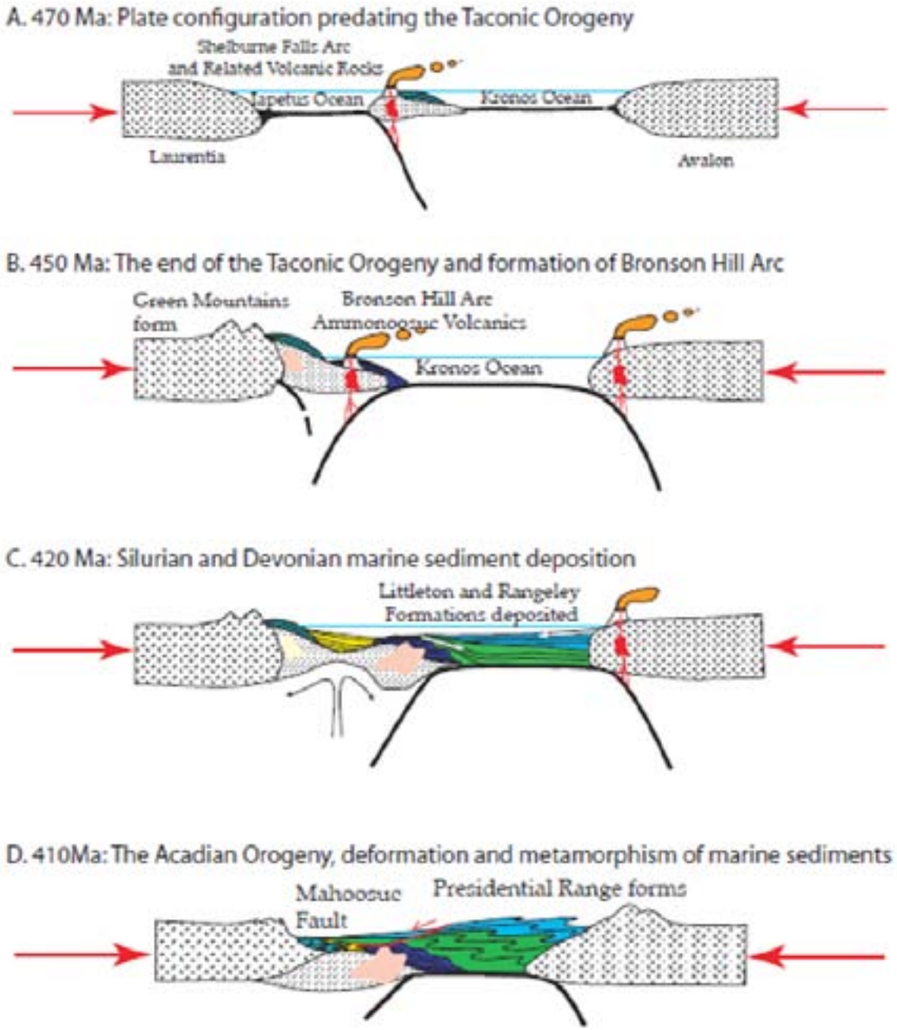


**Figure 1.4: Sequential schematic of Early Ordovician through Early Devonian orogenies, sedimentation and volcanism oriented west-to east (Eusden, 2010)**

oriented perpendicular to orogenic stress in a Ne-SW direction (Ludman and West, 1999). The Amonoosuc Fault lies on the boundary of New Hampshire and Vermont and extends from northern New Hampshire into southern Connecticut. Its origins and activity are similar to that of the Norumbega Fault.

While these faults were principally initiated by orogenic means, forcings from the asthenosphere outside normal collisional tectonism dictated fault behavior. Reactivation of the Norumbega and Amonoosuc Faults, and postorogenic extension, have affiliated the reactivation of these faults, along with other zones of crustal weakness, with some regional igneous provinces formed from localized asthenospheric upwelling (Faure et al., 1996). These events are similarly connected to the intrusion of primarily mafic dikes throughout the region, which loaded flood basalts into the rift basins of prior faulting (McHone, 2000).

*1. 3. b Local Geologic Setting*

The metamorphic formations that are included in this study are the Rangeley and Littleton Formations. The Rangeley Formation is Silurian in age, identified from shelly fauna in the formation (Moench and Zartman, 1976). Its origin is in the deep marine sediments of the Kronos Ocean. It is a gray gneiss that is subdivided based on compositional variations. The Rangeley Formation incorporates different units, including calc-silicate granofels, rusty schist and amphiboles (Eusden, 2010). These blocks range in size from cm to m scale.

Formations not included in the study area, but chronologically following the Rangeley's deposition, are the Perry Mountain, Smalls Falls and Madrid Formations. Also Silurian in age, these formations originated from sediments deposited above the Rangeley formation in the Kronos Ocean (Eusden, 2010). These formations are made of quartzites, rusty schists and calc-silicate granofels; they primarily occur in thin, discontinuous bands.

Above these formations is the Devonian Littleton Formation. The Littleton formation is derived from mud and sand sediments deposited in the deep Kronos Ocean approximately 410 Ma. Both have subsequently been metamorphosed during the Acadian Orogeny and now appear



as schists (from the mud deposits) and quartzites (from the sand deposits). The metasedimentary formations have undergone significant periods of deformation, resulting in a series of folds and faults throughout the range.

The youngest and lowest topographic unit in this study area is the Paleozoic Bretton Woods Granite, approximately 360 million years old. The age corresponds to two other low-elevation granites in the area: The Peabody River and Bickford Granites. They are approximately 40 million years younger than the peak of deformation and metamorphism associated with the onset of the Acadian orogeny.

These igneous intrusions originated from the release of the tectonic stress on the Presidential Range, which caused the range to collapse. As this occurred, the base of the crust rose and was heated by the mantle. The base of the crust then began to melt and new magma rose into the crust, creating these granitic intrusions (Eusden, 2010). Because the Bretton Woods granite and corresponding granites were formed at the end of the orogeny they were not subject to the extreme metamorphism and deformation of the Littleton and Rangeley Formations.

## 1.4 Regional Thermochronology and Paleozoic to Mesozoic Exhumation

Periods of long erosion and exhumation ensued from the Pangea rifting. While some of the unroofing can be attributed to Mesozoic rifting, other forcings were acting upon the Appalachinan Range causing it to decrease in elevation and shape the modern topography. Calculated exhumation rates detail the unroofing history and can potentially explain the driving erosional forces.

Based on $^{40}Ar/^{39}Ar$ mineral ages by the Auto Road using the relief method, Eusden and Lux (1994) calculated an exhumation rate of 0.04 mm/yr in the Middle Pennsylvanian through Early Permian. This slow initial exhumation was associated with the Acadian orogeny and stopped approximately 305 Ma. Eusden and Lux (1994) concluded that this initial exhumation did not create the present topography of the Mt. Washington massif, and thus a renewed period of exhumation occurred sometime after 274 Ma.

Exhumation resumed in the Jurassic period since when Doherty and Lyons (1980) have calculated an average erosion rate .031 mm/yr. This was calculated with a geothermal gradient of 25 to 30 °C. Therefore, the depth of emplacement ranged from 5.3 to 7.6 km in the Middle Jurassic to 3.0 to 3.6 km in the Middle Cretaceous. Ten Jurassic and Cretaceous plutons were analyzed using apatite fission tracks and zircon fission tracks of the White Mountain Plutonic-Volcanic Series. Site locations are scattered throughout New Hampshire and a few are in the border of Vermont. With the $^{40}Ar/^{39}Ar$ ages a preliminary exhumation reconstruction can begin to constrain the average cooling history from the Late Paleozoic into the Mesozoic.

Doherty and Lyons (1980) acknowledged that .031 mm/yr was a calculated average and periods of faster or slower exhumation were likely to have occurred throughout this time. Roden-Tice et. al (2009) collected new AFT ages and reexamined Doherty and Lyons' data to conclude that later in the Mesozoic, after the initial Jurassic exhumation renewal, there was a period of faster unroofing with rates ranging from 0.055 to 0.118 mm/yr in the Early Cretaceous. Rates returned to the relative slower rate of 0.01 to 0.04 mm/yr in the Late Cretaceous. Doherty and Lyons's (1980) erosion rate is comparable to that documented by Roden-Tice et. al (2009), who calculated an average erosion rate of 0.03 to 0.04 mm/yr from 100 to 60 Ma.

From the late Jurassic to the Early Cretaceous, exhumation rates stopped acting uniformly throughout northern New England as postorogenic extension was initiated (Figure 1.3). Cretaceous extension can result in both for the region's unroofing during this time and the reactivation of faults that led to localized differential unroofing.

West and Roden-Tice (2003) obtained AFT ages for opposite sides of the Norumbega Fault Zone in southern Maine. Their analysis indicated differential erosion rates on either side of the fault. AFT ages on the western side of the fault ranged from 113 to 89 Ma, while ages of the eastern side ranged from 159 to 140 Ma. This discontinuity was explained by the reactivation of the Norumbega Fault in the Late Cretaceous less than 80 Ma and was localized to the northern Casco Bay region of Maine.

AFT ages along other northern New England faults document localized reactivation



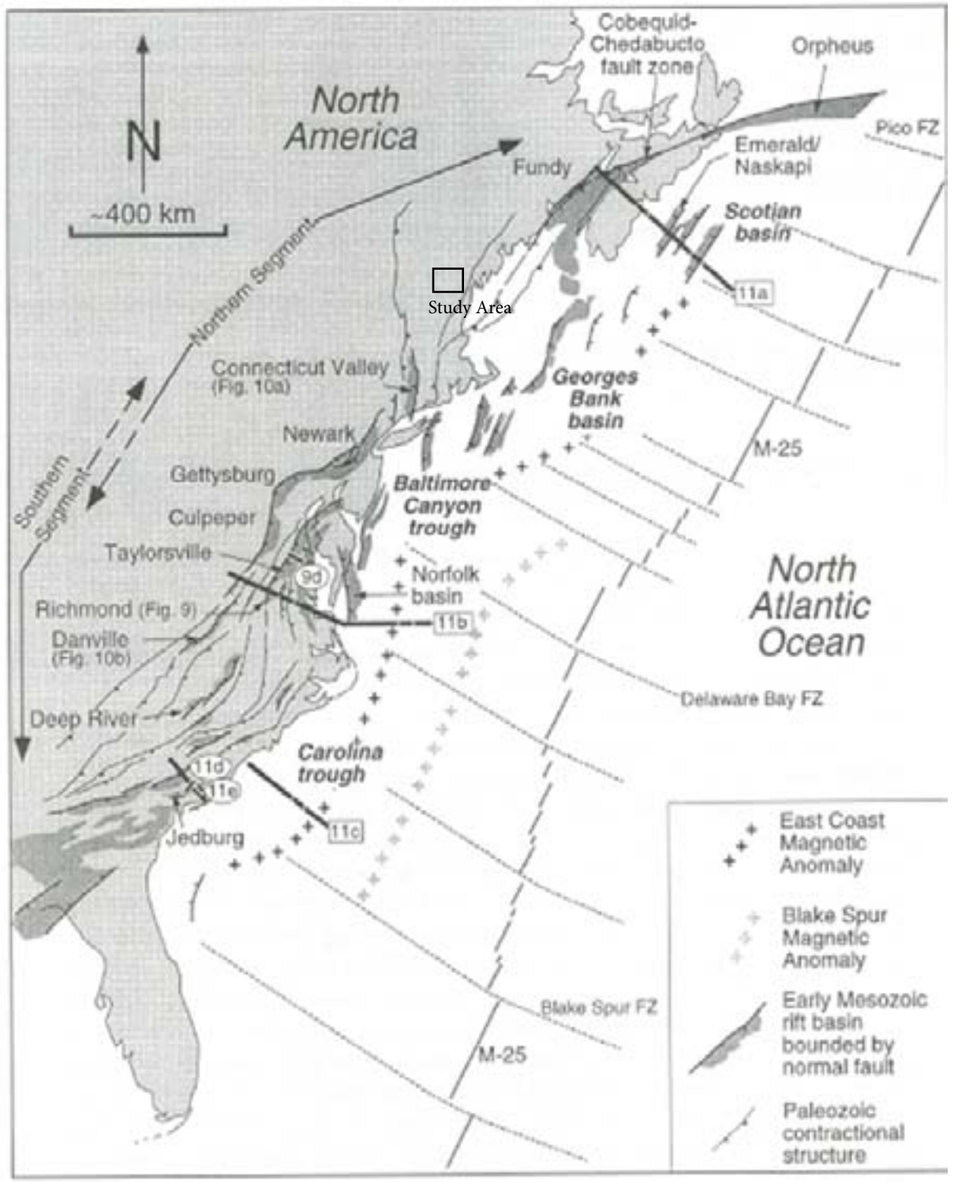


Figure 1.5: Mesozoic Rifting and corresponding faults and rift basins (Schlische et. al, 2004)

during the late Cretaceous. While there is no significant offset documented in AFT ages across the Ammonoosuc fault in the Connecticut River valley, there was a significant AFT age offset in northwestern New Hampshire between the Bill Little, Amonoosuc, and Northery Hill faults. This is also indicative of Cretaceous normal displacement at times <80 Ma (Roden Tice et. al., 2009).

All known studies present a relatively similar picture of Mesozoic average exhumation into Cretaceous differential unroofing and the reinstatement of uniform exhumation approximately 60 Ma. This is further evidenced in data explicitly applicable to this study.

AFT ages along Mt. Washington's Auto Road, on the eastern side of the mountain yield an average erosion rate of 0.2 mm/yr between ~160 Ma and ~100 Ma. Between ~140 Ma and ~120 Ma there was a period of slower erosion, 0.01 mm/yr, bounded by 0.03 mm/yr from ~140 mm/yr from ~140 Ma to ~160 Ma and 0.04 mm/yr from ~100 Ma to ~120 Ma. These generalized values, based solely on the AFT age from summit to base, are comparable to the average erosion rate, 0.04 mm/yr from 304 Ma to 274 Ma determined by Eusden and Lux's (1994) $^{40}Ar/^{39}Ar$ ages. It is also comparable to Doherty and Lyons' (1980) erosion rate of 0.03-0.04 mm/yr since the Jurassic (Roden-Tice et. al, 2011).

There is a large discrepancy, however, in the calculated geothermal gradient. Where Doherty and Lyons based their study on a geothermal gradient of 25 to 30°C, Roden-Tice et. al (2011) found an average geothermal gradient of ~ 40 °C during the Mesozoic. The relief method yielded a geothermal gradient of ~ 36 °C while the time-temperature history yielded a geothermal gradient of ~ 43 °C. Roden-Tice et. al (2011) extrapolated the data to extend back to ~ 300 Ma. These values are significantly higher than that of both Doherty and Lyons' (1980) study and Roden-Tice et.al's (2009) calculation that also assumed a geothermal gradient of ~25 – 30 °C for the same time period.

From 120 Ma to 60 Ma erosion patterns changed relative to the modern topographic profile. While samples from the summit of Mt. Washington and topographic middle of the mountain travel through the PAZ relatively synchronously, indicating uniform exhumation, the sample from the near Pinkham Notch diverges at approximately 120 Ma. The sample at the base



moved through the PAZ faster, cooling at approximately 0.6 °C/my from 100 Ma to 60 Ma while the summit and middle samples were cooled at 0.2 °C/my during this time.

Two theories exist to explain this period of differential exhumation. One attributes it to differential erosion from a paleo-drainage system. The other theory suggests that faults were reactivated in the region causing localized uplift. These two theories, however, are not mutually exclusive and a combination of the two is possible, if not more likely.

As studies along faults both east and west of the Presidential Region have revealed late Mesozoic fault reactivation a similar event is not unlikely, although it would require a fault to exist that spatially separates Mt. Washington's summit from base. This would allow the summit to stay put throughout the period of differential exhumation, while the base rocks were tilted upwards thus exhibiting higher exhumation rates.

AFT ages from this study add to the understanding of both regional and local Mesozoic and Cenozoic topographic setting and development. With the addition of AFT ages varying in elevation, previously limited to Roden-Tice et. al's (2011) study, an even more comprehensive chronology can be constructed.

# Methods

## 2.1 Field Sampling

Thirteen samples were collected from the summit of Mt. Washington at 2523.7 m to near the base at 539.5 m. during one day of field work in mid-June, 2011. Samples were collected approximately every 150 m. in vertical elevation along the Cog Railroad on the western ridge of Mt. Washington (Figure 2.1). The sites were chosen from elevation change determined by Garmin Etrek GPS unit. At each site, two sample bags were filled using both a 10 pound sledge hammer and smaller rock hammer.

The thirteen sample sites crossed through two metamorphic rock formations and one granitic intrusion. Samples CR01 through CR 07 (starting at high elevation) are from the Littleton Formation (Figure 2.2). Samples CR08 through CR11, intermediate elevations, are from the Rangeley Formation (Figure 2.2). Samples CR12 and CR13, at low elevations, are from Bretton Woods Granite (Figure 2.2). As mentioned previously, the rock formations are not integral for the purpose of this study. It is more important to note that each of samples rock is likely to contain enough apatite to perform this work.

| Sample # | Elevation (m) | Formation | Distance from Last Sample | Waypoint # | Error (m) |
|---|---|---|---|---|---|
| CR01 | 1914.14 | Littleton Schist | - | 001 | ±4.6 |
| CR02 | 1886.71 | Littleton Schist | 90 | 002 | ±7.3 |
| CR03 | 1743.46 | Littleton Schist | 470 | 003 | ±4.9 |
| CR04 | 1624.58 | Littleton Schist | 390 | 004 | ±3.1 |
| CR05 | 1482.24 | Littleton Schist | 467 | 005 | ±3.4 |
| CR06 | 1392.02 | Littleton Schist | 296 | 006 | ±2.7 |
| CR07 | 1325.88 | Littleton Schist | 217 | 007 | ±3.7 |
| CR08 | 1190.55 | Rangely Schist | 444 | 008 | ±4.0 |
| CR09 | 1089.66 | Rangely Schist | 331 | 009 | ±3.4 |
| CR10 | 930.55 | Rangely Schist | 522 | 010 | ±6.7 |
| CR11 | 842.77 | Rangely Schist | 288 | 011 | ±9.1 |
| CR12 | 647.09 | Bretton Woods Granite | 642 | 012 | ±6.4 |
| CR13 | 539.50 | Bretton Woods Granite | 353 | 013 | ±7.3 |

Table 2.1: Sample Locations

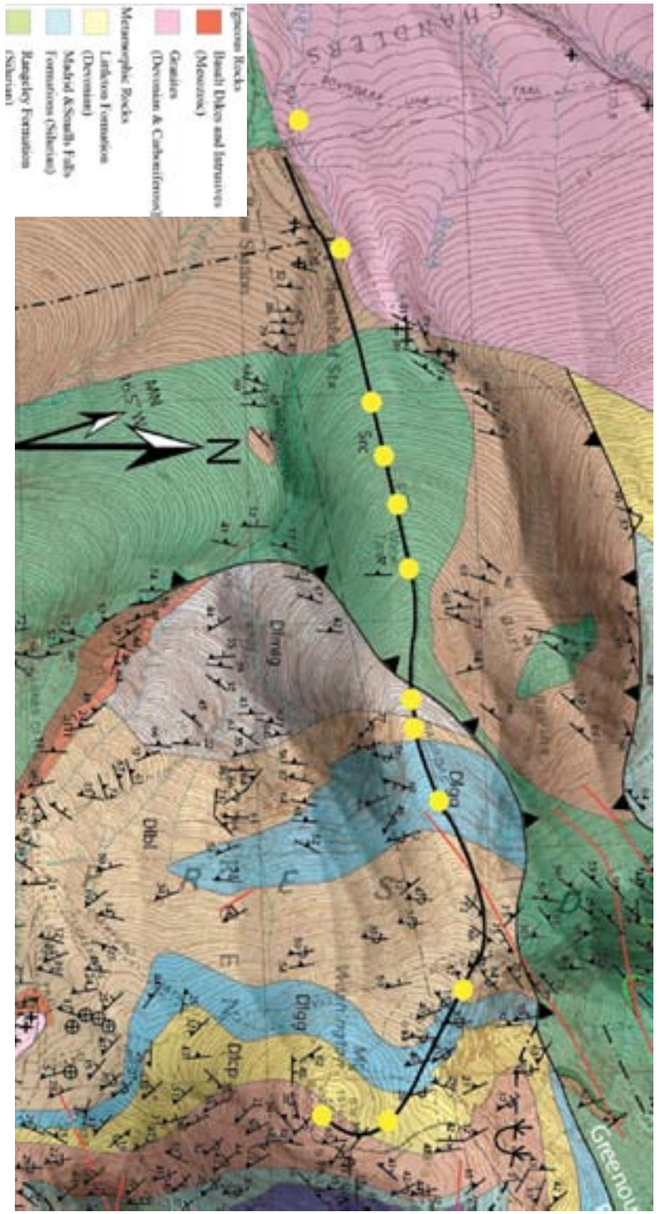





CR01: Littleton,1914.1 m


CR02: Littleton, 1886.7


CR03: Littleton,1743.5 m


CR04: Littleton, 1624.6 m


CR05: Littleton, 1482.2 m


CR06: Littleton, 1392.0 m


CR07: Littleton, 1325.9 m


CR08: Rangeley, 1190.6 m


CR09: Rangeley, 930.6 m


CR11: Rangely, 842.8 m


CR13: Bretton Woods, 539.5 m

Figure 2.2: Photo Locations

## 2.2 Crushing and Pulverizing

At least one hand sample from each site was archived prior to crushing. Remaining sample was crushed with a Braun Chipmunk jaw crusher (Figure 2.5). To eliminate cross-sample contamination the jaw crusher would be completely vacuumed, blown with compressed air and swept. After the initial cleaning, a small fragment of the sample would be crushed before another around of cleaning. If a sample is, then, contaminated with the previous run it would be contaminated with itself, thus reducing the risk of error in later results. During both crushing and pulverizing, an external vacuum was placed within the hood to remove airborne dust produced by the working machines. The cleaning process was extensive and most essential here because of the necessity to preserve the purity of all samples.

After the second round of cleaning, the remaining sample was crushed resulting in approximately 1 cm diameter fragments. Samples too large to fit in the mouth of the crusher were physically crushed first with a hammer before mechanically crushing them. If this was done, the surface where the rock was crushed was also extensively cleaned with a vacuum. After a sample was crushed, the resultant fragments were collected in 1L plastic containers. Each sample yielded different quantities of crushed rocks, but 1L was chosen to pulverize, while the remaining fragments were archived.

Using a 2hp belt drive Bico disc mill 1L of each sample was then pulverized with ceramic plates. An identical pre-screening cleaning was conducted to reduce the risk of cross-sample contamination. Once cleaned for a sample, the 1L of crushed rock was run twice through the pulverizer. First, the ceramic discs were approximately 0.5 cm apart which resulted in a mix of coarse sand size grains and powder. For the second run, the discs were approximately 1 mm apart resulting in fine sand to silt size grains and powder.



Figure 2.3: Chipmunk Crusher and Pulverizer

## 2.3 Sieving Samples

The pulverized samples were sieved using a fine cloth sieve. This removed the larger grains, primarily micas that were not able to be pulverized into a fine grain with the Bico discs. The same cloth sieve was used for all samples; between samples the cloth was washed with hand soap and scrubbed with a brush. It was blown with compressed air to dry and remove any remaining grains from a previous sample.

## 2.4 Rogers Table Separation

A Rogers Table was used to separate the pulverized and sieved material by specific gravity. To prepare, the table was scrubbed with a plastic brush and rinsed thoroughly to ensure that all residual grains were washed out. The table was cleaned before each sample was run. In addition,

buckets where sediment was collected were washed and rinsed. Water pressure combined with appropriate levels of shaking separated the minerals. When a sample was run, grains with intermediate and heavy specific gravity were collected in the smaller collecting buckets together while grains with light specific gravity were collected separately in the large bottom bucket (Figure 2.6). After one run, the light grains were archived back in the 1L containers. The intermediate and heavy grains were run again to separate out any residual light grains. The remaining intermediate and heavy grains were dried in small aluminum trays.

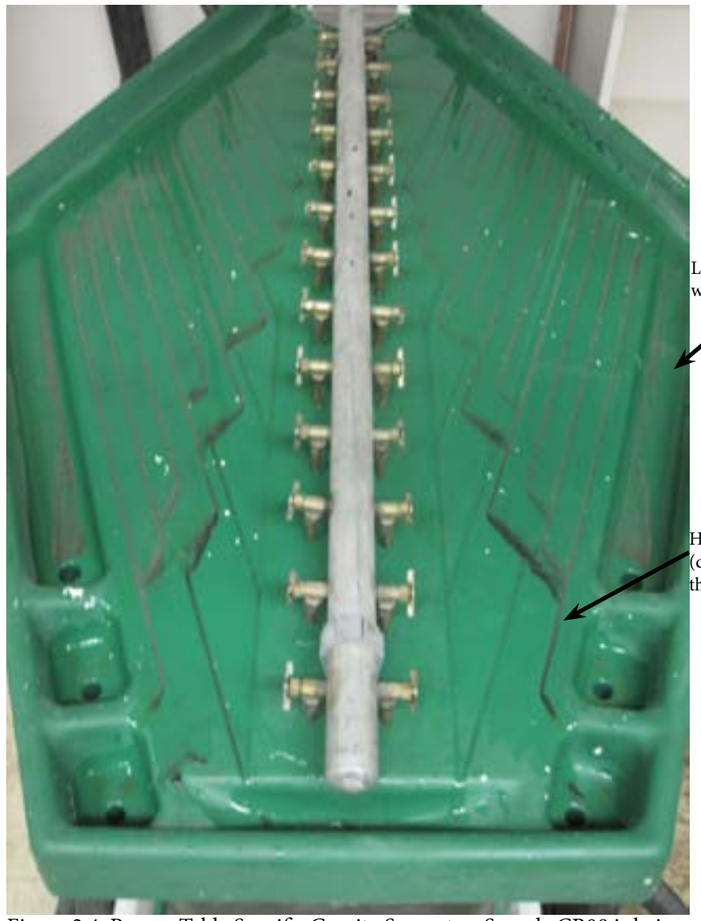

Figure 2.4: Rogers Table Specific Gravity Separator; Sample CR08 is being run



## 2.5 Magnetic Separation

After samples were dried, they were separated by magnetic susceptibility. A hand magnet was used to initially separate all the extremely high-magnetic minerals. The high-magnetic fractions were archived.

The samples were then run through a Frantz Isodynamic Magnetic Separator. The track was set with a forward tilt of 15° and a side tilt of 25° (Figure 2.5). Before each sample was run, the Frantz was disassembled and cleaned with compressed air and Kimwipes. The samples were first run at 0.5 Å. This removed the highly magnetic minerals, which were archived. They were then re-run at 1.2 Å. Apatite had a magnetic susceptibility of 1.3 Å (Rosenblum, 2000); at 1.2 Å was preserved while slightly more magnetic minerals were removed (Figure 2.6). Quartz, among others, remained after this step. All magnetic fractions were archived.

*Steps 2.6 to 2.10 took place at SUNY Plattsburgh*

## 2.6 Heavy Liquid Separation

LST (containing lithium heteropolytungstates) can be used for heavy liquid separation with a recommended density of 2.85 g/mL at 25°C was used for heavy liquid separation the initial separation (Figure 2.7). Apatite and the remaining heavy separates were then separated using Methylene Iodide (MI), which has a specific gravity of 3.32 g/mL. This second liquid is used to separate the apatites from the zircons, as zircon has a specific gravity greater than the MI and apatite less. Remaining grains were cleaned with 100, 300 mesh sieves (.152 mm and .044 mm respectively).

## 2.7 Grain Mount and Polishing

Grains were mounted on petrographic slides in epoxy; each sample was measured to be a 1 cm by 1.5 cm size rectangle. Using 400 grit paper, the surfaces of the grains were cut to expose the apatites before being briefly polished with 600 grit paper. 9 micron and 1 micron diamond paste was, sequentially, used to polish the mounts. Polishing was finalized with 0.3 micron $Al_8O_3$

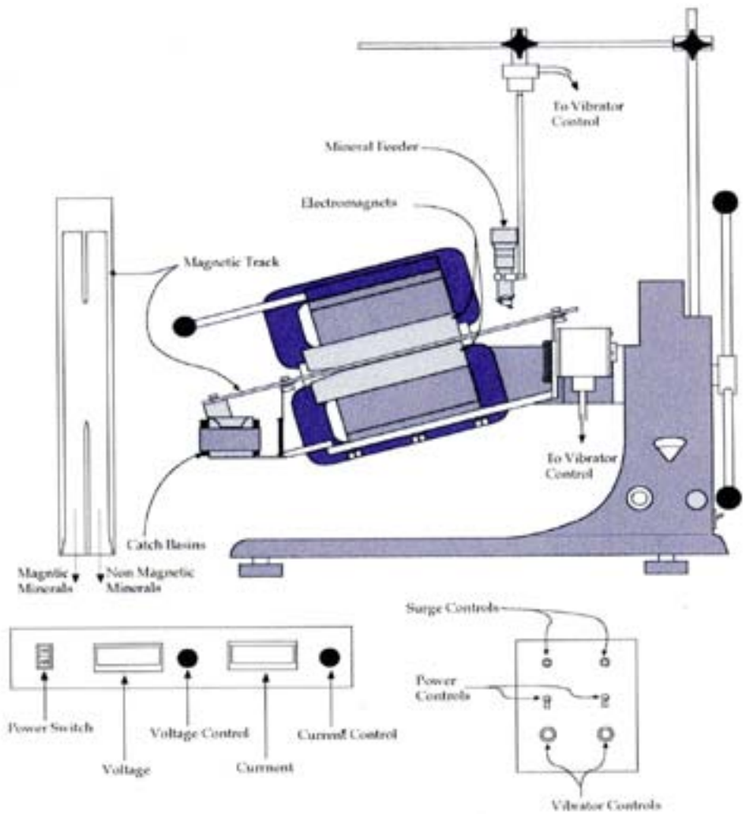


Figure 2.7: Frantz Isodynamic Magnetic Separator (Robinson, 1997)



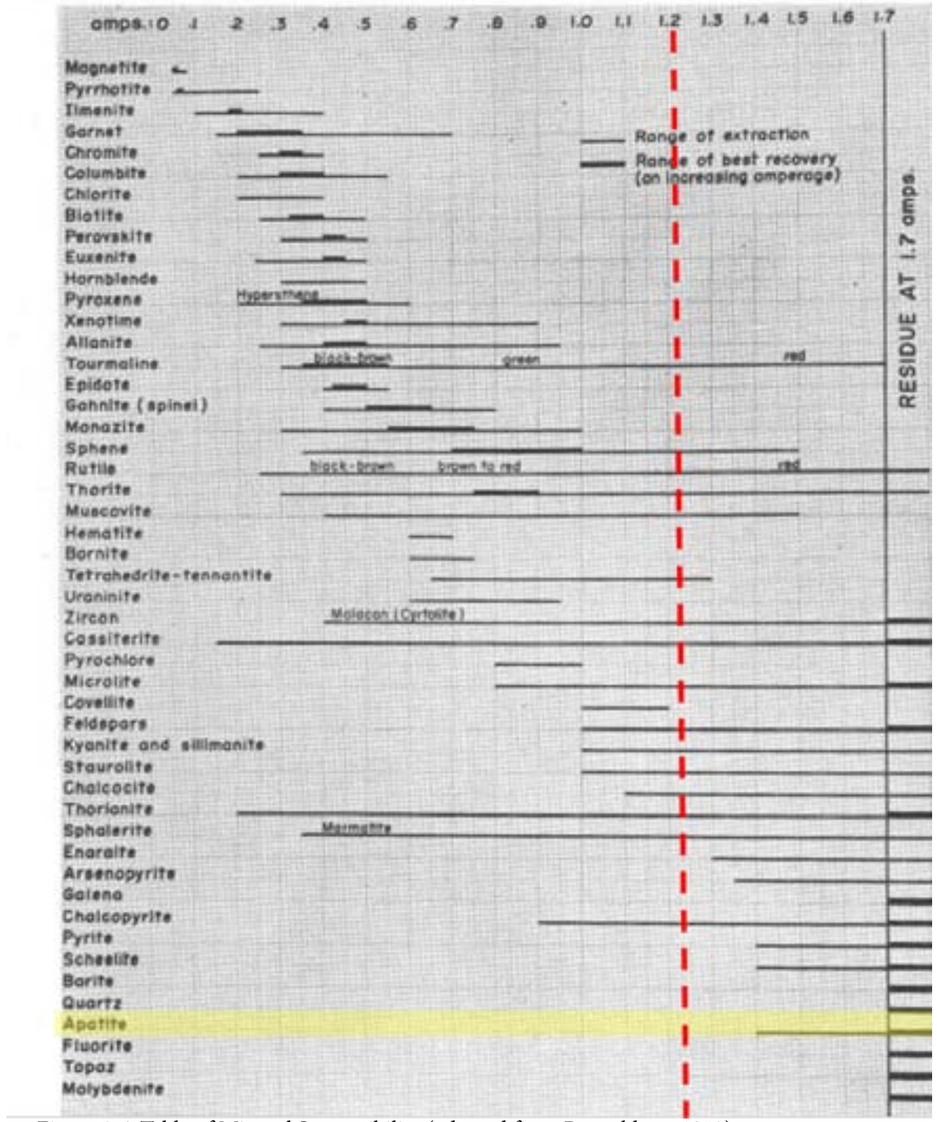


Figure 2.6: Table of Mineral Susceptibility (adapted from Rosenblum, 1953)

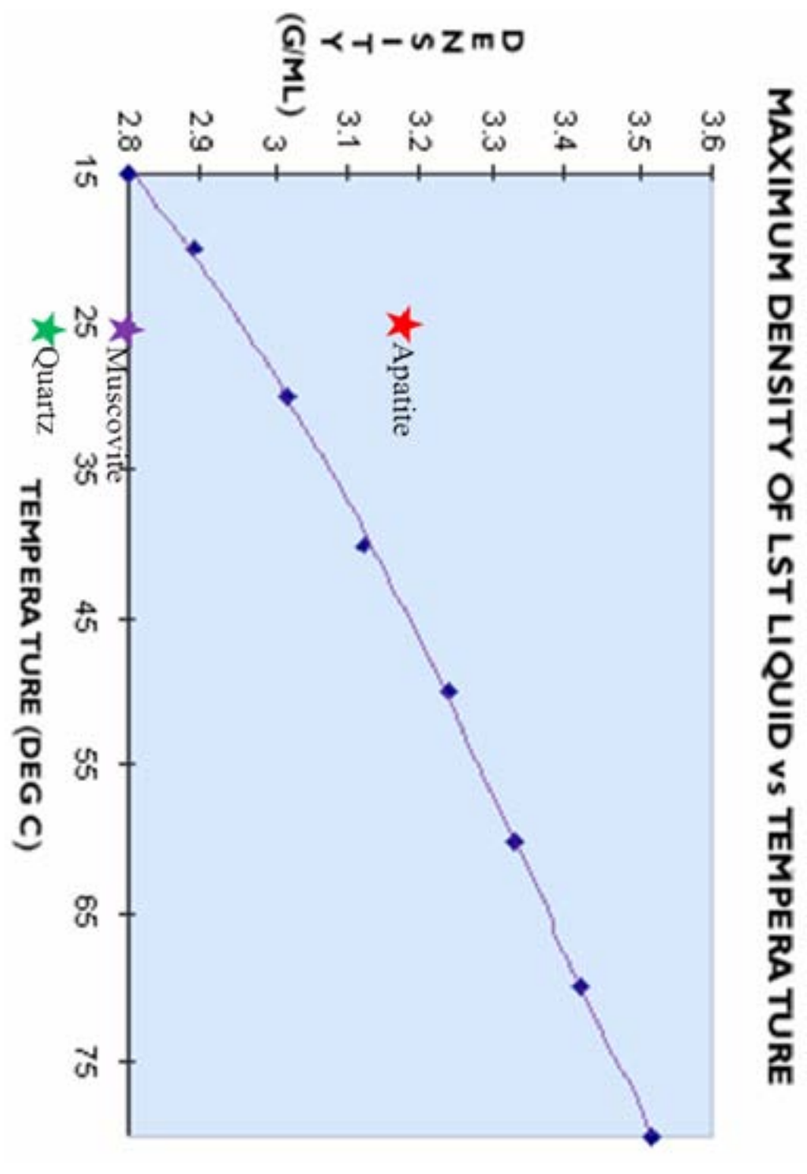


Figure 2.7: Heavy Liquid Density Comparison



powder twice for 3+ minutes until smooth.

## 2.8 Etching Tracks

Mounted slides were submerged in 5M $HNO_3$ for 20 seconds at 21°C. This revealed spontaneous fission tracks in the apatite grains.

## 2.9 External Detector Attachment

The mica detector was cut with an Exacto-Knife to fit over the epoxy mount; the mica was cut to be slightly smaller in size than the 1 cm x 1.5 cm rectangle mount. The samples and the detectors were taped together and tightly bound using the dull end of the Exacto-Knife.

## 2.10 Packaging Samples

The thirteen samples, with attached mica detectors, were stacked and bound with tape. Additionally, CN1 dosimeter glasses with attached mica detectors were placed at the top and the bottom of the stack in order to later monitor neutron flux during irradiation. Samples CR01 to CR08 were in a package with CN1 L dosimeter. Samples CR09 to CR13 were in a separate package with CN1 N dosimeter. Together, the stack was packaged in a polyTRIGA tube and sent to Oregon State University.

## 2.11 Irradiation and $U^{235}$ Track Etching

The samples were irradiated at the Oregon State University TRIGA reactor using a nominal flux of 8.0 x $10^{15}$ n/$cm^2$. This induced $U^{235}$ fission tracks in the samples; only the tracks in the mica replicas were etched after this point such that $U^{238}$ tracks are only visible on the apatite samples and $U^{235}$ tracks are only visible on the mica replicas.

## 2.13 Zeta Calculation

In order to quantify potential error, tracks on known samples were counted. The samples

used were Durango apatite from Durango, Mexico. Tracks on twenty grains were counted for Durango A and Durango B over a given area for each grain. Tracks were counted on the replica of each grain over the same area. Brandon age calculation computer program generated ages for each grain and averaged them. These ages were compared to the known age of the sample to define personal error. As this was done for both Durango A and Durango B, the two error scores were averaged to attain one standard zeta score to be used for all calculations of Mt. Washington samples.

## 2.14 Fluence Calculation

In order to later accurately calculate AFT ages, the fluence was determined for each package containing Mt. Washington samples. Approximately 1000 tracks were counted for each mica glass (four in total at the top and bottom of each package). The exact number counted was divided by the total area tracks were counted within to reach 1000, giving a total density of tracks within the glass. This is proportional to the flux of particles intersecting the mica glass. Fluence for the individual samples was determined by interpolating between the two measured dosimeters.

## 2.15 Track Counting and Calculation

For each sample, tracks on approximately 20 grains were counted with an Olympus BMAX 60 microscope at x 1600. For each grain, tracks were counted within in a certain area representing the spontaneous fission. The same grain on the mica replica, representing the induced tracks, was found and tracks were counted within the same area.

These values, along with the area counted, were entered into the Brandon age calculation program. This program, using the counted track values, the decomposition half-life of $U^{238}$ and relative abundances of $U^{235}$ to $U^{238}$ generated ages for each grain. The program also takes into account the previously determined personal zeta score (which is constant for all samples) and fluence (which differs for each sample). The average for all of the grains was used for the final



measured age, indicated by the program as the central age. Based on the zeta score, an error histogram was also generated.

## 2.16 Track Measurement

Track lengths were measured for samples CR01 (summit) and CR13 (base). 77 tracks were measured for CR01 and 57 tracks were measured for CR13. Data was then input into a386 Zenith PC to generate track length frequency histograms. These histograms were used to model the time temperature path of the sample through the PAZ using Cal Comp Model 31120 program.

## 2.17 Microprobe Composition Analysis

Slides were prepared for Samples CR13, CR12, CR10, CR08, CR06 and CR01. These samples represent all formations being studied. Once mounted in epoxy, the slides were polished first with 400 and 600 grit papers. Slides were then polished with 60/90 grit silicon carbine and 500/600 grit silicon carbide. The polishing was finalized with Alumina G. Slides were finally carbon coated. F and P were calibrated using an apatite standard while Na and Cl were calibrated with a tungtapite standard. Samples CR01, CR08, CR12 and CR13 were scanned with a MAC 400S electron microprobe at UMaine Orono to determine the weight percent of F, Cl and Ce. For CR01, five grains were analyzed with ten points run for each grain. For CR08, three grains were analyzed with seven points run for each grain. For CR13, five grains were analyzed with ten points run for each grain.

# Results

## 3.1 Microprobe

Grains from samples CR01, CR08, CR12 and CR13 were analyzed for F, Cl and Ce content. Grains C 01 is Littleton Formation. Grains CR08 is Rangeley Formation and CR12 and CR13 are Bretton Woods Granite. The five grains analyzed for CR01 yielded an average F weight percent of 3.41, Cl weight percent of .029 and Ce weight percent of 0.03 (Figure 3.1). The three grains analyzed for CR08 yielded an average F weight percent of 4.14, Cl weight perfect of 0.00 and Ce weight percent of .12 (Figure 3.2). The five grains analyzed for CR12 yielded an average F weight percent of 3.42, Cl weight percent of 0.03 and Ce weight percent of 0.08 (Figure 3.3). Only one grain was analyzed for CR13 and had a Fl weight percent of 3.96, Cl weight percent of 0.00 and Ce weight percent of 0.05 (Figure 3.4). Given that these are all fluoroapatites, the closing temperature of apatite does not need to be adjusted to account for excess Cl content.

## 3.2 Zeta Score

Standard deviations of age are based on the zeta score determined off a measured variance from a known standard (Durango apatite of Durango, Mexico). The zeta score was determined on samples 2A, 6A, 7A, 11A and 13A. The mean zeta was determined to be 101.6 +/- 7.18. This is an average of the error calculations from two Durango samples. All other samples are calculated with a zeta score of 98.4 ± 1.7 from Roden-Tice.

## 3.3 Fluence

For Package PL061, the measured fluence for the top and bottom mica glasses, acting as fluence dosimeters for the package, were 3.8403E+06 at the top (CN1 N) and 4.1310E+06 at the bottom (CN1 O). Fluence values for the samples within this package were interpolated (Table 3.5) accordingly. This package included samples CR09 to CR13.

For Package PL060, the measured fluence for the top mica glass was 3.7431E+06. The fluence for the bottom mica glass was 4.3383E+06. Fluence values were interpolated in this package for samples CR01 to CR 08 (Table 3.6). These values are similar to those determined by

| Grain # | F | Cl | H2O | Na2O | CaO | MnO | FeO | Ce2O3 | SO2 | P2O5 | Total | O=F , Cl | Total |
|---|---|---|---|---|---|---|---|---|---|---|---|---|---|
| 1 | 3.66 | 0.033 | -0.039 | 0.102 | 54.653 | 0.336 | 0.104 | 0.039 | 0.006 | 42.882 | 100.837 | 1.544 | 99.313 |
| 2 | 3.701 | 0.008 | -0.033 | 0.093 | 54.386 | 0.258 | 0.037 | 0.025 | 0.012 | 42.985 | 100.73 | 1.56 | 99.171 |
| 3 | 3.282 | 0.033 | 0.146 | 0.083 | 54.732 | 0.28 | 0.042 | 0.021 | 0.001 | 42.024 | 100.638 | 1.392 | 99.246 |
| 4 | 3.522 | 0.002 | 0.039 | 0.072 | 54.766 | 0.224 | -0.0006 | -0.029 | 0.002 | 42.133 | 100.78 | 1.485 | 99.297 |
| 5 | 2.981 | 0.032 | 0.294 | 0.106 | 54.641 | 0.277 | 0.021 | -0.013 | 0 | 42.189 | 100.364 | 1.267 | 99.299 |
| Total | 3.4252 | 0.0364 | 0.077 | 0.092 | 54.676 | 0.275 | 0.044 | 0.0082 | 0.0042 | 42.6424 | 100.7178 | 1.4496 | 99.2694 |

Table 3.3: CR12 Microprobe Data

| Run | F | Cl | H2O | Na2O | CaO | MnO | FeO | Ce2O3 | SO2 | P2O5 | Total | O=F , Cl | Total |
|---|---|---|---|---|---|---|---|---|---|---|---|---|---|
| 1 / 1 . | 3.32 | 0.01 | 0.13 | 0.07 | 55.73 | 0.03 | 0.01 | 0.06 | 0.02 | 11.31 | 101.7 | 1.4 | 100.3 |
| 1 / 2 . | 3.99 | 0.01 | 0.19 | 0.06 | 55.31 | 0.07 | 0.01 | 0.03 | 0 | 11.38 | 102.03 | 1.68 | 100.35 |
| 1 / 3 . | 1.26 | 0 | 0.34 | 0.02 | 55.43 | 0.06 | 0.03 | 0 | 0.01 | 11.03 | 101.83 | 1.8 | 100.03 |
| 1 / 4 . | 1.02 | 0 | 0.21 | 0.06 | 55.16 | 0.07 | 0.03 | 0.07 | 0.03 | 11.13 | 101.36 | 1.69 | 99.67 |
| 1 / 5 . | 1.11 | 0 | 0.26 | 0.03 | 55.03 | 0.03 | 0.01 | 0.03 | 0.01 | 11.33 | 101.33 | 1.73 | 99.8 |
| 1 / 6 . | 1.03 | 0 | 0.27 | 0.03 | 55.86 | 0.03 | 0.03 | 0.07 | 0.01 | 11.39 | 101.71 | 1.7 | 100.01 |
| Average | 3.96 | 0.01 | 0.18 | 0.03 | 55.33 | 0.06 | 0.02 | 0.03 | 0.01 | 11.31 | 101.73 | 1.67 | 100.06 |

Table 3.4: CR13 Microprobe Data



| Grain # | F | Cl | H2O | Na2O | CaO | MnO | FeO | Ce2O3 | SO2 | P2O5 | Total | O=F , Cl | Total |
|---|---|---|---|---|---|---|---|---|---|---|---|---|---|
| 1 | 3,989 | 0,034 | -0,201 | 0,099 | 51,632 | 0,377 | 0,084 | 0,013 | -0,003 | 12,052 | 101 296 | 1,687 | 99,61 |
| 2 | 3,244 | 0,031 | 0,168 | 0,1 | 51,414 | 0,418 | 0,242 | 0,029 | 0,003 | 12,244 | 100 694 | 1,371 | 99,322 |
| 3 | 3,287 | 0,036 | 0,285 | 0,104 | 51,388 | 0,438 | 0,234 | 0,032 | -0,002 | 11,764 | 100 262 | 1,349 | 98,911 |
| 4 | 3,273 | 0,024 | 0,296 | 0,232 | 51,124 | 0,495 | 0,257 | 0,029 | -0,003 | 11,949 | 100 264 | 1,342 | 98,922 |
| 5 | 3,437 | 0,022 | 0,068 | 0,097 | 51,383 | 0,286 | 0,039 | 0,047 | 0,003 | 11,962 | 100 373 | 1,436 | 98,922 |
| Total | 3,4064 | 0,0294 | 0,0832 | 0,2064 | 51,3932 | 0,4028 | 0,2092 | 0,03 | -0,00008 | 11,9702 | 100 3776 | 1,4404 | 99 1374 |

Table 3.1: CR01 Microprobe Data

| Grain # | F | Cl | H2O | Na2O | CaO | MnO | FeO | Ce2O3 | SO2 | P2O5 | Total | O=F , Cl | Total |
|---|---|---|---|---|---|---|---|---|---|---|---|---|---|
| 1.00 | 4.65 | 0.00 | -0.52 | 0.12 | 54.68 | 0.30 | 0.03 | 0.07 | -0.01 | 42.17 | 102.03 | 1.96 | 100.07 |
| 2.00 | 3.68 | 0.01 | -0.04 | 0.14 | 53.82 | 0.38 | 0.07 | 0.25 | 0.01 | 42.41 | 100.76 | 1.55 | 99.21 |
| 3.00 | 3.89 | 0.00 | -0.14 | 0.16 | 54.18 | 0.38 | 0.05 | 0.05 | 0.00 | 42.26 | 100.97 | 1.64 | 99.33 |
| Total | 4.14 | 0.00 | -0.26 | 0.14 | 54.28 | 0.35 | 0.05 | 0.12 | 0.00 | 42.27 | 101.35 | 1.74 | 99.60 |

Table 3.2: CR08 Microprobe Data

Roden-Tice, therefore can confindently be used to compared ages between Anderson and Roden-Tice.

## 3.4 Ages

Thirteen samples from the Cog Railroad, Mt. Washington yielded ages ranging from 148.0 +/- 15 Ma to 89.2 +/- 10 Ma, therefore ranging from late Jurassic to Late Cretaceous. The samples yielded an average exhumation rate of .0215 mm/yr during this period (Table 3.7).

Near the summit, elevations 1914.14 m (CR-01) and 1886.71 m (CR-02) yielded ages, respectively, 180.0 +/- 15 Ma and 147.3 +/- 25 Ma. The latter age was confirmed by Roden-Tice's determined age of 147.2 +/- 15 Ma at the same elevation.

Between 1743.5 m elevation and 1089.7 m elevation, ages show small variations and range between 110.1 +/- 13 Ma and 126.6 +/- 13 Ma. The previously established trend of increasing age with elevation is similarly neglected during this period (Figure 3.1). Ages for elevations 1743.5 m (CR03), 1624.6 m (CR04), 1482.2 m (CR05), 1392.0 m (CR06), 1325.9 m (CR07), 1190.6 m (CR08) and 1089.7 m (CR09) are, respectively, 114.5 +/- 17 Ma, 114.4 +/- 12 Ma, 119.3 +/- 13 Ma, 125.8 +/- 22 Ma, 117.7 +/- 22 Ma, 118.4 +/- 12 Ma and 110.1 +/- 13 Ma. CR06 and CR07 ages were confirmed by Roden-Tice. The Roden-Tice ages were 126.6 +/-15 Ma for CR06 and 114.4 +/- 16 Ma.

| Sample | Elevation (m) | MRT Age (Ma) | Error + | Error - | BPA Age (Ma) | Error + | Error - |
|---|---|---|---|---|---|---|---|
| CR01 | 1914.14 | 180.0 | 15.5 | 14.8 | | | |
| CR02 | 1886.71 | 147.2 | 15.7 | 14.2 | 147.3 | 25.0 | 22.8 |
| CR03 | 1743.56 | 114.5 | 14.0 | 15.3 | | | |
| CR04 | 1624.58 | 114.4 | 13.1 | 11.8 | | | |
| CR05 | 1482.21 | 119.3 | 13.5 | 12.2 | | | |
| CR06 | 1392.02 | 126.6 | 15.5 | 13.0 | 126.6 | 24.3 | 20.5 |
| CR07 | 1325.88 | 114.4 | 15.5 | 17.8 | 117.7 | 23.6 | 20.5 |
| CR08 | 1190.59 | 118.4 | 13.2 | 11.9 | | | |
| CR09 | 1089.66 | 110.1 | 13.6 | 12.1 | | | |
| CR10 | 960.66 | 102.9 | 11.6 | 10.5 | | | |
| CR11 | 812.72 | 95.5 | 9.3 | 8.5 | 95.5 | 9.3 | 8.5 |
| CR12 | 617.69 | 85.5 | 8.0 | 7.3 | | | |
| CR13 | 554.05 | 89.2 | 10.0 | 10.0 | 89.7 | 17.6 | 16.7 |

Table 3.4: AFT Ages from Cog Railroad



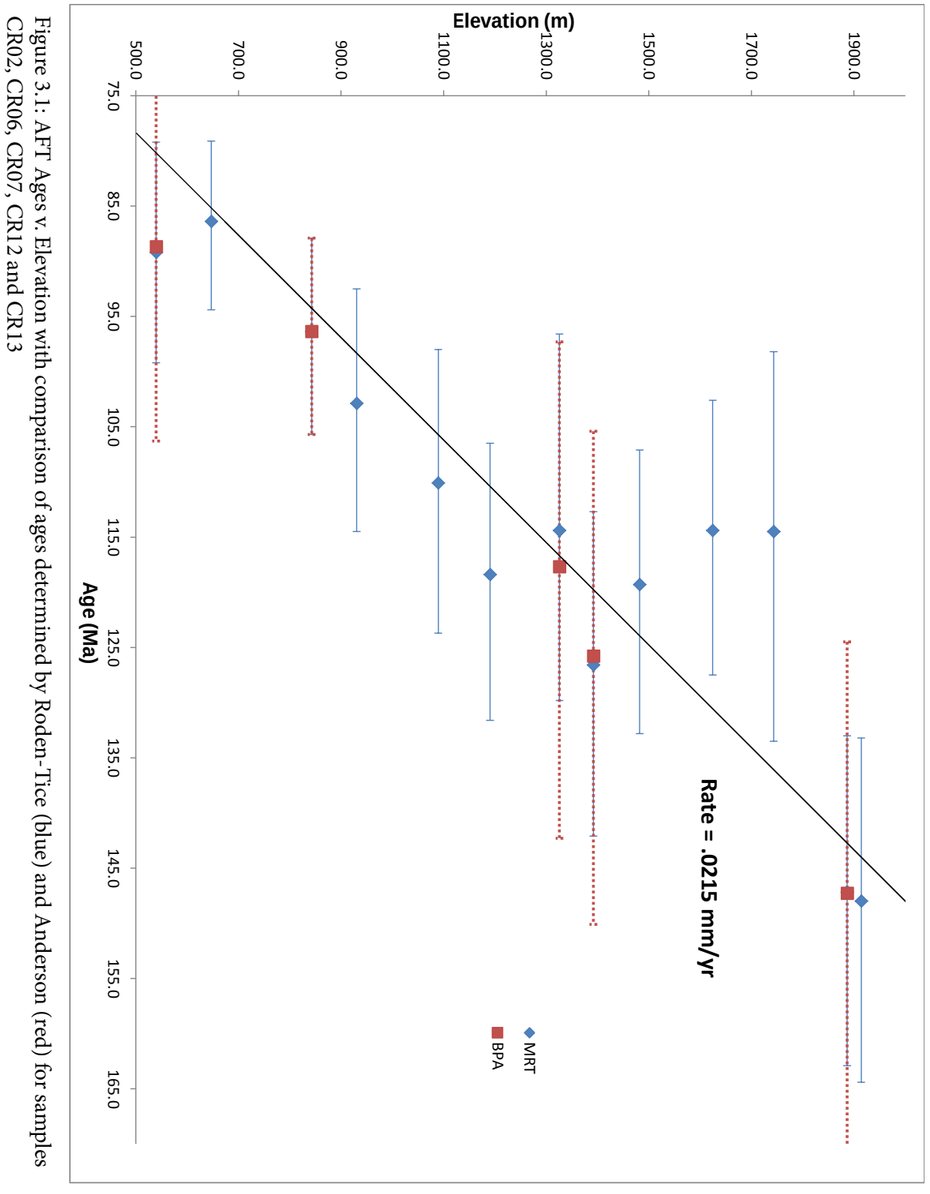


Figure 3.1: AFT Ages v. Elevation with comparison of ages determined by Roden-Tice (blue) and Anderson (red) for samples CR02, CR06, CR07, CR12 and CR13

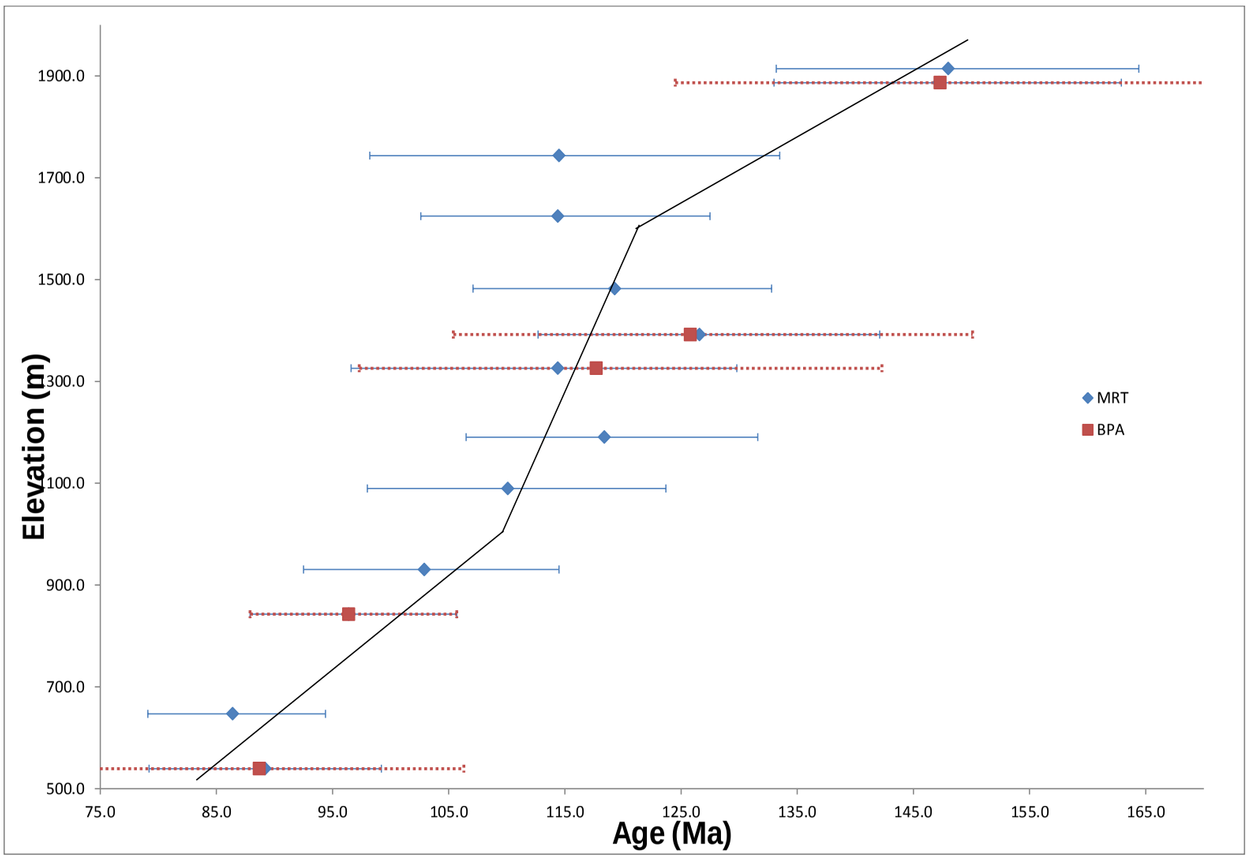


Figure 3.3: AFT Ages with exhumation rates separated by elevation



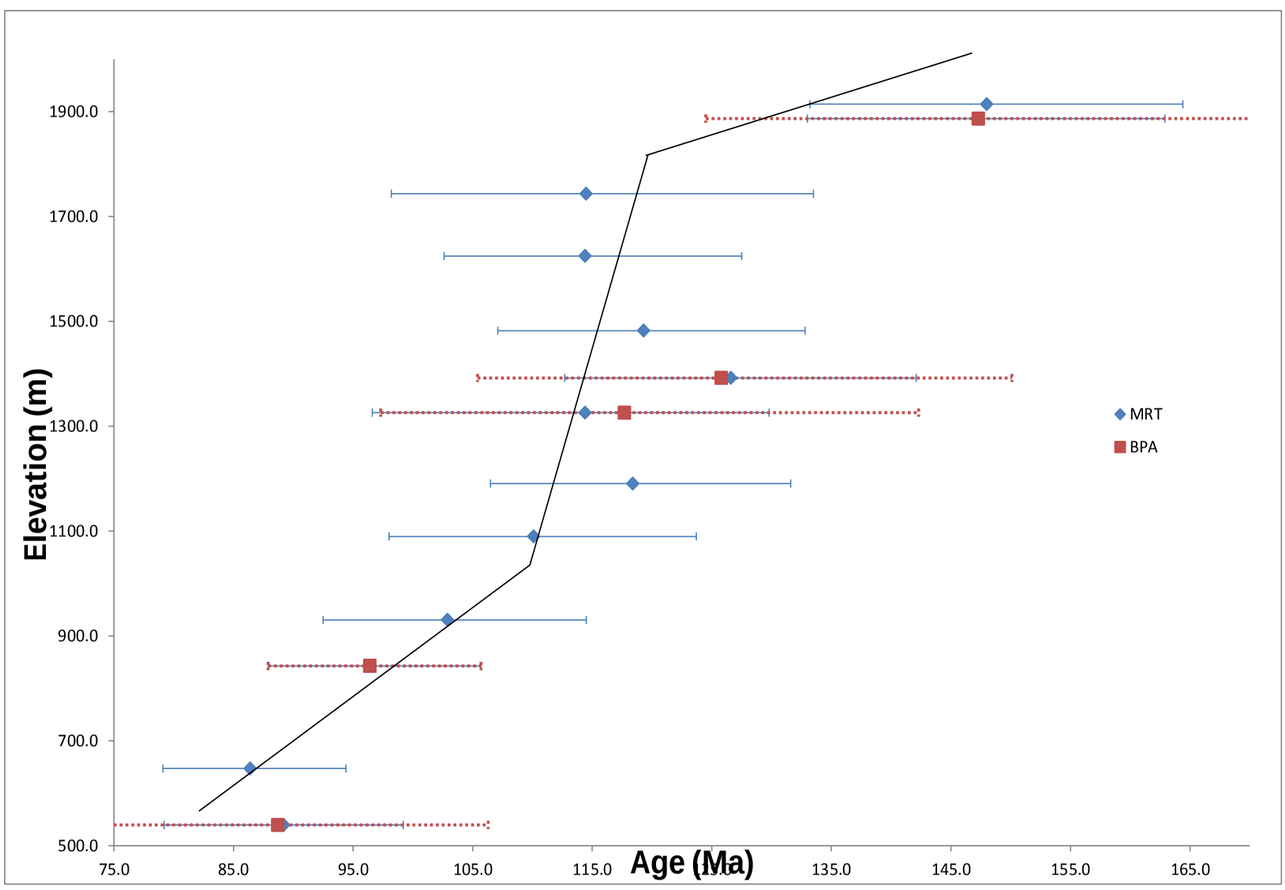


Figure 3.2: AFT ages with exhumation rates separated by trends in age

Bottom samples are similarly all within error of each other. Elevation 930.6 m (CR10) yielded an age of 102.9 +/- 11 Ma. Elevation 842.8 (CR11) yielded an age of 96.4 +/- 9 Ma. This sample had a confirmed age of 96.4 +/- 9 Ma, calculated by Roden-Tice. The lowest elevation samples, Bretton Woods Granite, had ages 86.4 +/- 8 Ma (at elevation 647.1; CR 12) and 88.7 +/- 16 Ma (at elevation 539.5 m; CR13). Roden-Tice calculated an age of 89.2 +/-10 Ma for this sample.

### 3.5 Exhumation Rate

The samples yield an average exhumation rate of .0234 mm/yr during this period. Exhumation, however, does not appear to be constant throughout. There is no obvious separation of distinct exhumation rates, but there is one clear trend from 110 Ma to 125 Ma, where all AFT are nearly uniform (Figure 3.2). Samples CR03 to CR09 are represented in this period, ranging in elevation from 1743.5 m to 1089.7 m. The exhumation rate of these samples jumps to .03924 mm/yr. Keeping consistent with this separation, the remaining low elevation samples, CR10 to CR13 yield an exhumation rate of.0350 mm/yr. The high elevation samples, CR01 and CR02 yield an exhumation rate of .0342 mm/yr. These upper two samples, however, are extremely close both in elevation and age that this upper exhumation rate is relatively insignificant.

If the exhumation separations presented by Roden-Tice et. al (2011) are followed, groups are based on similarities in elevation more so than ages. Doing this, Samples CR01 to CR04 would yield an exhumation rate of .0285 mm/yr between elevations 1914.14 m and 1624.58 m (Figure 3.3). Samples CR05 to CR09 would yield an exhumation rate of .0427 mm/yr between elevations 1482.24 m and 1089.66 m. Finally, samples CR10 to CR13 would again be grouped together yielding that exhumation rate of .0342 mm/yr between elevations 930.55 m and 539.50 m.

### 3.6 AFT Ages of Separate Rock Units

The Littleton Formation encompasses samples CR01 to CR07 from elevations 1914.14 m to 1325.88 m. Littleton Formation ages range from 148.0 +/- 15 Ma to 114.4 +/-16 Ma (Figure 3.4). Rangeley Formation encompasses samples from CR08 to CR11 from elevations 1190.55 m to 842.77 m. These ages range from 118.4 +/- 12 Ma 96.4 +/- 9 Ma. Bretton Woods Granite is represented in samples CR12 and CR13 from elevations 647.09 m to 539.50 m. Bretton Woods Granite ages range from 89.2 +/- 10 Ma to 86.4 +/- 8 Ma. Evaluating the differences in slopes between rock type does not yield any significant trends so it can be assumed that lithology does not play a role in differences of exhumation rate throughout the study period.

### 3.7 Track Length Modeling

Track lengths were measured for samples CR1 at elevation 1914.1 m and CR13 at 539.5 m.

For CR1, 77 tracks were measured and yielded a mean track length of 12.3 +/-1.8 μm. Lengths ranged from approximately 6 μm to 17 μm. For CR13, 57 tracks were measured and yielded a mean track length of 13.1+/- 1.2 μm. Lengths ranged from 9 μm to 16 μm. CR1 had a relatively normal distribution around the mean track length (Figure 3.5), while CR13 was slightly skewed to the left (Figure 3.6).

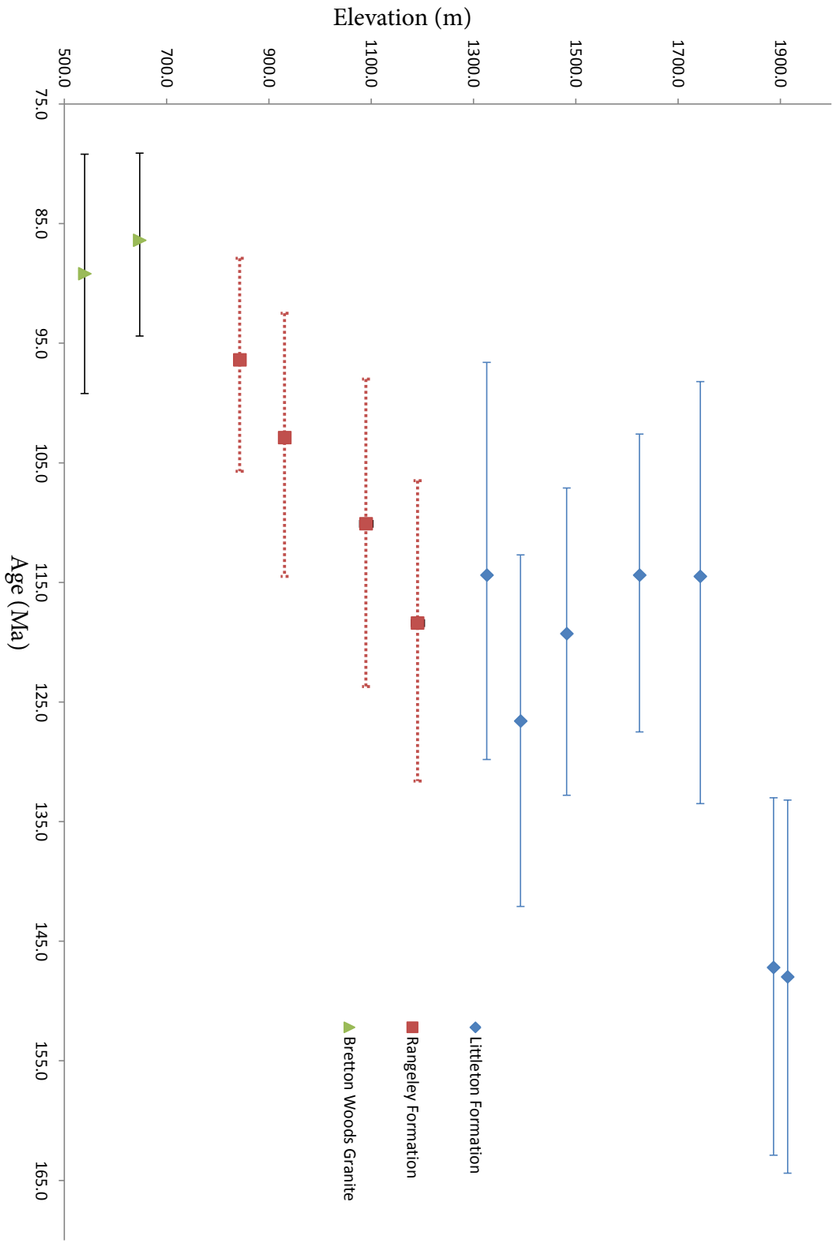


Figure 3.4: AFT Ages by lithography



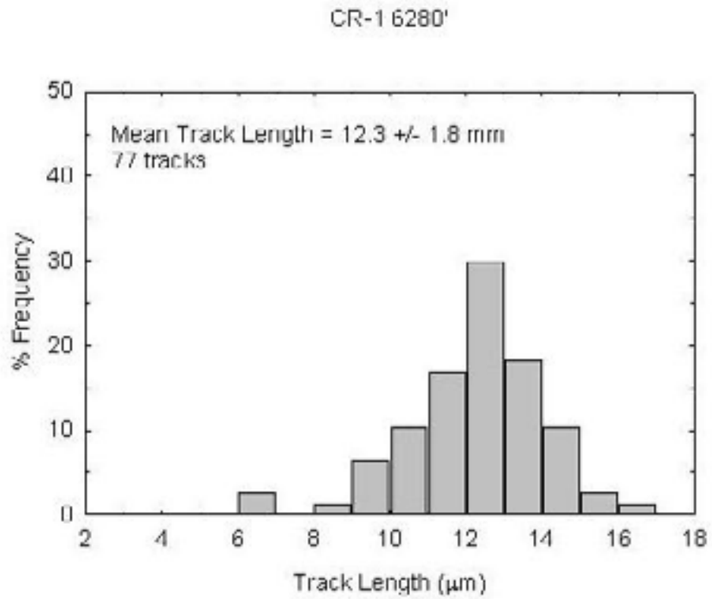


Figure 3.5: CR1 Track length frequency distribution

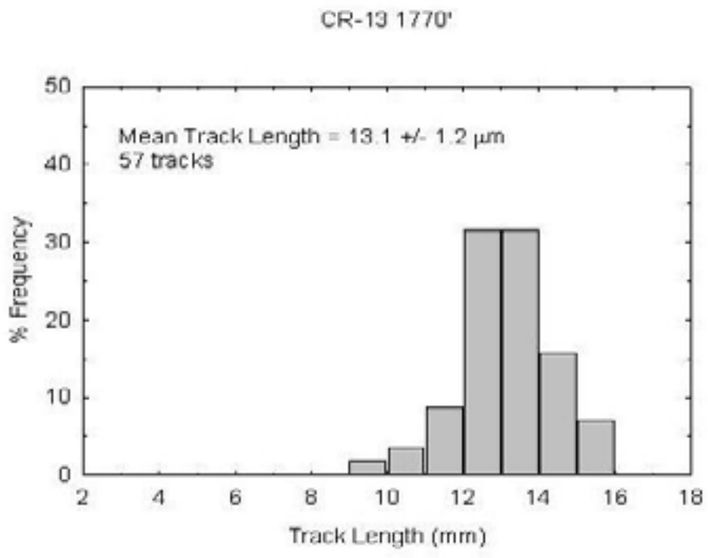


Figure 3.6: CR13 Track length frequency distribution

# Discussion

## 4.1 AFT Ages

AFT ages from the Cog Railroad display a significant period of rapid exhumation that correlates chronologically with differential exhumation also evidenced in the Auto Road time-temperature history lasting from approximately 125 Ma to 60 Ma. This period of geologic time is well documented in the sedimentary record from Georges Bank off of the North Atlantic continental margin. As these sediments are derived from mountainous interior of New England there should be a temporal correlation between rapid sedimuent influx offshore and rapid exhumation on land. AFT ages from this study also align with a local and regional tilt when compared with AFT ages throughout New England and northern New York. These models typically invoke fault reactivation and/or paleo-drainage systems both of which contribute to the measured accelerated and differential exhumation.

## 4.2 Rapid Exhumation

Contrary to the separation of exhumation rates from the Auto Road proposed by Roden-Tice et. al (2012) (Figure 4.1), comparing the Cog Railroad ages suggests that - while times of different exhumation are evident - grouping data by AFT age rather than elevation is more significant. This teases out the trend of rapid exhumation from approximately 125 Ma to 110 Ma. Samples between 1743.5 m and 1089.7 m show a period of rapid exhumation documented with ages ranging from only (not respectively) 126. 6 +/- 15 Ma to 110.2+/- 13 Ma.

A similar trend it evident in Auto Road samples, with ages between elevations 1762 m and 1173 m ranging from 143.8 +/-19 Ma to 123.5 +/- 14 Ma (Figure 4.2). Although there is a gap of approximately 10 my, consistent with the general offset between sample sets, rapid exhumation evidenced from both Cog Railroad and Auto Road coincide with magmatic events.This period lies within the Cretaceous Peri-Atlantic Alkaline Pulse (PAAP) (Matton and Jebrak, 2009). PAAP describes a surge of alkaline activity during the Cretaceous, specifically from 125 Ma to 80 Ma (Figure 4.3) that was caused by local shallow asthenospheric upwelling that reactivated zones of crustal weakness initially formed during Atlantic rift-drift tectonism (Matton and Jebrak, 2009).

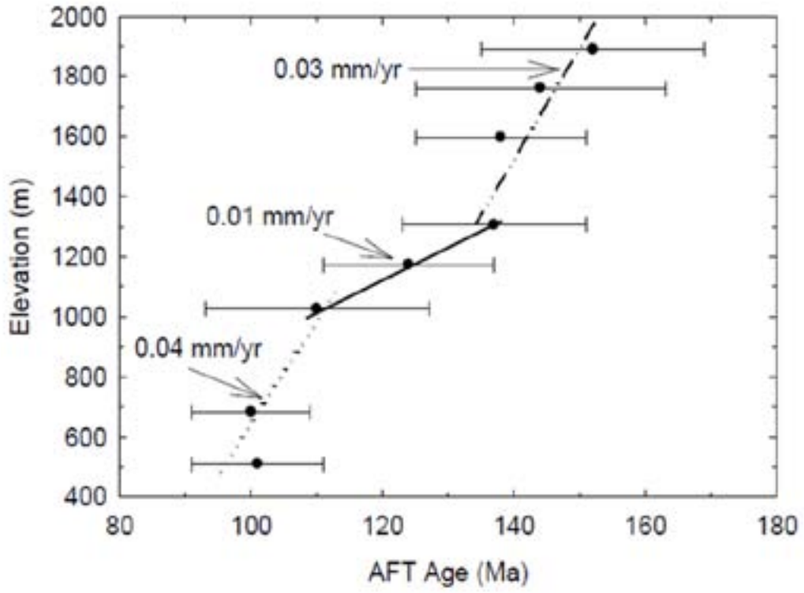


Figure 4.1: Separations of Exhumations Rates fro mAuto Road AFT Ages (Roden-Tice et. al,. 2011)

This further aligns with the formation of the Monteregian Hills alkaline province (MHAP) in Quebec, Canada to the northwest of Mt. Washington. It consists of nine alkaline intrusions approximately 124 my old. While the original explanation for the hills was the passage of North America over the Great Meteor Hot Spot, this theory has been dismissed because of inconsistencies in the their age relative to the Hot Spot's path.

McHone (1996) first rejected the hot spot theory and introduced an alternative one involving alkaline basalts from the mantle occurring in concert with tectonic reactivation of lithospheric structures. Roulleau et. al (2010) concluded that the hills formed during continental rifting associated with upper mantle source upwelling.

The MHAP is the northwestern bound to the New England-Quebec Igneous Province (NEQ), a series that extends into southern New England (Figure 4.4) composed of Cretaceous



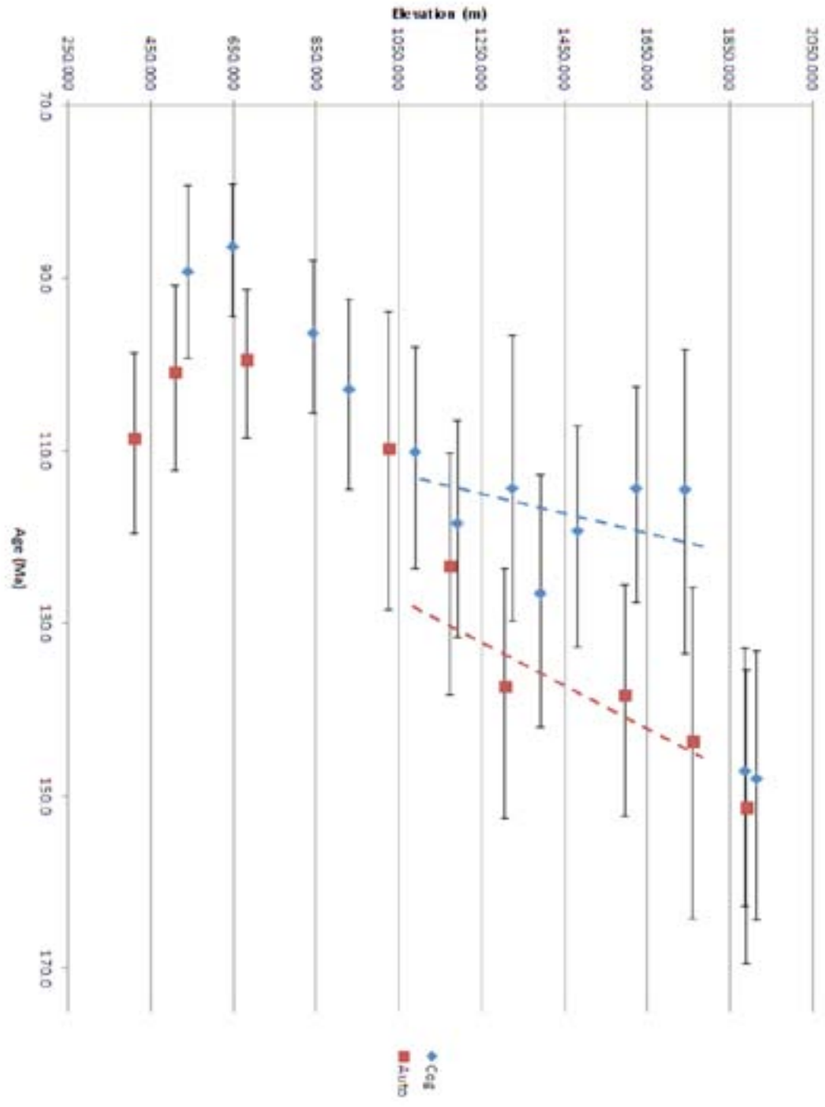


Figure 4.2: Cog Railroad Ages v. Auto Road Ages; slopes indicate period of potential rapid exhumation in both data sets

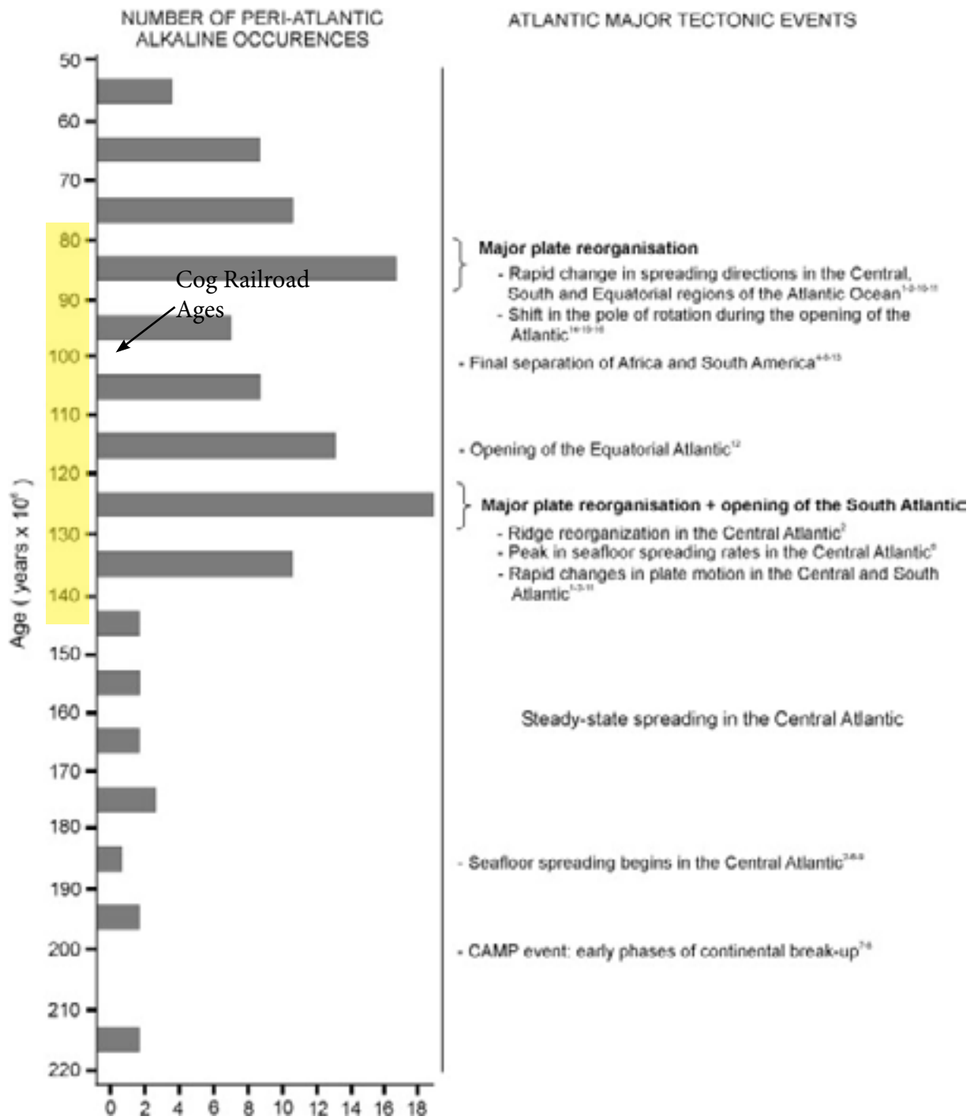


Figure 4.3: Timing of PAAP and tectonic activity synchronous with rapid exhumation (Matton and Jébrak, 2007)



gabbro-syenite alkali plutons and dikes (McHone and Butler, 1984). As with MHAP, the source of the NEQ is asthenospheric upwelling that caused zones of crustal weakness to be reactivated (Faure et al, 1996).

Local evidence of this reactivation has been recently documented by the presence of a dike in Huntington Ravine (Kindley, 2011; Gardner, 2010). This dike, the Escape Hatch dike, with an E-W orientation, is an alkali dolerite, similar to the composition of features in the Cretaceous NEQ (Figure 4.5). Kindley (2011) asserts, then, that this dike is related to the N-S extensional stress field throughout New England and into Quebec. Faure et. al (1996) links E-W striking dike intrusions to the rifting event approximately 125 mya that marks the final stages of the breakup of Pangea and accelerated plate motion (Figure 4.6). Along with the upwelling, the NEQ-aged dikes could have introduced increased heat just west of the present day summit, causing the cluster of Cog Railroad ages not found in the Auto Road data set.

This is all synchronous with the rapid period of exhumation evidenced in AFT ages along the Cog Railroad. Upwelling from these magmatic events, therefore, is likely to have triggered the onset of increased rates of exhumation.

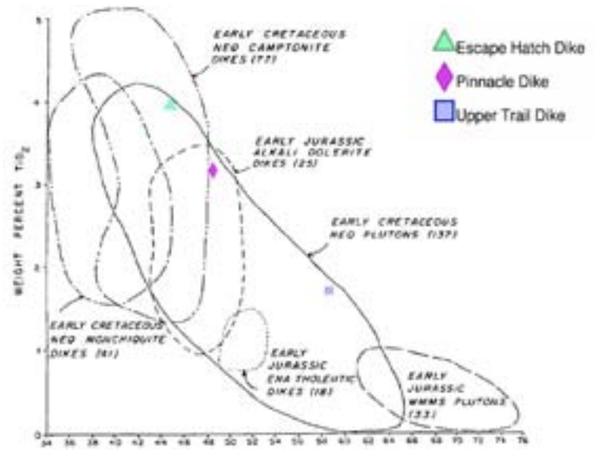


Figure 4.5: Huntington Ravine Dikes geochemical classifcation against those put forth by McHone and Butler (1984) (Gardner, 2010)

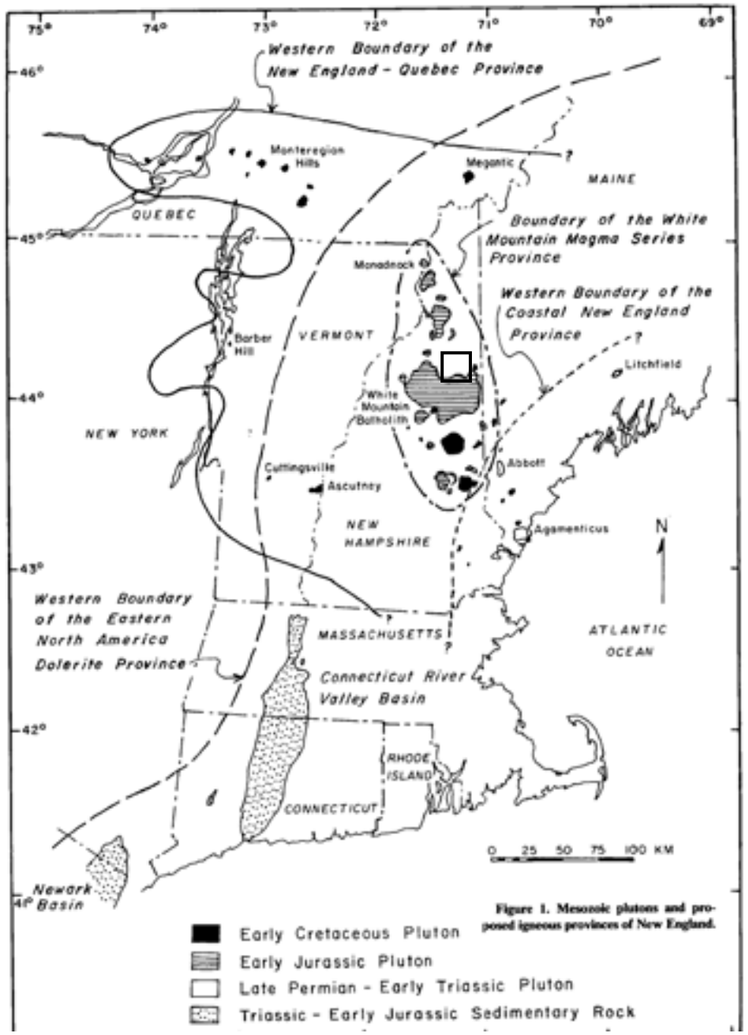


Figure 4.4: Map of Mesozoic Igneous intrustions through New England and Quebec (McHone and Butler, 1984)



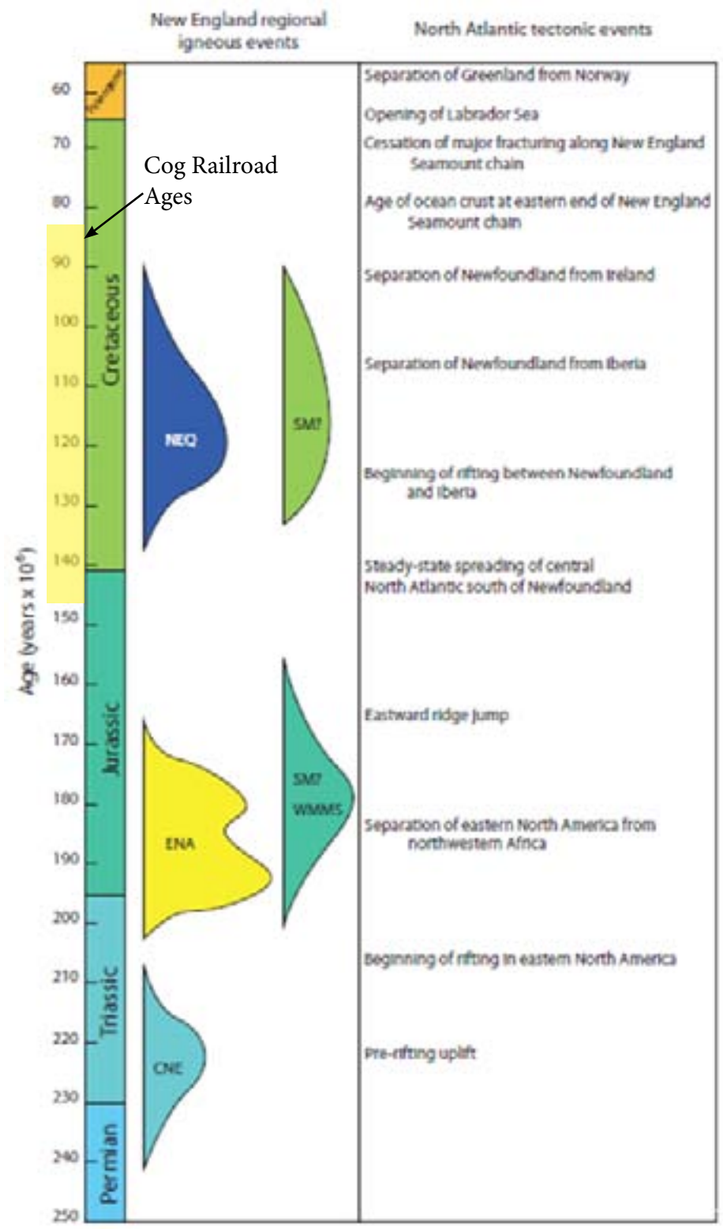


Figure 4.6: Timing of North Atlantic Tectonism and New England Igneous Provinces (McHone and Butler, 1984)

## 4.3 Differential Exhumation

*4.3a Evidence in Track Length Measurement*

Track length measurements for the summit and base samples yielded nearly identical frequency distributions to the Auto Road measurements (Figure 4.7), allowing the use of the time-temperature path for the Auto Road samples to be applied to the Cog Railroad samples. The model suggests that the base and summit samples underwent uniform exhumation between approximately 160 and 130 Ma of 1.5 – 2.0 °C/my (Figure 4.8). At 130 Ma the summit samples, in the case of the Auto Road at elevation 1762 m, was essentially at a standstill, while base same at elevation 510 m experienced exhumation of 0.6 °C/my. At 60 Ma, the base and summit resumed a uniform exhumation of 0.6 °C/my with the current topographic relief in place.

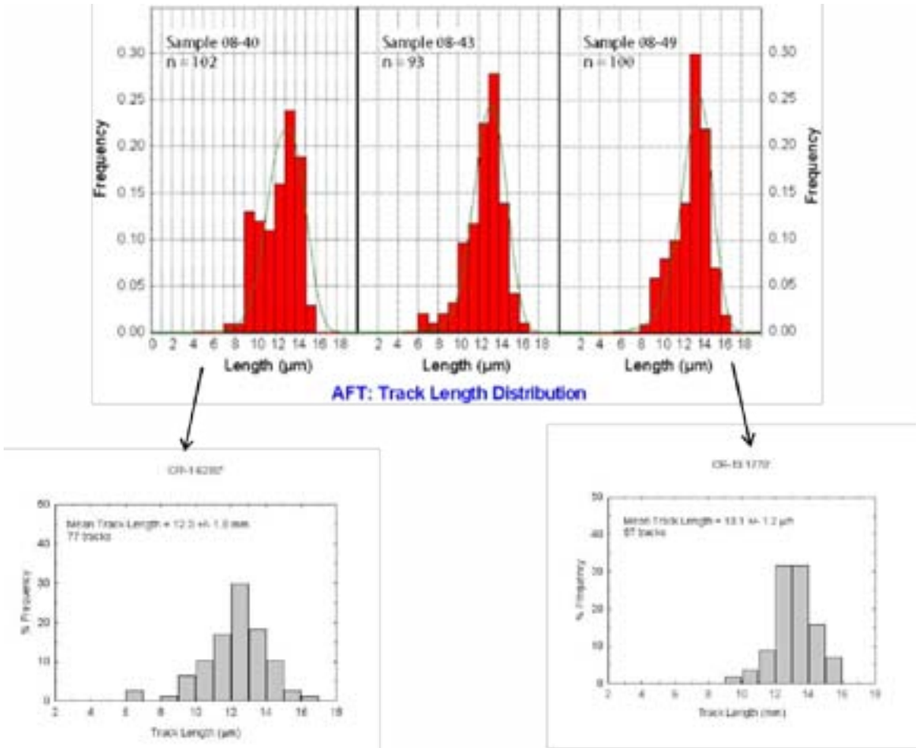


Figure 4.7: Frequency Track Length Histograms; Top figure is from Auto Road (Roden-Tice et. al, 2011) and bottom two graphs are from Cog Railroad



The onset of differential exhumation roughly coincides with the phase of rapid exhumation for middle-elevation Cog Railroad samples between approximately 100 and 125 Ma. As middle elevation samples were passing quickly through the 100°C isotherm, they continued to exhume through the PAZ with relative speed.

Roden-Tice et. al (2012) suggest that this differential erosion is a result solely of a paleo-drainage system that cut down topography east of the present day summit. The uniformity of track lengths between Cog Railroad and Auto Road would suggest that a paleo-drainage system likewise existed to the west of the present day summit somewhere in the vicinity of Crawford Notch. This suggets that the initiation of Pinkham and Crawford Notches, and perhaps others in the White Mountains, such as Evans and Franconia Notches, began along N-S trending paleo-river systems in response to magmatic uplift associated with the NEQ Cretaceous magmatic events.

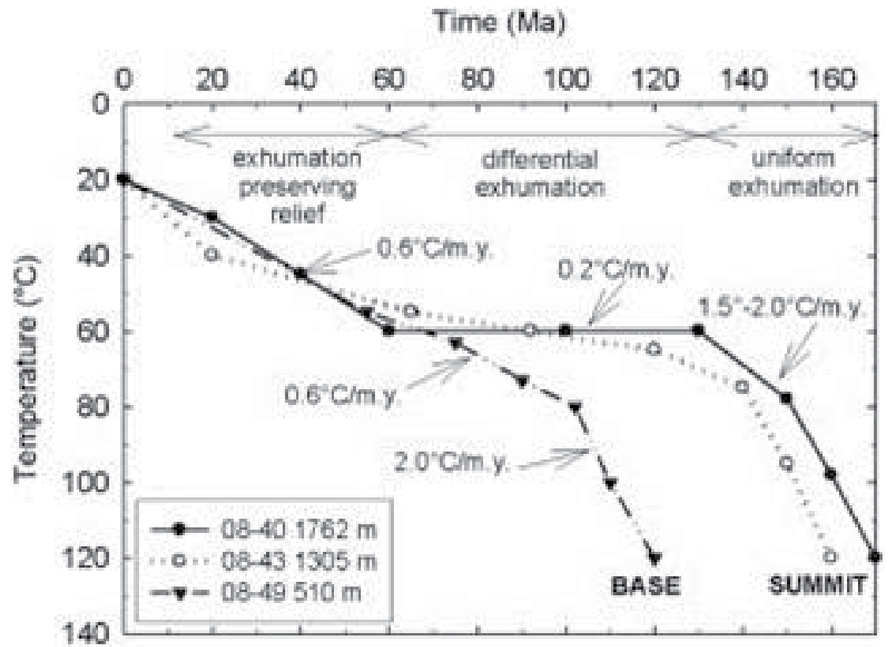


Figure 4.8: Time-Temperature Path of Auto Road Samples through PAZ (Roden-Tice et. al, 2012)

*4.3b Sedimentation Record*

It would be expected that a large influx of clastic, as opposed to marine-influenced limestone, would be present to account for unroofing of Mt. Washington during the same time period of rapid exhumation. There is unlikely to be too long of a response time between rapid exhumation and sediment inflow to Georges Bank and it would certainly have within the 10-20 my uncertainty of the AFT ages reported here and by Roden-Tice et al. (2012).

Marine core logs reveal an inflow of terrestrial-derived sediment that could be in response to rapid mountain incision. The stratigraphic column from the USGS Wells Cost No. G-2 from Georges Bank off of North Atlantic (Figure 4.9) continental margin shows an influx of clastic sediment during the Aptian and Albian, between approximately 125 Ma and 100 Ma (Figure 4.10).

This period is marked by a mudstone unit commencing right after the Barremian – Aptian (130 Ma) border and lasting just past the Aptian- Albian border (112 Ma). The mudstone is primarily silty with interbeds of sandstone. After this is a thin layer of very coarse, rounded sand and medium to fine grained sandstone. Stratigraphy above and below these clastic are biogenic units of limestone, reflecting a quiet water, equatorial setting without significant clastic influx. Carbonate unites define most of the rest of the Cost No. G-2 stratigraphic column which extends from the Late Triassic to the Tertiary (Figure 4.10).

The mudstone and sandstone layers that are interpreted here to be synchronous with the rapid and differential exhumation seen in the Mt. Washington region are relatively atypical. These sediments can be attributed to this exhumation as sediment from Mt. Washington would have entered the Gulf of Maine to Georges Bank through the local Cretaceous river systems. The stratigraphic record also reveals a decrease in organic carbon during this period that would be related to marine-origin sediments, possibly confirming the mountainous source of sediments then.

Cost No. G-1 Well similarly reveals an influx of clastic material and decrease in organic carbon content during the Albian and Aptian (Figure 4.11). This well further shows sandstone



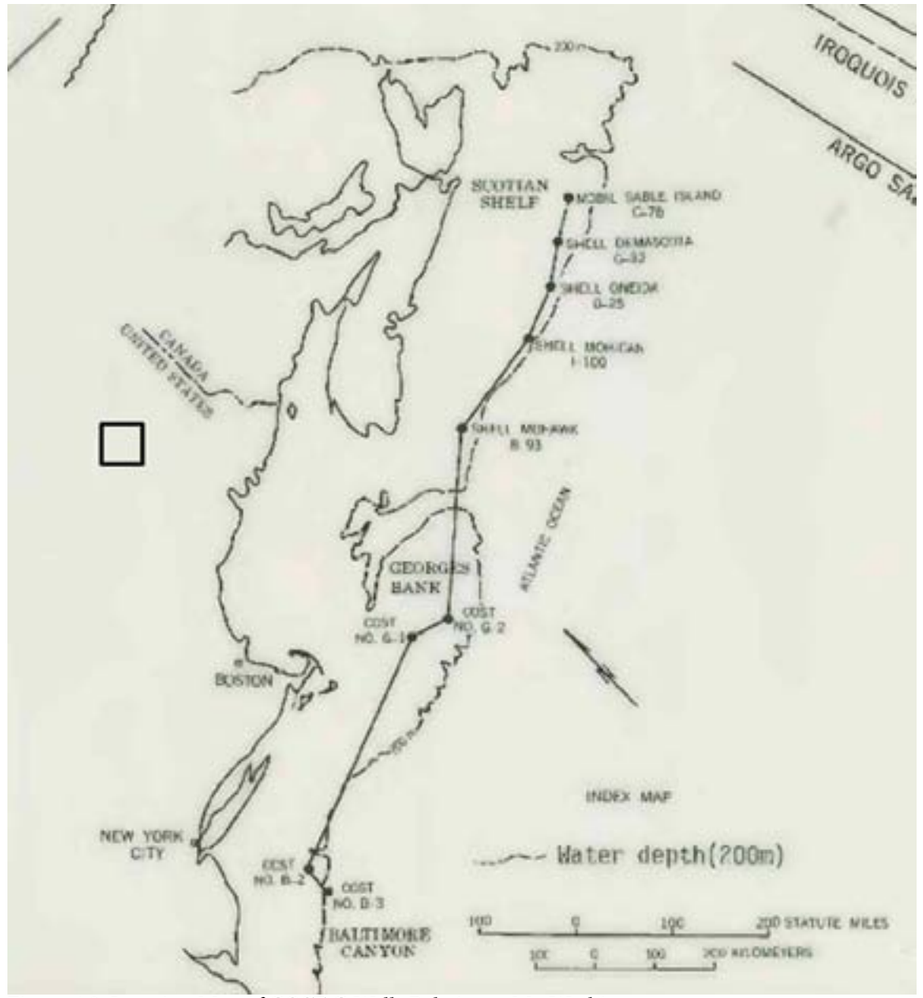

Figure 4.9: Location Map of COST G Wells Relative to Mt. Washington

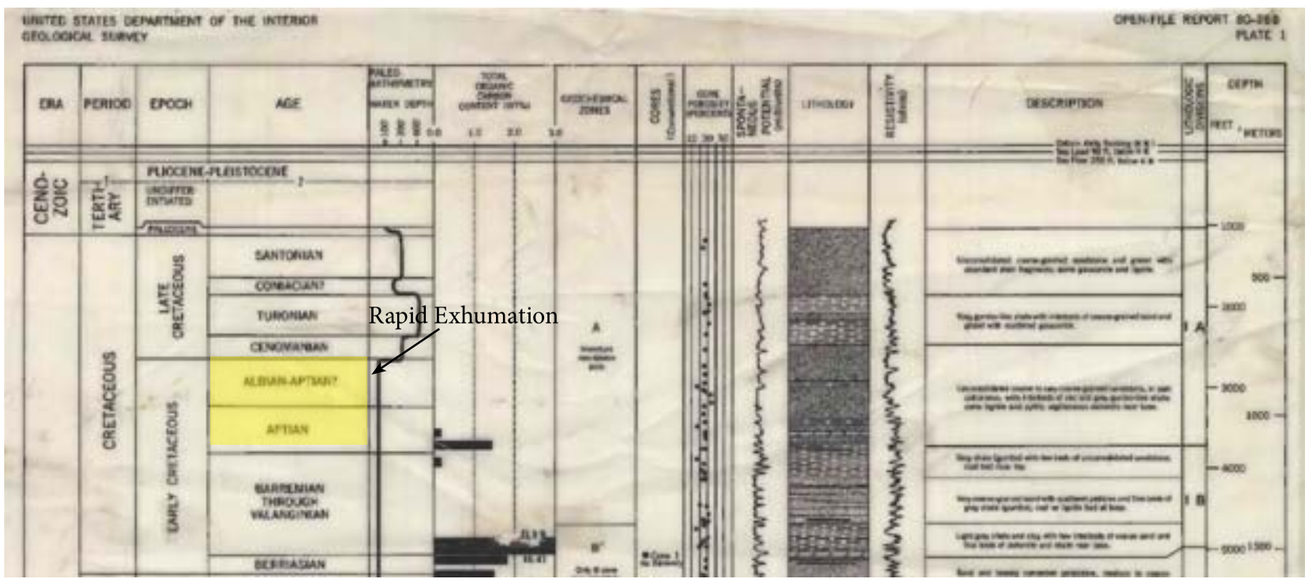


Figure 4.11: Cost G-1 Well Stratigraphic Column from Cretaceous to Tertiary (USGS, 1980)



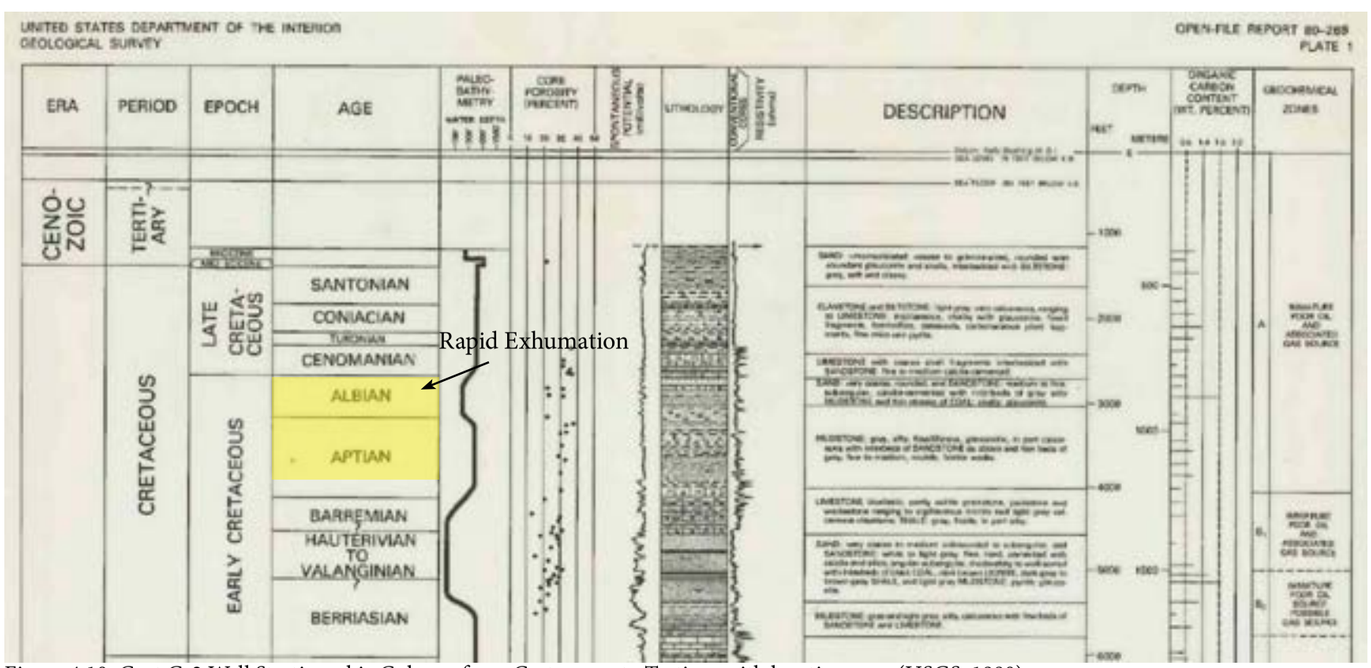


Figure 4.10: Cost G-2 Well Stratigraphic Column from Cretaceous to Tertiary with location map (USGS, 1980)

layers extending to Santonian, approximately 80 Ma, corresponding further with the period of differential exhumation that lasted from approximately 120 Ma to 60 Ma. It is described as unconsolidated coarse to very coarse grained sanstone. Surrounding this layer on both sides are beds of gumbo-like shale, which is along with the limestone some of the most commonly occuring sediments found throughout the core log. The unconsolidated sandstone, on the other hand, is more anomalous requiring an external event separate from the regular cycles of sedimentation.

This explanation could be the increased inflow of sediment from rapid exhumation on Mt. Washington. Like with Cost G-2, the response time is likely to be relatively sudden, therefore an offset of rapid exhumation on Mt. Washington and sediment appearing in the Georges Bank core would not be vastly significant.

## 4.4 Age Gradation

*4.4a Local Tilt*

Cog Railroad samples from the western slope are all within error of the Auto Road samples on the eastern side of the mountain. Cog Railroad ages are, however, consistently younger at comparable elevations; similarly, at comparable ages, Cog Railroad samples are higher in elevation. While ages are within error, this undeviating relationship is indicative of a westward surficial tilt during the period of cooling of no more than 5° W (Figure 4.12).

AFT ages from Mt. Washington align with a general trend of AFT ages from Roden-Tice et. al (2009). These samples were taken along roads and riverbeds, and their elevations are likely relatively low-lying and vertical relief is therefore negligible. Given that, the westward tilt evidenced on Mt. Washington can be extended locally through the Amonoosuc Fault on the New Hampshire/Vermont border (Figure 4.13) . The region of lower-lying elevation surrounding the Mt. Washington massif is characterized by younger ages, approximately 80 to 90 Ma. Ages generally increase to both the east (southeast) and west (northwest).



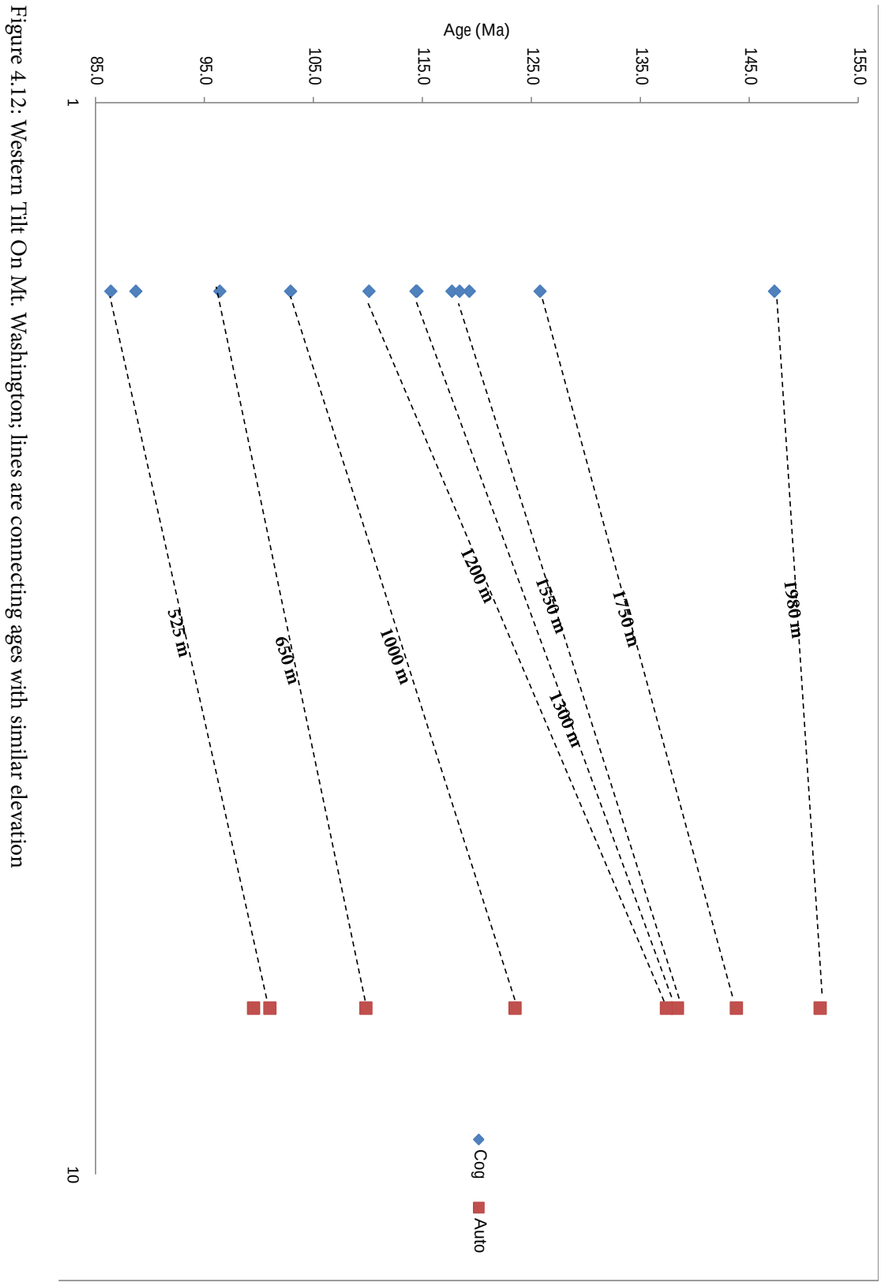


Figure 4.12: Western Tilt On Mt. Washington; lines are connecting ages with similar elevation

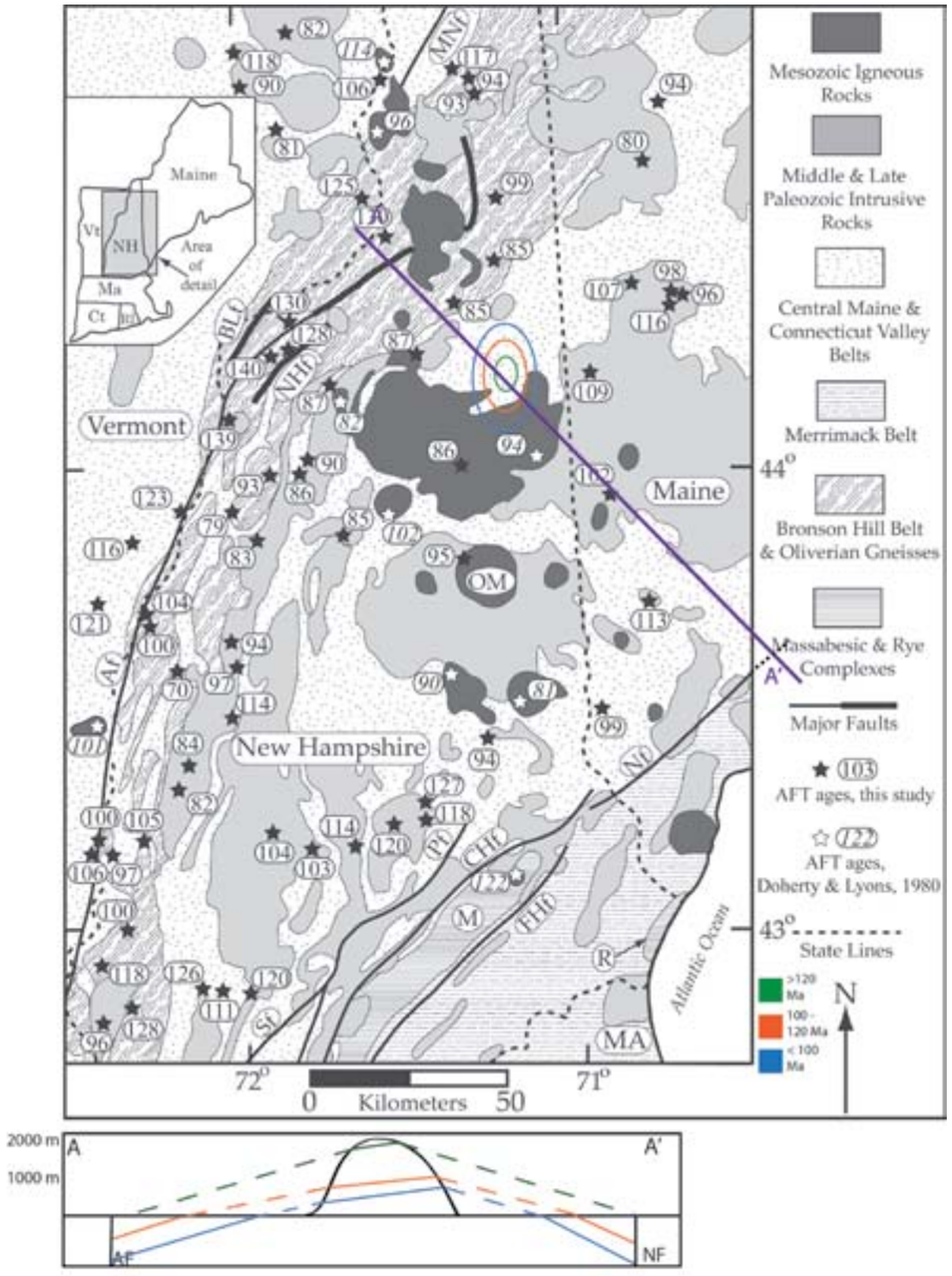


Figure 4.13: Local Age Gradation of AFT Ages across New Hampshire and proposed western tilt and regional arc (modified from Roden-Tice et. al, 2009)



*4.4bRegion Tilt Trend Westward*

Adding in data from Roden-Tice and Tice (2005), this tilt extends further westward into the Adirondacks (Figure 4.14). Excluding age discrepancies on either side of Adirondack faults, AFT ages increase westward. Again assuming that samples were taken at low-lying elevations (presumably along riverbeds or roadways), westward-most ages past the Adirondacks correlate with high-elevation Mt. Washington samples with ages approximately 120 Ma and above. Middle elevation Mt. Washington Samples at approximately 100 to 120 Ma fall east of the oldest AFT ages right in and just east of the Adirondacks. Youngest and lowest-elevation Mt. Washington AFT ages correspond with nearby AFT ages of less than 100 Ma in neighboring Vermont.

*4.4c Region Tilt Trend Southward*

This data could further fit into a regional W-E age gradation proposed by Roden-Tice and Wintsch (2002) based on AFT and ZFT ages of southern New England, primarily in the Connecticut River Valley. In Massachusetts, AFT ages rise to the east from 106 to 146 Ma and in Connecticut from 113 to 164 Ma (Roden-Tice and Wintsch, 2002). The Bronson Hill Terrane lies just west of the Central Maine Terrane, in which Mt. Washington lies, and has elevations significantly lower (Figure 4.15).

The west- to-east gradient in the Early Cretaceous was approximately a 40 my difference. The gradient measured from the Cog Railroad to the Auto Road on Mt. Washington is 20 my at most. Roden-Tice and Wintsch (2002) proposed that a rotation to account for the lack of such tilt now was Early Cretaceous or younger in age. With the noted decrease in age gradient from west to east between the studies, it appears that the corrective rotation was occurring in the Early Cretaceous into the Late Cretaceous.

## 4.5 Faulting and Pale-drainage Systems

Roden-Tice and Wintsch (2002) attributed the initial gradation to a faulting event that occurred between 120 Ma and 60 Ma and up-threw the Bronson Hill Terrane rocks along the

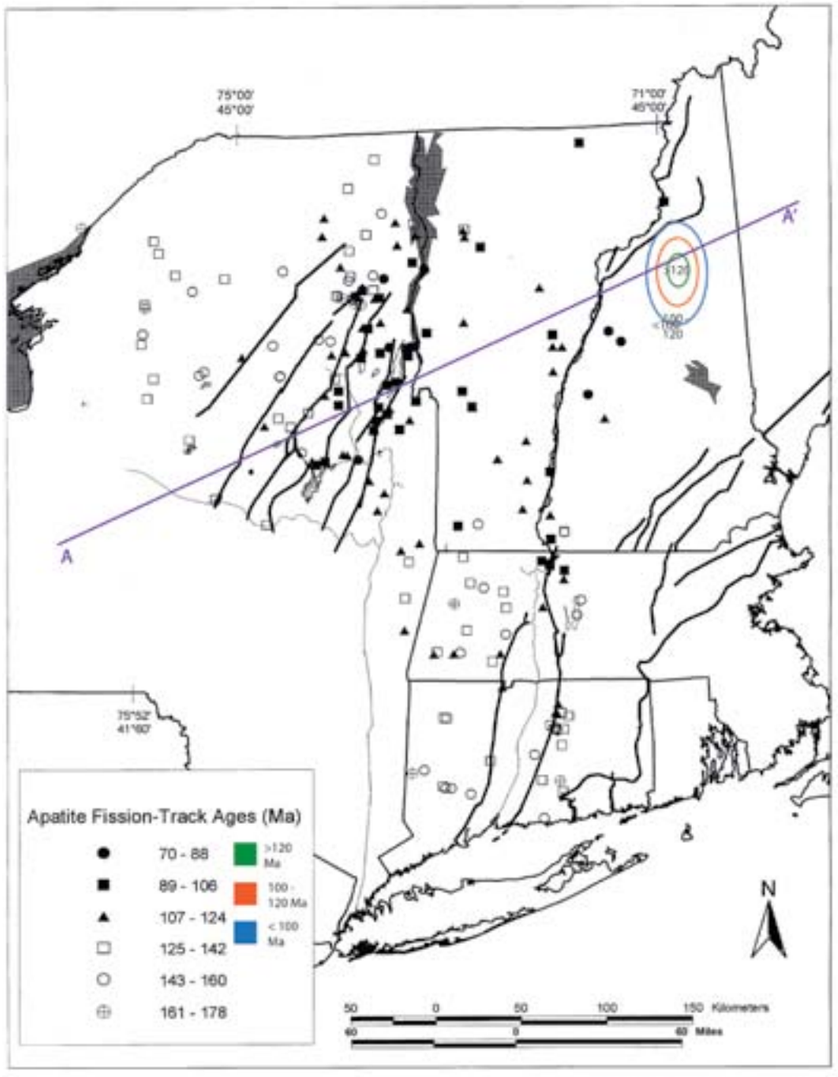


Figure 4.14: Regional Westward Tilt from AFT Ages of Cog Railroad and AFT Ages of the Adirondacks; offset from Ammonoosuc Fault is estimated (modified from Roden-Tice and Tice, 2005)



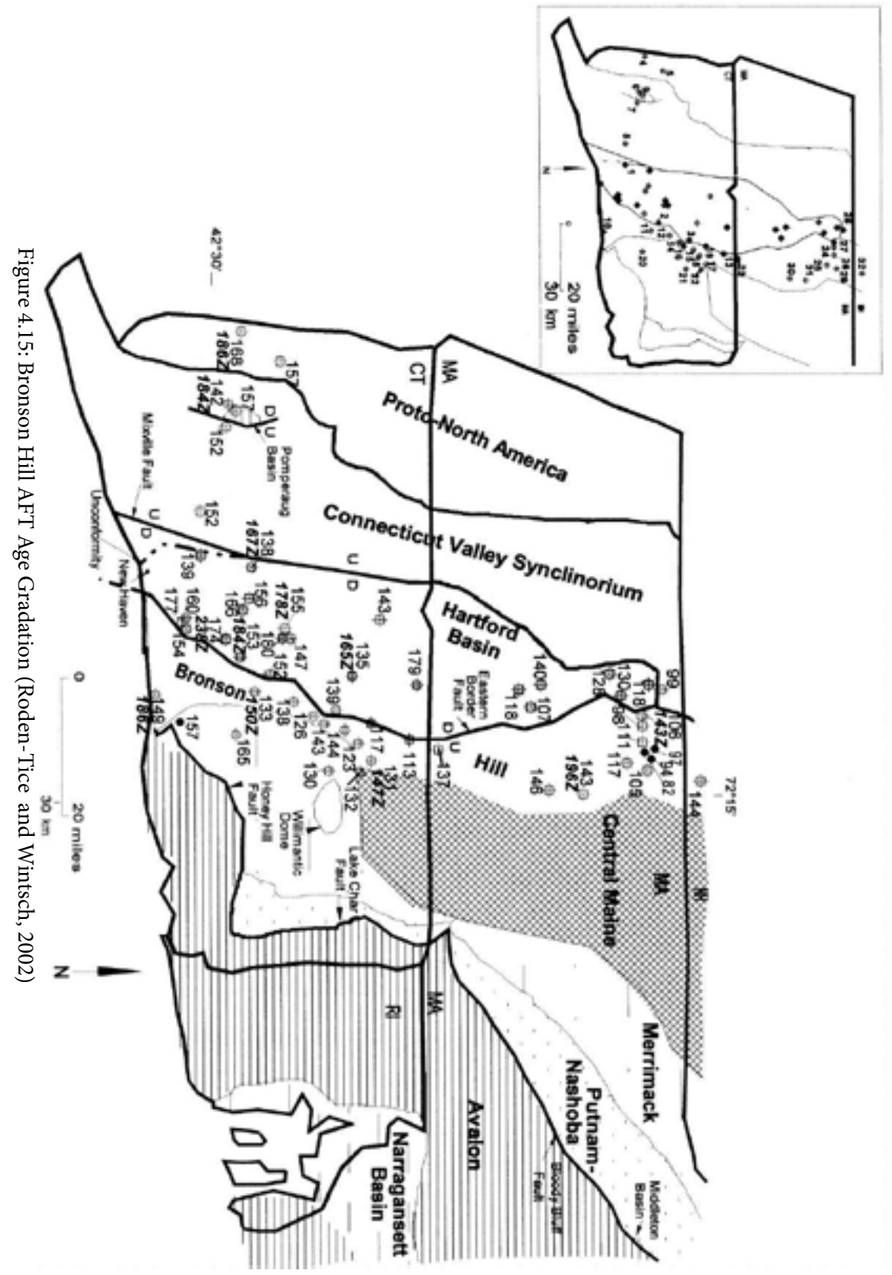


Figure 4.15: Bronson Hill AFT Age Gradation (Roden-Tice and Wintsch, 2002)

Eastern Border Fault. The Bronson Hill Faulting event was followed by the reactivation of normal faulting in the Norumbega Fault Zone east of Mt. Washington (West and Roden-Tice, 2003). Kindley (2011) asserted that the Norumbega Fault reactivation initiated the Pinkham Notch drainage, east of Mt. Washington and accounted for in the Auto Road data.

On the eastern side of Mt. Washington, this paleo-drainage system that downcut into the mountain eroded away the eastern limb as Pinkham "Mountain" became Pinkham Notch (Figure 4.16). As the same trend of differential exhumation, rapid exhumation and age gradation is apparently evident on the western side of the mountain, it is possible that a Great Gulf drainage system was acting to remove sediment on the west. Kindley (2011) suggested that the paleo-drainage system was in fact fault driven and that faults on either side of Mt. Washington would have created a graben-like structure in which the down-cutting of reactivated faults would have driven the onset of such paleo-drainage system.

As it is now evident that there was fault reactivation to the west of Mt. Washington with the Bronson Hill event, it is likely that a paleo-drainage system was, in fact, initiated to explain the period of differential exhumation on the western slope of the mountain.

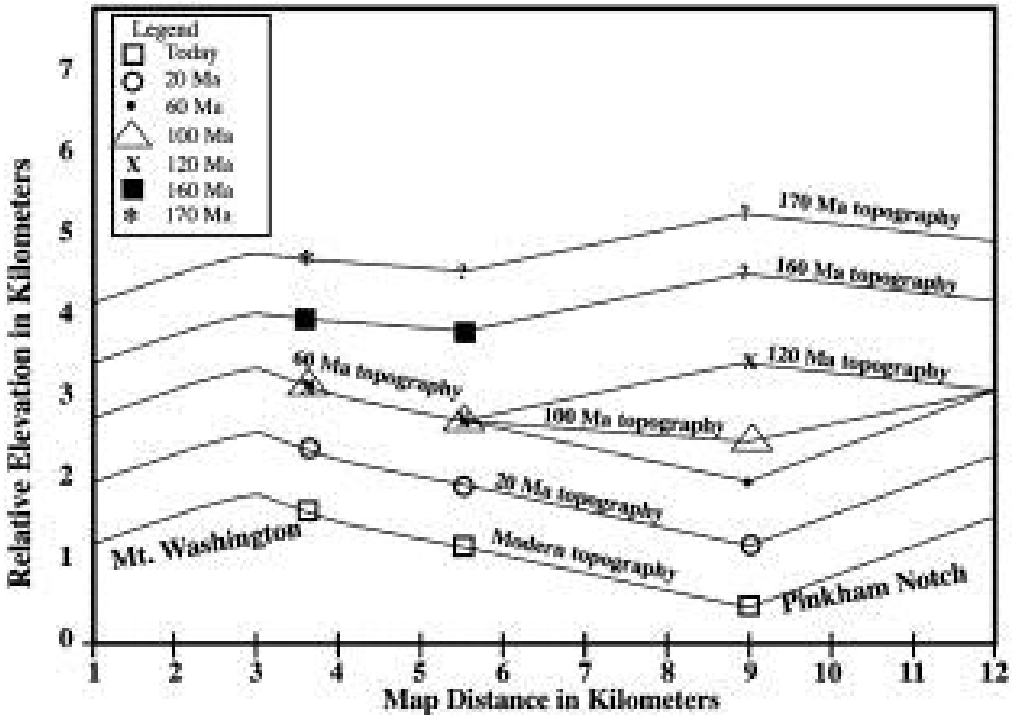


Figure 4.16: Profile of Topographic Evolution (Roden-Tice et. al, 2012)

## Conclusion

This project added thirteen AFT ages to a local data set on Mt. Washington. It further contributed to a greater regional data set of AFT ages throughout New England and upstate New York. Ages ranged from 148.0 +/- 15 Ma at 1914.1 m to 89.2 +/- 10 Ma at 539.5 m. Ages revealed a west-down tilt when compared to ages on the eastern Auto Road that fits into a greater regional west-down tilt when compared to ages from Roden-Tice et. al (2009) throughout New Hampshire and Roden-Tice and Tice (2005) into the Adirondacks.

Mt. Washington Cog Railroad ages themselves revealed a period of rapid exhumation from approximately 125 to 80 Ma that is synchronous with magmatic events. These events include the Peri-Atlantic Alkaline Pulse, formation of the Monteregian Hills and New England-Quebec Igneous Province and the intrusion of alkalic dikes proximal to Mt. Washington documented by Kindley (2011) and Gardner (2010). Local asthenospheric upwelling is thought to have reactivated zones of crustal weakness and, along with the onset of paleo-drainage systems, contributed to this period of rapid exhumation.

While Mt. Washington provided the ideal location for this study given the topographic variation, other mountains in the Presidential Range of New Hampshire provide significant enough topographic relief to collect AFT ages by change in elevation. This would provide further insight to the local extent of trends on Mt. Washington.

With the archived samples from both the Auto Road and Cog Railroad, zircon fission track ages could be analyzed. Zircon has a closure temperature of 200°C as composed to apatite at 100°C. This would extend the cooling history further back in the Mesozoic. This would add further texture to the Mesozoic cooling history of the Presidential Range region.

## Appendix A: AFT Counting Data and Grain Sheets





CR2A-BA

==========ZetaAge Program v. 4.7 (Brandon 4/11/97)==========

DATE/TIME: 01-19-2012/10:40:30 FILENAME: C:\FTDATA\CR2A-BA.TXT

Cr-2A Littleton schisht 6190' Mt Washington PL060-4 B Anderson 1/19/12

>>NEW PARAMETERS--ZETA METHOD<<

EFFECTIVE TRACK DENSITY FOR FLUENCE MONITOR (tracks/cm^2): 3.855E+06

RELATIVE ERROR (%): 2.53

EFFECTIVE URANIUM CONTENT OF MONITOR (ppm): 39.20

ZETA FACTOR AND STANDARD ERROR (yr cm^2): 101.60 7.20

SIZE OF COUNTER SQUARE (cm^2): 3.600E-07

------ GRAIN AGES IN ORIGINAL ORDER ------

| Grain no. | RhoS (cm^-2) | (Ns) | RhoI (cm^-2) | (Ni) | Squares | U+/-2s | | Grain Age | Age (Ma) --95% CI-- | |
|---|---|---|---|---|---|---|---|---|---|---|
| 1 | 1.02E+06 | 33 | 1.45E+06 | 47 | 90 | 15 | 4 | 136.3 | 84.5 | 216.2 |
| 2 | 1.42E+06 | 46 | 1.57E+06 | 51 | 90 | 16 | 5 | 174.3 | 114.6 | 263.9 |
| 3 | 2.22E+06 | 40 | 2.22E+06 | 40 | 50 | 23 | 7 | 192.9 | 121.6 | 305.1 |
| 4 | 1.55E+06 | 39 | 1.98E+06 | 50 | 70 | 20 | 6 | 151.1 | 96.8 | 233.4 |
| 5 | 1.28E+06 | 37 | 1.70E+06 | 49 | 80 | 17 | 5 | 146.4 | 92.9 | 228.0 |
| 6 | 1.25E+06 | 45 | 2.08E+06 | 75 | 100 | 21 | 5 | 116.6 | 78.6 | 170.7 |
| 7 | 1.39E+06 | 50 | 1.89E+06 | 68 | 100 | 19 | 5 | 142.5 | 96.8 | 207.9 |
| 8 | 1.32E+06 | 38 | 1.77E+06 | 51 | 80 | 18 | 5 | 144.5 | 92.3 | 223.3 |
| 9 | 2.22E+06 | 80 | 3.19E+06 | 115 | 100 | 32 | 6 | 134.9 | 99.9 | 181.1 |
| 10 | 1.11E+06 | 40 | 1.78E+06 | 64 | 100 | 18 | 5 | 121.4 | 79.6 | 182.6 |
| 11 | 2.50E+06 | 63 | 2.54E+06 | 64 | 70 | 26 | 7 | 190.0 | 132.1 | 272.6 |
| 12 | 1.42E+06 | 51 | 1.94E+06 | 70 | 100 | 20 | 5 | 141.3 | 96.4 | 205.1 |
| 13 | 2.54E+06 | 64 | 3.06E+06 | 77 | 70 | 31 | 7 | 160.8 | 113.5 | 226.6 |
| 14 | 1.98E+06 | 50 | 2.38E+06 | 60 | 70 | 24 | 6 | 161.3 | 108.5 | 238.0 |
| 15 | 1.25E+06 | 27 | 1.71E+06 | 37 | 60 | 17 | 6 | 141.6 | 82.9 | 237.4 |
| 16 | 1.71E+06 | 37 | 2.82E+06 | 61 | 60 | 29 | 7 | 117.9 | 76.1 | 179.7 |
| 17 | 1.11E+06 | 40 | 1.75E+06 | 63 | 100 | 18 | 5 | 123.4 | 80.7 | 185.7 |
| 18 | 1.39E+06 | 45 | 1.73E+06 | 56 | 90 | 18 | 5 | 155.6 | 102.7 | 233.8 |
| 19 | 1.92E+06 | 69 | 2.22E+06 | 80 | 100 | 23 | 5 | 166.8 | 119.0 | 232.8 |
| 20 | 2.62E+06 | 51 | 3.29E+06 | 64 | 54 | 33 | 9 | 154.3 | 104.6 | 225.9 |


==========ZetaAge Program v. 4.7 (Brandon 4/11/97)==========

DATE/TIME: 01-19-2012/10:40:30 FILENAME: C:\FTDATA\CR2A-BA.TXT

Cr-2A Littleton schisht 6190' Mt Washington PL060-4 B Anderson 1/19/12


Number of grains = 20

------ GRAIN AGES ORDERED WITH INCREASING AGE ------

| Grain no. | RhoS (cm^-2) | (Ns) | RhoI (cm^-2) | (Ni) | Grain age (Ma) Age | --95% CI-- | | P(x2) (%) | Sum age (Ma) Age | --95% CI-- | |
|---|---|---|---|---|---|---|---|---|---|---|---|
| 6 | 1.25E+06 | 45 | 2.08E+06 | 75 | 116.6 | 78.6 | 170.7 | 100.0 | 116.6 | 78.6 | 170.7 |
| 16 | 1.71E+06 | 37 | 2.82E+06 | 61 | 117.9 | 76.1 | 179.7 | 96.9 | 117.1 | 87.7 | 155.3 |
| 10 | 1.11E+06 | 40 | 1.78E+06 | 64 | 121.4 | 79.6 | 182.6 | 98.9 | 118.1 | 90.5 | 154.1 |
| 17 | 1.11E+06 | 40 | 1.75E+06 | 63 | 123.4 | 80.7 | 185.7 | 99.7 | 119.3 | 93.6 | 152.0 |
| 9 | 2.22E+06 | 80 | 3.19E+06 | 115 | 134.9 | 99.9 | 181.1 | 97.1 | 124.0 | 99.9 | 154.0 |
| 1 | 1.02E+06 | 33 | 1.45E+06 | 47 | 136.3 | 84.5 | 216.2 | 98.4 | 125.4 | 101.6 | 154.5 |
| 12 | 1.42E+06 | 51 | 1.94E+06 | 70 | 141.3 | 96.4 | 205.1 | 98.5 | 127.6 | 104.3 | 156.0 |
| 15 | 1.25E+06 | 27 | 1.71E+06 | 37 | 141.6 | 82.9 | 237.4 | 99.2 | 128.5 | 105.5 | 156.6 |
| 7 | 1.39E+06 | 50 | 1.89E+06 | 68 | 142.5 | 96.8 | 207.9 | 99.4 | 130.1 | 107.3 | 157.6 |
| 8 | 1.32E+06 | 38 | 1.77E+06 | 51 | 144.5 | 92.3 | 223.3 | 99.6 | 131.2 | 108.6 | 158.4 |
| 5 | 1.28E+06 | 37 | 1.70E+06 | 49 | 146.4 | 92.9 | 228.0 | 99.7 | 132.3 | 109.8 | 159.3 |
| 4 | 1.55E+06 | 39 | 1.98E+06 | 50 | 151.1 | 96.8 | 233.4 | 99.7 | 133.5 | 111.1 | 160.3 |
| 20 | 2.62E+06 | 51 | 3.29E+06 | 64 | 154.3 | 104.6 | 225.9 | 99.7 | 135.1 | 112.8 | 161.8 |
| 18 | 1.39E+06 | 45 | 1.73E+06 | 56 | 155.6 | 102.7 | 233.8 | 99.7 | 136.5 | 114.2 | 163.0 |
| 13 | 2.54E+06 | 64 | 3.06E+06 | 77 | 160.8 | 113.5 | 226.6 | 99.5 | 138.4 | 116.1 | 165.0 |
| 14 | 1.98E+06 | 50 | 2.38E+06 | 60 | 161.3 | 108.5 | 238.0 | 99.4 | 139.8 | 117.5 | 166.3 |
| 19 | 1.92E+06 | 69 | 2.22E+06 | 80 | 166.8 | 119.0 | 232.8 | 99.0 | 141.8 | 119.4 | 168.3 |
| 2 | 1.42E+06 | 46 | 1.57E+06 | 51 | 174.3 | 114.6 | 263.9 | 98.7 | 143.2 | 120.8 | 169.8 |
| 11 | 2.50E+06 | 63 | 2.54E+06 | 64 | 190.0 | 132.1 | 272.6 | 95.5 | 145.7 | 123.1 | 172.5 |
| 3 | 2.22E+06 | 40 | 2.22E+06 | 40 | 192.9 | 121.6 | 305.1 | 93.3 | 147.2 | 124.4 | 174.2 |
| POOL | 1.61E+06 | 945 | 2.11E+06 | 1242 | | | | 93.3 | 147.2 | 124.4 | 174.2 |
| 95% CI BRACKETS FOR POOLED AGE (Ma): | | | | | | | | | | -22.8 | +26.9 |

Page 1

**Figure A.1: CR2 Data Sheet 1**

CR2A-BA

CENTRAL AGE (Ma): AGE DISPERSION = 0.00 147.3 124.5 174.2
95% CI BRACKETS FOR MEAN AGE (Ma): -22.8 +26.9

CHI^2 AGE (number & percentage of grains: 20, 100%) 147.2 124.4 174.2
95% CI BRACKETS FOR CHI^2 AGE (Ma): -22.8 +26.9

MEAN URANIUM CONCENTRATION +/- 2 SE (ppm): 21.5 1.6

```
▯==========ZetaAge Program v. 4.7  (Brandon 4/11/97)==========
DATE/TIME: 01-19-2012/10:40:30 FILENAME: C:\FTDATA\CR2A-BA.TXT
Cr-2A Littleton schisht 6190' Mt Washington PL060-4 B Anderson 1/19/12
Kernel factor =  .6  (Ratio of kernel window size to standard error)
Number of grains =  20
PEAKS IN PROBABILITY DISTRIBUTION
The modes in the distribution are found by inspecting the derivatives
of the probability density as a function of Z.
Probability distribution uses grain-only standard errors.
Total probability mass integrates to N (= number of grains).
Probability density is given as grains per delta Z=0.1.
At 50 Ma, delta Z=0.1 is equivalent to a time interval of 5 m.y.

Total range for grain ages =   116.94 to   192.90 Ma

First Search: peaks with zero first derivatives.

       AGE      PROBABILTY DENSITY AT PEAK     EST. N
       (Ma)           (grains/DZ=0.1)          (grains)

Second search: find minima in the second derivative of the Gaussian
probability density function.

       AGE      PROBABILTY DENSITY AT PEAK     EST. N
       (Ma)           (grains/DZ=0.1)          (grains)
     156.09                4.049                20.13
▯==========ZetaAge Program v. 4.7  (Brandon 4/11/97)==========
DATE/TIME: 01-19-2012/10:40:30 FILENAME: C:\FTDATA\CR2A-BA.TXT
Cr-2A Littleton schisht 6190' Mt Washington PL060-4 B Anderson 1/19/12
Kernel factor =  .6  (Ratio of kernel window size to standard error)
Number of grains =  20     Barwidth (Z units) =  .1
Histogram shown by asterisks and probability distribution by circles.

                PROBABILITY DENSITY (GRAINS PER DELTA Z=0.1)
          0         1         2         3         4         5         6
 AGE   COUNT|.........|.........|.........|.........|.........|.........|
  67.8 -   0 :o
  74.8 -   0 :o
  82.7 -   0 :o
  91.3 -   0 :o
 100.8 -   0 :    o
 111.3 -   1 :**********   o
 122.9 -   3 :*****************************o***
 135.7 -   4 :****************************************o**
 149.8 -   6 :**************************************************o*****************
 165.4 -   3 :*****************************     o
 182.6 -   2 :******************** o
 201.5 -   1 :*********o
 222.3 -   0 :   o
 245.2 -   0 :o
▯
```



**Figure A.2: CR2 Data Sheet 2**



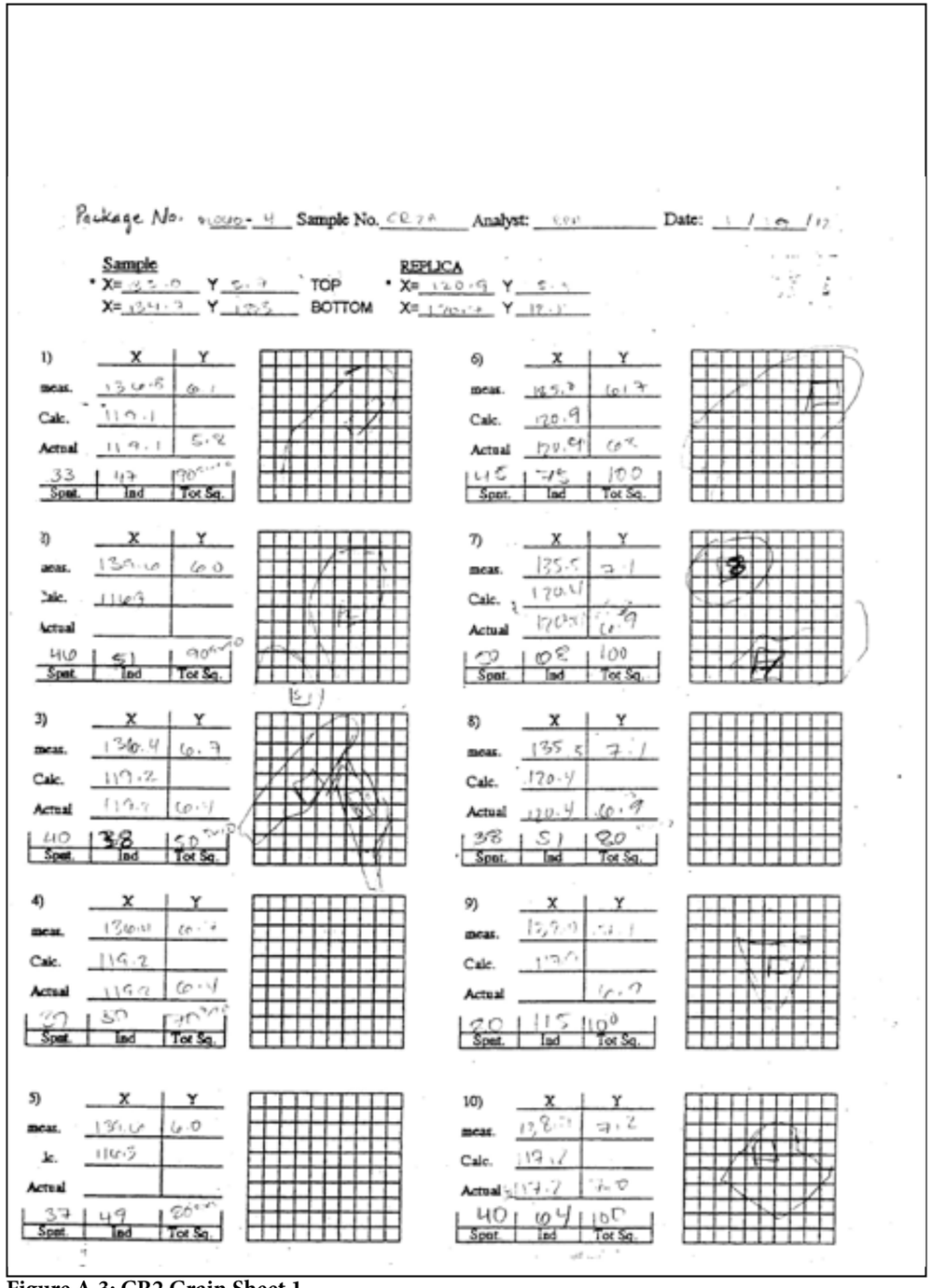


**Figure A.3: CR2 Grain Sheet 1**

Irradiation

Irradiation Num. PL060-4 Sample No. CR-2B Analyst: EEP Date: 1/17/12

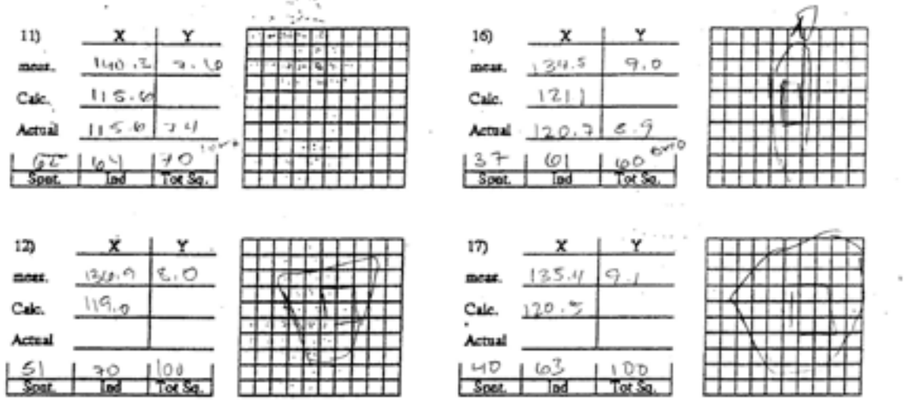


**Figure A.4: CR2 Grain Sheet 1**



```
                                                CR6B-BA
==================ZetaAge Program v. 4.7  (Brandon 4/11/97)==================
DATE/TIME: 01-17-2012/16:33:03 FILENAME: C:\FTDATA\CR6B-BA.TXT
Cr-6b  Littleton Schist 4567' Mt Washington PL060-13 B Anderson 1/17/12

>>NEW PARAMETERS--ZETA METHOD<<
EFFECTIVE TRACK DENSITY FOR FLUENCE MONITOR (tracks/cm^2):      4.190E+06
                                                RELATIVE ERROR (%):      2.29
                                EFFECTIVE URANIUM CONTENT OF MONITOR (ppm):     39.20
                                  ZETA FACTOR AND STANDARD ERROR (yr cm^2):    101.60      7.20
                                                SIZE OF COUNTER SQUARE (cm^2):      3.600E-07
------ GRAIN AGES IN ORIGINAL ORDER ------
Grain    RhoS      (Ns)     RhoI      (Ni)  Squares  U+/-2s      Grain  Age (Ma)
 no.    (cm^-2)             (cm^-2)                              Age     --95% CI--
   1  1.45E+06 (  47)  2.50E+06 (  81)   90      23    5  122.5   83.6  177.2
   2  1.11E+06 (  28)  1.87E+06 (  47)   70      17    5  125.9   75.9  204.0
   3  1.44E+06 (  26)  1.89E+06 (  34)   50      18    6  161.0   92.9  274.2
   4  1.11E+06 (  40)  2.00E+06 (  72)  100      19    4  117.4   77.6  174.6
   5  1.50E+06 (  26)  2.31E+06 (  40)   48      22    7  137.2   80.4  228.8
   6  1.67E+06 (  30)  2.28E+06 (  41)   50      21    7  154.2   93.0  251.3
   7  2.14E+06 (  77)  3.67E+06 ( 132)  100      34    6  123.1   91.5  164.3
   8  1.89E+06 (  34)  3.22E+06 (  58)   50      30    8  123.9   78.6  191.5
   9  1.11E+06 (  24)  2.59E+06 (  56)   60      24    7   91.0   53.7  148.3
  10  2.22E+06 (  48)  2.73E+06 (  59)   60      26    7  171.0  114.5  253.6
  11  1.72E+06 (  62)  3.17E+06 ( 114)  100      30    6  114.9   82.8  157.7
  12  2.01E+06 (  58)  3.85E+06 ( 111)   80      36    7  110.4   78.8  152.9
  13  1.87E+06 (  47)  2.86E+06 (  72)   70      27    6  137.7   93.2  200.9
  14  1.39E+06 (  30)  2.31E+06 (  50)   60      22    6  126.8   77.8  202.2
==================ZetaAge Program v. 4.7  (Brandon 4/11/97)==================
DATE/TIME: 01-17-2012/16:33:03 FILENAME: C:\FTDATA\CR6B-BA.TXT
Cr-6b  Littleton Schist 4567' Mt Washington PL060-13 B Anderson 1/17/12
Number of grains =  14
------ GRAIN AGES ORDERED WITH INCREASING AGE ------
Grain  RhoS      (Ns)     RhoI      (Ni)     Grain age (Ma)  P(X2)      Sum age (Ma)
 no.  (cm^-2)             (cm^-2)           Age    --95% CI--  (%)     Age    --95% CI--
  9  1.11E+06 (  24)  2.59E+06 (  56)   91.0   53.7  148.3  100.0    91.0   53.7  148.3
 12  2.01E+06 (  58)  3.85E+06 ( 111)  110.4   78.8  152.9   49.8   103.8   78.5  136.1
 11  1.72E+06 (  62)  3.17E+06 ( 114)  114.9   82.8  157.7   70.7   108.0   84.4  138.1
  4  1.11E+06 (  40)  2.00E+06 (  72)  117.4   77.6  174.6   84.4   109.9   87.4  138.0
  1  1.45E+06 (  47)  2.50E+06 (  81)  122.5   83.6  177.2   89.5   112.2   90.5  139.0
  7  2.14E+06 (  77)  3.67E+06 ( 132)  123.1   91.5  164.3   92.5   114.7   93.9  140.0
  8  1.89E+06 (  34)  3.22E+06 (  58)  123.9   78.6  191.5   96.0   115.5   95.1  140.4
  2  1.11E+06 (  28)  1.87E+06 (  47)  125.9   75.9  204.0   97.8   116.2   95.9  140.8
 14  1.39E+06 (  30)  2.31E+06 (  50)  126.8   77.8  202.2   98.8   116.9   96.8  141.2
  5  1.50E+06 (  26)  2.31E+06 (  40)  137.2   80.4  228.8   99.0   118.0   97.9  142.1
 13  1.87E+06 (  47)  2.86E+06 (  72)  137.7   93.2  200.9   98.8   119.7   99.7  143.6
  6  1.67E+06 (  30)  2.28E+06 (  41)  154.2   93.0  251.3   97.7   121.3  101.2  145.3
  3  1.44E+06 (  26)  1.89E+06 (  34)  161.0   92.9  274.2   96.2   122.8  102.6  146.9
 10  2.22E+06 (  48)  2.73E+06 (  59)  171.0  114.5  253.6   86.8   125.7  105.3  150.0

POOL 1.62E+06(  577) 2.72E+06(  967)                           86.8   125.7  105.3  150.0
95% CI BRACKETS FOR POOLED AGE (Ma):                                        -20.4  +24.3

CENTRAL AGE (Ma):          AGE DISPERSION =  0.00                          125.8  105.3  150.1
95% CI BRACKETS FOR MEAN AGE (Ma):                                          -20.4  +24.3

CHI^2 AGE (number & percentage of grains:  14, 100%)                       125.7  105.3  150.0
95% CI BRACKETS FOR CHI^2 AGE (Ma):                                         -20.4  +24.3

MEAN URANIUM CONCENTRATION +/- 2 SE (ppm):   25.4    2.0
==================ZetaAge Program v. 4.7  (Brandon 4/11/97)==================
DATE/TIME: 01-17-2012/16:33:03 FILENAME: C:\FTDATA\CR6B-BA.TXT
Cr-6b  Littleton Schist 4567' Mt Washington PL060-13 B Anderson 1/17/12
Kernel factor =  .6  (Ratio of kernel window size to standard error)

                                        Page 1
```

**Figure A.5: CR6 Data Sheet 1**

```
Number of grains =  14
PEAKS IN PROBABILITY DISTRIBUTION
The modes in the distribution are found by inspecting the derivatives
of the probability density as a function of Z.
Probability distribution uses grain-only standard errors.
Total probability mass integrates to N (= number of grains).
Probability density is given as grains per delta Z=0.1.
At 50 Ma, delta Z=0.1 is equivalent to a time interval of 5 m.y.

Total range for grain ages =    91.63 to   171.19 Ma

First Search: peaks with zero first derivatives.

       AGE      PROBABILTY DENSITY AT PEAK     EST. N
       (Ma)           (grains/DZ=0.1)          (grains)

Second search: find minima in the second derivative of the Gaussian
probability density function.

       AGE      PROBABILTY DENSITY AT PEAK     EST. N
       (Ma)           (grains/DZ=0.1)          (grains)
      79.58              0.176                   0.92
     120.32              3.118                  16.38
     172.45              0.979                   5.14
▯==================ZetaAge Program v. 4.7  (Brandon 4/11/97)==================
DATE/TIME: 01-17-2012/16:33:03 FILENAME: C:\FTDATA\CR6B-BA.TXT
Cr-6b  Littleton Schist 4567' Mt Washington PL060-13 B Anderson 1/17/12
Kernel factor =  .6  (Ratio of kernel window size to standard error)
Number of grains =  14     Barwidth (Z units) =  .1
Histogram shown by asterisks and probability distribution by circles.
                    PROBABILITY DENSITY (GRAINS PER DELTA Z=0.1)
                    0         1         2         3         4         5         6
 AGE    COUNT|.........|.........|.........|.........|.........|.........|
  55.5 -    0 :o
  61.3 -    0 :o
  67.8 -    0 :o
  74.8 -    0 :o
  82.7 -    0 : o
  91.3 -    1 :***o******
 100.8 -    0 :         o
 111.3 -    2 :********************   o
 122.9 -    6 :****************************o****************************
 135.7 -    2 :********************    o
 149.8 -    1 :**********       o
 165.4 -    2 :***********o********
 182.6 -    0 :          o
 201.5 -    0 :   o
 222.3 -    0 :o
▯
```

Page 2

**Figure A.6: CR6 Data Sheet 2**



Package No. PL060-13 Sample No. CR-6B Analyst: BAB Date: 1/17/12

Sample
* X=1311.0 Y=7.1 TOP
X=1252.3 Y=10.2 BOTTOM

REPLICA
* X=1341.9 Y=10.2
X=1317.4 Y=9.6

| | X | Y |
|---|---|---|
| 1) meas. | 1397 | 7.1 |
| Calc. | 120.4 | |
| Actual | 120.2 | 7.5 |
| | 47 Spot. | 81 Ind. | 80 Tot Sq. |

| | X | Y |
|---|---|---|
| 6) meas. | 1341.9 | 10.2 |
| Calc. | 117.0 | |
| Actual | 117.4 | 9.6 |
| | 30 Spot. | 41 Ind. | 50 (100) Tot Sq. |

| | X | Y |
|---|---|---|
| 2) meas. | 1320 | 5.1 |
| Calc. | 121.9 | |
| Actual | 121.7 | 8.0 |
| | 28 Spot. | 47 Ind. | 70 Tot Sq. |

| | X | Y |
|---|---|---|
| 7) meas. | 1360.9 | 11.41 |
| Calc. | 123.1 | |
| Actual | 122.8 | 10.7 |
| | 77 Spot. | 132 Ind. | 100 Tot Sq. |

| | X | Y |
|---|---|---|
| 3) meas. | 1324.4 | 8.1 |
| Calc. | 121.5 | |
| Actual | 121.3 | 7.5 |
| | 26 Spot. | 24 Ind. | 50 (91) Tot Sq. |

| | X | Y |
|---|---|---|
| 8) meas. | 1387.5 | 11.9 |
| Calc. | 122.6 | |
| Actual | 122.1 | 11.0 |
| | 34 Spot. | 58 Ind. | 50 (97) Tot Sq. |

| | X | Y |
|---|---|---|
| 4) meas. | 1327.5 | 9.1 |
| Calc. | 121.4 | |
| Actual | 121.1 | 8.2 |
| | 40 Spot. | 42 Ind. | 100 Tot Sq. |

| | X | Y |
|---|---|---|
| 9) meas. | 1421.2 | 135.5 |
| Calc. | 129.9 | |
| Actual | 129.0 | 12.2 |
| | 24 Spot. | 56 Ind. | 66 (100) Tot Sq. |

| | X | Y |
|---|---|---|
| 5) meas. | 1382.3 | 10.3 |
| Calc. | 121.4 | |
| Actual | 121.0 | 9.5 |
| | 26 Spot. | 40 Ind. | 48 (100) Tot Sq. |

| | X | Y |
|---|---|---|
| 10) meas. | 1430 | 13.3 |
| Calc. | 116.9 | |
| Actual | 116.3 | 10.9 |
| | 48 Spot. | 59 Ind. | 60 (100) Tot Sq. |

**Figure A.7: CR2 Grain Sheet 1**

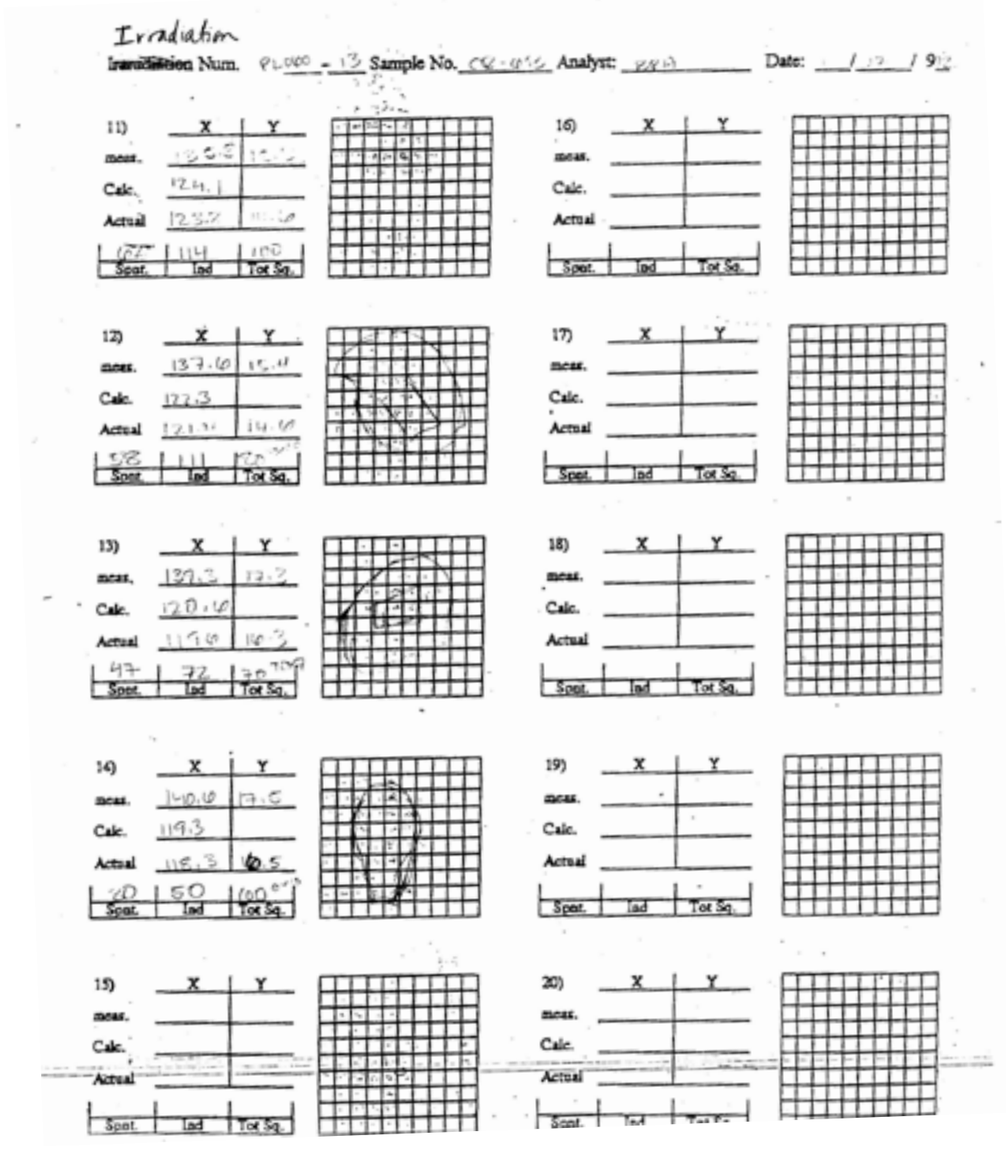


**Figure A.8: CR2 Grain Sheet 2**



```
                                                    CR7A-BA
==================ZetaAge Program v. 4.7  (Brandon 4/11/97)==================
DATE/TIME: 01-17-2012/16:32:30 FILENAME: C:\FTDATA\CR7A-BA.TXT
Cr-7a  Littleton Schist 4350' Mt Washington PL060-14 B Anderson 1/17/12

>>NEW PARAMETERS--ZETA METHOD<<
EFFECTIVE TRACK DENSITY FOR FLUENCE MONITOR (tracks/cm^2):      4.227E+06
                                                RELATIVE ERROR (%):      2.38
                    EFFECTIVE URANIUM CONTENT OF MONITOR (ppm):     39.20
                      ZETA FACTOR AND STANDARD ERROR (yr cm^2):   101.60      7.20
                                    SIZE OF COUNTER SQUARE (cm^2):    3.600E-07
------ GRAIN AGES IN ORIGINAL ORDER ------
Grain    RhoS      (Ns)     RhoI      (Ni)  Squares  U+/-2s      Grain  Age (Ma)
 no.     (cm^-2)           (cm^-2)                              Age    --95% CI--
   1  9.92E+05 (  15) 2.31E+06 (  35)   42     21   7    91.9   46.4  171.0
   2  7.50E+05 (  27) 2.56E+06 (  92)  100     24   5    63.0   39.2   97.2
   3  1.39E+06 (  15) 3.06E+06 (  33)   30     28  10    97.5   49.0  182.6
   4  1.43E+06 (  36) 3.17E+06 (  80)   70     29   7    96.2   62.8  143.8
   5  1.19E+06 (  30) 1.67E+06 (  42)   70     15   5   151.8   91.8  246.8
   6  1.39E+06 (  20) 1.74E+06 (  25)   40     16   6   169.8   89.7  315.0
   7  7.87E+05 (  17) 1.34E+06 (  29)   60     12   5   125.2   64.4  233.1
   8  2.61E+06 (  94) 5.08E+06 ( 183)  100     47   7   109.1   82.0  145.2
   9  1.91E+06 (  33) 3.24E+06 (  56)   48     30   8   125.6   79.0  195.5
  10  1.91E+06 (  33) 3.24E+06 (  56)   48     30   8   125.6   79.0  195.5
  11  1.67E+06 (  30) 2.39E+06 (  43)   50     22   7   148.3   89.9  240.5
  12  1.57E+06 (  34) 2.41E+06 (  52)   60     22   6   139.1   87.5  217.4
  13  8.33E+05 (  18) 1.39E+06 (  30)   60     13   5   128.0   67.2  234.9
  14  1.11E+06 (  20) 1.67E+06 (  30)   50     15   6   142.0   76.4  256.0
  15  1.70E+06 (  49) 2.15E+06 (  62)   80     20   5   167.6  112.9  246.9
  16  1.08E+06 (  39) 1.86E+06 (  67)  100     17   4   124.0   81.2  186.1
  17  9.88E+05 (  32) 1.45E+06 (  47)   90     13   4   144.8   89.4  230.5
  18  1.02E+06 (  11) 1.67E+06 (  18)   30     15   7   130.6   55.7  287.4
  19  1.69E+06 (  61) 4.67E+06 ( 168)  100     43   7    77.6   56.7  104.7
  20  1.16E+06 (  25) 1.94E+06 (  42)   60     18   6   126.9   74.1  211.7
==================ZetaAge Program v. 4.7  (Brandon 4/11/97)==================
DATE/TIME: 01-17-2012/16:32:30 FILENAME: C:\FTDATA\CR7A-BA.TXT
Cr-7a  Littleton Schist 4350' Mt Washington PL060-14 B Anderson 1/17/12
Number of grains =  20
------ GRAIN AGES ORDERED WITH INCREASING AGE ------
Grain    RhoS      (Ns)     RhoI      (Ni)    Grain age (Ma)   P(X2)      Sum age (Ma)
 no.     (cm^-2)           (cm^-2)           Age    --95% CI--   (%)    Age    --95% CI--
   2  7.50E+05 (  27) 2.56E+06 (  92)  63.0   39.2   97.2  100.0   63.0   39.2   97.2
  19  1.69E+06 (  61) 4.67E+06 ( 168)  77.6   56.7  104.7   42.1   72.2   54.5   95.5
   1  9.92E+05 (  15) 2.31E+06 (  35)  91.9   46.4  171.0   56.5   74.4   57.0   97.1
   4  1.43E+06 (  36) 3.17E+06 (  80)  96.2   62.8  143.8   50.9   79.0   62.0  100.6
   3  1.39E+06 (  15) 3.06E+06 (  33)  97.5   49.0  182.6   61.1   80.5   63.6  101.7
   8  2.61E+06 (  94) 5.08E+06 ( 183) 109.1   82.0  145.2   27.1   89.4   72.7  110.0
  16  1.08E+06 (  39) 1.86E+06 (  67) 124.0   81.2  186.1   19.7   92.9   76.1  113.5
   7  7.87E+05 (  17) 1.34E+06 (  29) 125.2   64.4  233.1   22.2   94.3   77.3  114.9
  10  1.91E+06 (  33) 3.24E+06 (  56) 125.6   79.0  195.5   20.6   96.6   79.6  117.2
   9  1.91E+06 (  33) 3.24E+06 (  56) 125.6   79.0  195.5   20.5   98.6   81.5  119.2
  20  1.16E+06 (  25) 1.94E+06 (  42) 126.9   74.1  211.7   22.2  100.0   82.9  120.6
  13  8.33E+05 (  18) 1.39E+06 (  30) 128.0   67.2  234.9   25.4  101.0   83.8  121.6
  18  1.02E+06 (  11) 1.67E+06 (  18) 130.6   55.7  287.4   29.9  101.6   84.4  122.2
  12  1.57E+06 (  34) 2.41E+06 (  52) 139.1   87.5  217.4   25.7  103.6   86.3  124.4
  14  1.11E+06 (  20) 1.67E+06 (  30) 142.0   76.4  256.0   25.9  104.8   87.4  125.6
  17  9.88E+05 (  32) 1.45E+06 (  47) 144.8   89.4  230.5   22.5  106.6   89.1  127.6
  11  1.67E+06 (  30) 2.39E+06 (  43) 148.3   89.9  240.5   19.8  108.3   90.7  129.4
   5  1.19E+06 (  30) 1.67E+06 (  42) 151.8   91.8  246.8   17.2  110.0   92.2  131.2
  15  1.70E+06 (  49) 2.15E+06 (  62) 167.6  112.9  246.9    8.3  113.0   94.9  134.6
   6  1.39E+06 (  20) 1.74E+06 (  25) 169.8   89.7  315.0    7.3  114.2   96.0  135.9

POOL 1.38E+06(  639) 2.57E+06( 1190)                          7.3  114.2   96.0  135.9
95% CI BRACKETS FOR POOLED AGE (Ma):                                        -18.2 +21.6

                                    Page 1
```

**Figure A.9: CR7 Data Sheet 1**

CR7A-BA

```
CENTRAL AGE (Ma):          AGE DISPERSION =  0.16              117.7  97.3 142.3
95% CI BRACKETS FOR MEAN AGE (Ma):                                    -20.4 +24.6

CHI^2 AGE (number & percentage of grains:  20, 100%)           114.2  96.0 135.9
95% CI BRACKETS FOR CHI^2 AGE (Ma):                                   -18.2 +21.6

MEAN URANIUM CONCENTRATION +/- 2 SE (ppm):    23.8    1.8
□==================ZetaAge Program v. 4.7  (Brandon 4/11/97)==================
DATE/TIME: 01-17-2012/16:32:30 FILENAME: C:\FTDATA\CR7A-BA.TXT
Cr-7a  Littleton Schist 4350' Mt Washington PL060-14 B Anderson 1/17/12
Kernel factor =  .6  (Ratio of kernel window size to standard error)
Number of grains =  20
PEAKS IN PROBABILITY DISTRIBUTION
The modes in the distribution are found by inspecting the derivatives
of the probability density as a function of Z.
Probability distribution uses grain-only standard errors.
Total probability mass integrates to N (= number of grains).
Probability density is given as grains per delta Z=0.1.
At 50 Ma, delta Z=0.1 is equivalent to a time interval of 5 m.y.

Total range for grain ages =    63.52 to   170.34 Ma

First Search: peaks with zero first derivatives.

       AGE      PROBABILTY DENSITY AT PEAK     EST. N
       (Ma)           (grains/DZ=0.1)          (grains)

Second search: find minima in the second derivative of the Gaussian
probability density function.

       AGE      PROBABILTY DENSITY AT PEAK     EST. N
       (Ma)           (grains/DZ=0.1)          (grains)
      59.83                0.298                 1.86
      77.61                0.846                 5.29
     110.42                2.428                15.20
     136.83                3.049                19.08
□==================ZetaAge Program v. 4.7  (Brandon 4/11/97)==================
DATE/TIME: 01-17-2012/16:32:30 FILENAME: C:\FTDATA\CR7A-BA.TXT
Cr-7a  Littleton Schist 4350' Mt Washington PL060-14 B Anderson 1/17/12
Kernel factor =  .6  (Ratio of kernel window size to standard error)
Number of grains =  20     Barwidth (z units) =  .1
Histogram shown by asterisks and probability distribution by circles.

                PROBABILITY DENSITY (GRAINS PER DELTA Z=0.1)
            0         1         2         3         4         5         6
  AGE   COUNT|.........|.........|.........|.........|.........|.........|
  37.3 -    0 :o
  41.2 -    0 :o
  45.5 -    0 :o
  50.3 -    0 :o
  55.5 -    0 : o
  61.3 -    1 :**o*******
  67.8 -    0 :    o
  74.8 -    1 :*******o**
  82.7 -    0 :         o
  91.3 -    1 :*********o
 100.8 -    2 :***************o****
 111.3 -    1 :**********           o
 122.9 -    6 :****************************o******************************
 135.7 -    2 :********************          o
 149.8 -    4 :****************************o*************
 165.4 -    2 :********************o*
```



**Figure A.10: CR7 Data Sheet 2**



Package No. Plaeo-14 Sample No. CR-7A Analyst: KBM Date: 1 / 13 / 12

Sample: X= 123.5 Y 3.0 TOP; X= 123.7 Y 3.2 BOTTOM

REPLICA: X= 126.3 Y 10.7; X= 125.9 Y 10.1

| | X | Y |
|---|---|---|
| 1) meas. | 139.9 | 12.7 |
| Calc. | 119.9 | |
| Actual | 120.0 | 10.2 |
| Spnt. 15 | Ind 35 | Tot Sq. 112 (80%) |

| | X | Y |
|---|---|---|
| 6) meas. | 136.3 | 12.3 |
| Calc. | 123.5 | |
| Actual | 123.0 | 12.1 |
| Spnt. 20 | Ind 25 | Tot Sq. 40 (100%) |

| | X | Y |
|---|---|---|
| 2) meas. | 136.2 | 10.7 |
| Calc. | 123.9 | |
| Actual | 122.2 | 10.5 |
| Spnt. 27 | Ind 92 | Tot Sq. 100 |

| | X | Y |
|---|---|---|
| 7) meas. | 140.2 | 13.0 |
| Calc. | 119.6 | |
| Actual | 119.0 | 12.8 |
| Spnt. 17 | Ind 29 | Tot Sq. 60 (100%) |

| | X | Y |
|---|---|---|
| 3) meas. | 134.4 | 10.2 |
| Calc. | 136.2 | |
| Actual | 126.1 | 10.4 |
| Spnt. 15 | Ind 33 | Tot Sq. 30 |

| | X | Y |
|---|---|---|
| 8) meas. | 135.6 | 13.8 |
| Calc. | 124.2 | |
| Actual | 124.3 | 13.8 |
| Spnt. 94 | Ind 183 | Tot Sq. 100 |

| | X | Y |
|---|---|---|
| 4) meas. | 138.1 | 11.2 |
| Calc. | 121.7 | |
| Actual | 121.3 | 10.6 |
| Spnt. 36 | Ind 80 | Tot Sq. 40 (100%) |

| | X | Y |
|---|---|---|
| 9) meas. | 135.8 | 14.1 |
| Calc. | 124.4 | |
| Actual | 124.3 | 13.9 |
| Spnt. 33 | Ind 56 | Tot Sq. 45 (100%) |

| | X | Y |
|---|---|---|
| 5) meas. | 141.1 | 11.5 |
| Calc. | 118.7 | |
| Actual | 118.3 | 11.4 |
| Spnt. 30 | Ind 42 | Tot Sq. 70 (90%) |

| | X | Y |
|---|---|---|
| 10) meas. | 135.0 | 14.4 |
| Calc. | 124.8 | |
| Actual | 124.2 | 14.3 |
| Spnt. 30 | Ind 43 | Tot Sq. 50 (90%) |

**Figure A.11: CR7 Grain Sheet 1**

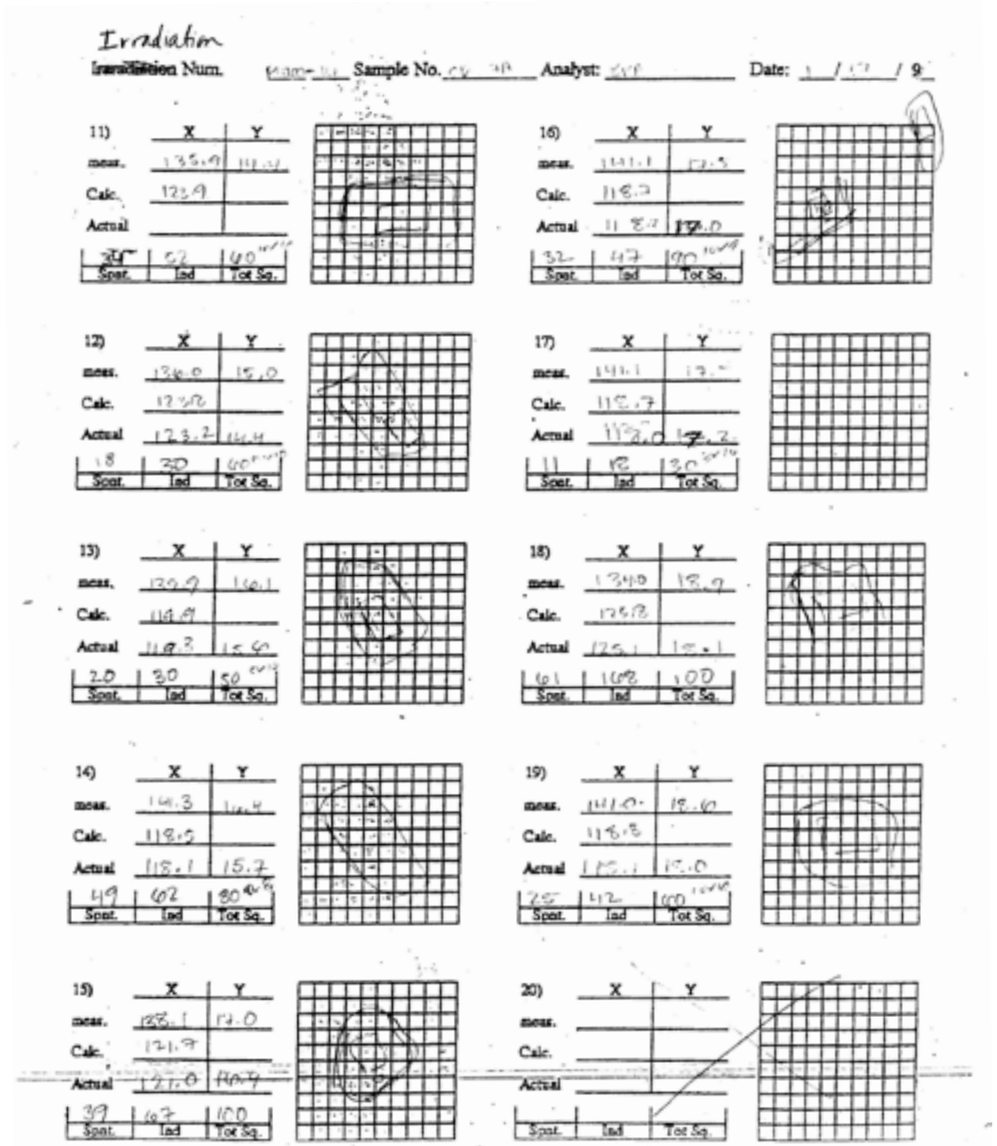


**Figure A.12: CR2 Grain Sheet 2**



```
                                                CR-11A
==================ZetaAge Program v. 4.7  (Brandon 4/11/97)==================
DATE/TIME: 01-03-2012/18:08:07 FILENAME: C:\FTDATA\CR-11A.TXT
CR-11a Rangeley schist 2765' Mt Washington PL061-6 mrt 1/3/12

>>NEW PARAMETERS--ZETA METHOD<<
EFFECTIVE TRACK DENSITY FOR FLUENCE MONITOR (tracks/cm^2):      4.042E+06
                                                RELATIVE ERROR (%):      2.25
                                EFFECTIVE URANIUM CONTENT OF MONITOR (ppm):      39.20
                                  ZETA FACTOR AND STANDARD ERROR (yr cm^2):      98.40      1.70
                                                SIZE OF COUNTER SQUARE (cm^2):      3.600E-07
------ GRAIN AGES IN ORIGINAL ORDER ------
Grain    RhoS      (Ns)     RhoI      (Ni)  Squares  U+/-2s      Grain  Age (Ma)
 no.   (cm^-2)             (cm^-2)                              Age    --95% CI--
   1 4.00E+06 (  72) 7.17E+06 ( 129)   50     70  13   109.7   82.0  146.6
   2 1.39E+06 (  30) 3.24E+06 (  70)   60     31   8    84.9   53.3  131.5
   3 5.56E+05 (  16) 1.87E+06 (  54)   80     18   5    59.1   31.3  103.9
   4 3.05E+06 (  79) 5.98E+06 ( 155)   72     58  10   100.3   76.3  131.8
   5 2.06E+06 (  74) 4.47E+06 ( 161)  100     43   7    90.5   68.5  119.5
   6 1.87E+06 (  47) 2.82E+06 (  71)   70     27   7   130.5   88.2  190.7
   7 6.94E+05 (  10) 1.32E+06 (  19)   40     13   6   104.6   43.3  232.7
   8 3.11E+06 (  56) 6.83E+06 ( 123)   50     66  12    90.1   64.3  124.4
   9 2.47E+06 (  89) 4.75E+06 ( 171)  100     46   7   102.4   79.0  132.7
  10 3.00E+06 (  54) 7.50E+06 ( 135)   50     73  13    79.2   56.5  109.3
  11 2.70E+06 (  68) 5.83E+06 ( 147)   70     57  10    91.1   68.2  121.7
  12 4.31E+06 (  93) 8.98E+06 ( 194)   60     87  13    94.4   73.5  121.3
  13 1.08E+06 (  39) 2.17E+06 (  78)  100     21   5    98.9   65.4  146.6
  14 6.11E+05 (  22) 1.75E+06 (  63)  100     17   4    69.4   40.5  113.7
  15 1.94E+06 (  28) 4.72E+06 (  68)   40     46  11    81.7   50.4  128.0
  16 1.56E+06 (  56) 2.81E+06 ( 101)  100     27   6   109.5   77.4  153.0
  17 2.08E+06 (  60) 3.96E+06 ( 114)   80     38   7   104.0   74.6  143.2
  18 2.55E+06 (  55) 5.69E+06 ( 123)   60     55  10    88.5   63.0  122.4
  19 2.78E+06 (  60) 4.40E+06 (  95)   60     43   9   124.5   88.5  173.6
  20 6.67E+05 (  24) 1.14E+06 (  41)  100     11   3   115.7   66.8  194.7
1==================ZetaAge Program v. 4.7  (Brandon 4/11/97)==================
DATE/TIME: 01-03-2012/18:08:07 FILENAME: C:\FTDATA\CR-11A.TXT
CR-11a Rangeley schist 2765' Mt Washington PL061-6 mrt 1/3/12
Number of grains =  20
------ GRAIN AGES ORDERED WITH INCREASING AGE ------
Grain  RhoS      (Ns)     RhoI      (Ni)    Grain age (Ma)   P(X2)      Sum age (Ma)
 no.   (cm^-2)             (cm^-2)          Age   --95% CI--  (%)     Age   --95% CI--
   3 5.56E+05 (  16) 1.87E+06 (  54)  59.1  31.3 103.9 100.0   59.1  31.3 103.9
  14 6.11E+05 (  22) 1.75E+06 (  63)  69.4  40.5 113.7  66.3   64.5  43.3  93.5
  10 3.00E+06 (  54) 7.50E+06 ( 135)  79.2  56.5 109.3  63.9   72.1  56.5  91.9
  15 1.94E+06 (  28) 4.72E+06 (  68)  81.7  50.4 128.0  77.6   74.1  59.7  91.8
   2 1.39E+06 (  30) 3.24E+06 (  70)  84.9  53.3 131.5  84.5   76.0  62.5  92.3
  18 2.55E+06 (  55) 5.69E+06 ( 123)  88.5  63.0 122.4  84.8   78.9  66.6  93.5
   8 3.11E+06 (  56) 6.83E+06 ( 123)  90.1  64.3 124.4  86.8   81.0  69.5  94.5
   5 2.06E+06 (  74) 4.47E+06 ( 161)  90.5  68.5 119.5  88.6   83.0  72.3  95.3
  11 2.70E+06 (  68) 5.83E+06 ( 147)  91.1  68.2 121.7  91.2   84.3  74.1  95.8
  12 4.31E+06 (  93) 8.98E+06 ( 194)  94.4  73.5 121.3  91.2   86.1  76.4  96.9
  13 1.08E+06 (  39) 2.17E+06 (  78)  98.9  65.4 146.6  92.5   86.9  77.4  97.5
   4 3.05E+06 (  79) 5.98E+06 ( 155) 100.3  76.3 131.8  91.0   88.4  79.2  98.6
   9 2.47E+06 (  89) 4.75E+06 ( 171) 102.4  79.0 132.7  88.7   90.0  81.1  99.9
  17 2.08E+06 (  60) 3.96E+06 ( 114) 104.0  74.6 143.2  88.9   90.9  82.2 100.7
   7 6.94E+05 (  10) 1.32E+06 (  19) 104.6  43.3 232.7  92.0   91.1  82.3 100.8
  16 1.56E+06 (  56) 2.81E+06 ( 101) 109.5  77.4 153.0  90.3   92.1  83.5 101.7
   1 4.00E+06 (  72) 7.17E+06 ( 129) 109.7  82.0 146.6  87.7   93.3  84.8 102.8
  20 6.67E+05 (  24) 1.14E+06 (  41) 115.7  66.8 194.7  88.3   93.8  85.3 103.2
  19 2.78E+06 (  60) 4.40E+06 (  95) 124.5  88.5 173.6  77.8   95.2  86.7 104.6
   6 1.87E+06 (  47) 2.82E+06 (  71) 130.5  88.2 190.7  66.4   96.4  87.9 105.7

POOL 1.99E+06( 1032) 4.07E+06( 2112)                    66.4   96.4  87.9 105.7
95% CI BRACKETS FOR POOLED AGE (Ma):                                  -8.5  +9.3

                                Page 1
```

**Figure A.13: CR11 Data Sheet 1**

CR-11A

CENTRAL AGE (Ma): AGE DISPERSION = 0.00 96.4 87.9 105.8
95% CI BRACKETS FOR MEAN AGE (Ma): -8.5 +9.3

CHI^2 AGE (number & percentage of grains: 20, 100%) 96.4 87.9 105.7
95% CI BRACKETS FOR CHI^2 AGE (Ma): -8.5 +9.3

MEAN URANIUM CONCENTRATION +/- 2 SE (ppm): 39.5 2.5

□==========ZetaAge Program V. 4.7 (Brandon 4/11/97)==========
DATE/TIME: 01-03-2012/18:08:07 FILENAME: C:\FTDATA\CR-11A.TXT
CR-11a Rangeley schist 2765' Mt Washington PL061-6 mrt 1/3/12
Kernel factor = .6 (Ratio of kernel window size to standard error)
Number of grains = 20
PEAKS IN PROBABILITY DISTRIBUTION
The modes in the distribution are found by inspecting the derivatives
of the probability density as a function of Z.
Probability distribution uses grain-only standard errors.
Total probability mass integrates to N (= number of grains).
Probability density is given as grains per delta Z=0.1.
At 50 Ma, delta Z=0.1 is equivalent to a time interval of 5 m.y.

Total range for grain ages = 59.92 to 130.76 Ma

First Search: peaks with zero first derivatives.

| AGE (Ma) | PROBABILTY DENSITY AT PEAK (grains/DZ=0.1) | EST. N (grains) |
|---|---|---|
| 56.20 | 0.318 | 1.59 |
| 95.33 | 4.310 | 21.50 |
| 132.71 | 1.117 | 5.57 |

□==========ZetaAge Program v. 4.7 (Brandon 4/11/97)==========
DATE/TIME: 01-03-2012/18:08:07 FILENAME: C:\FTDATA\CR-11A.TXT
CR-11a Rangeley schist 2765' Mt Washington PL061-6 mrt 1/3/12
Kernel factor = .6 (Ratio of kernel window size to standard error)
Number of grains = 20 Barwidth (Z units) = .1
Histogram shown by asterisks and probability distribution by circles.

PROBABILITY DENSITY (GRAINS PER DELTA Z=0.1)

```
          0         .83       1.67       2.5       3.33       4.17       5
 AGE   COUNT|.........|.........|.........|.........|.........|.........|
 37.3 -   0 :o
 41.2 -   0 :o
 45.5 -   0 :o
 50.3 -   0 : o
 55.5 -   0 :   o
 61.3 -   1 :*****o******
 67.8 -   1 :********o***
 74.8 -   0 :             o
 82.7 -   3 :*******************************o*****
 91.3 -   5 :**************************************************o************
100.8 -   4 :************************************************** o
111.3 -   4 :***********************************o**************
122.9 -   1 :************          o
135.7 -   1 :**********o*
149.8 -   0 :    o
165.4 -   0 :o
```



**Figure A.14: CR11 Data Sheet 2**



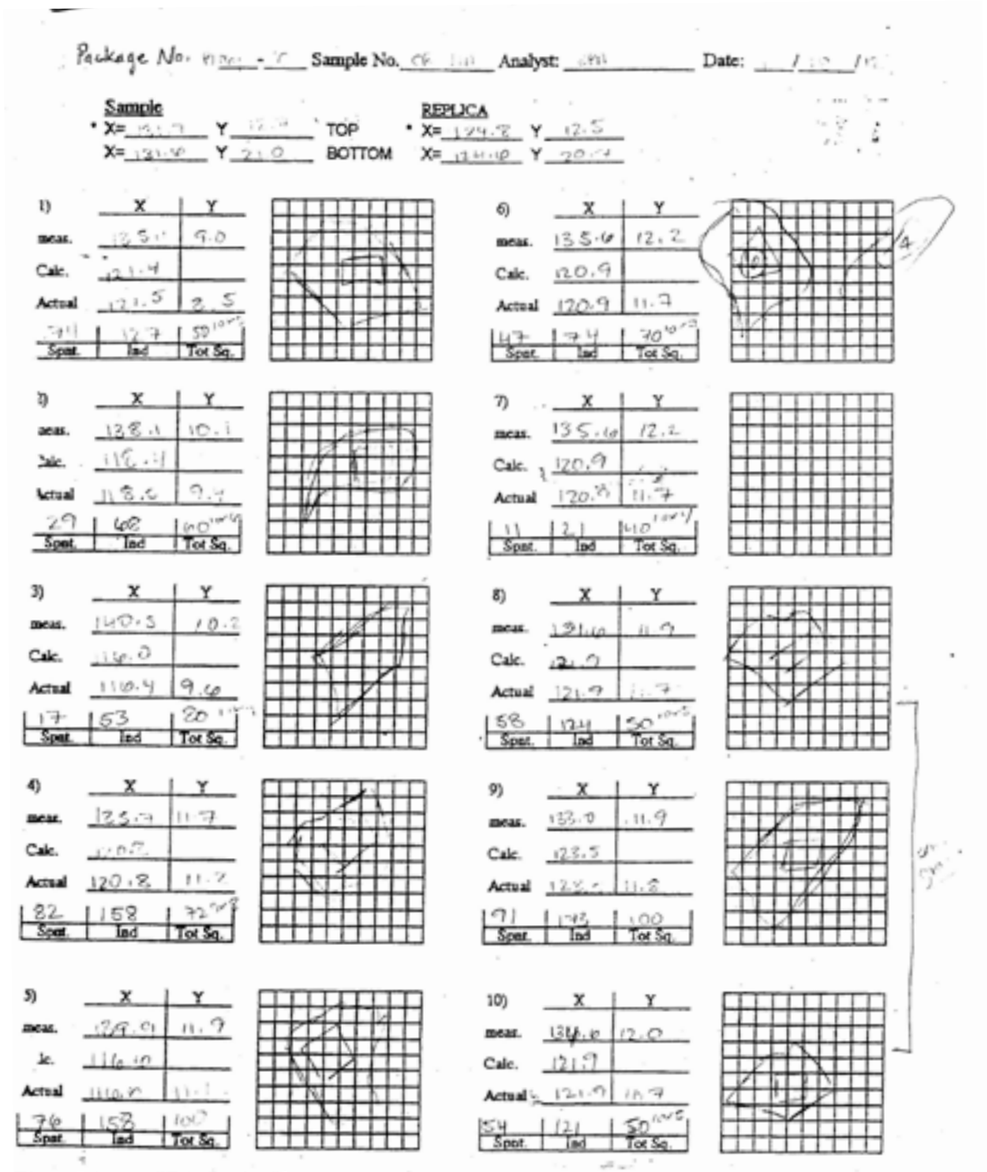


**Figure A.15: CR2 Grain Sheet 1**

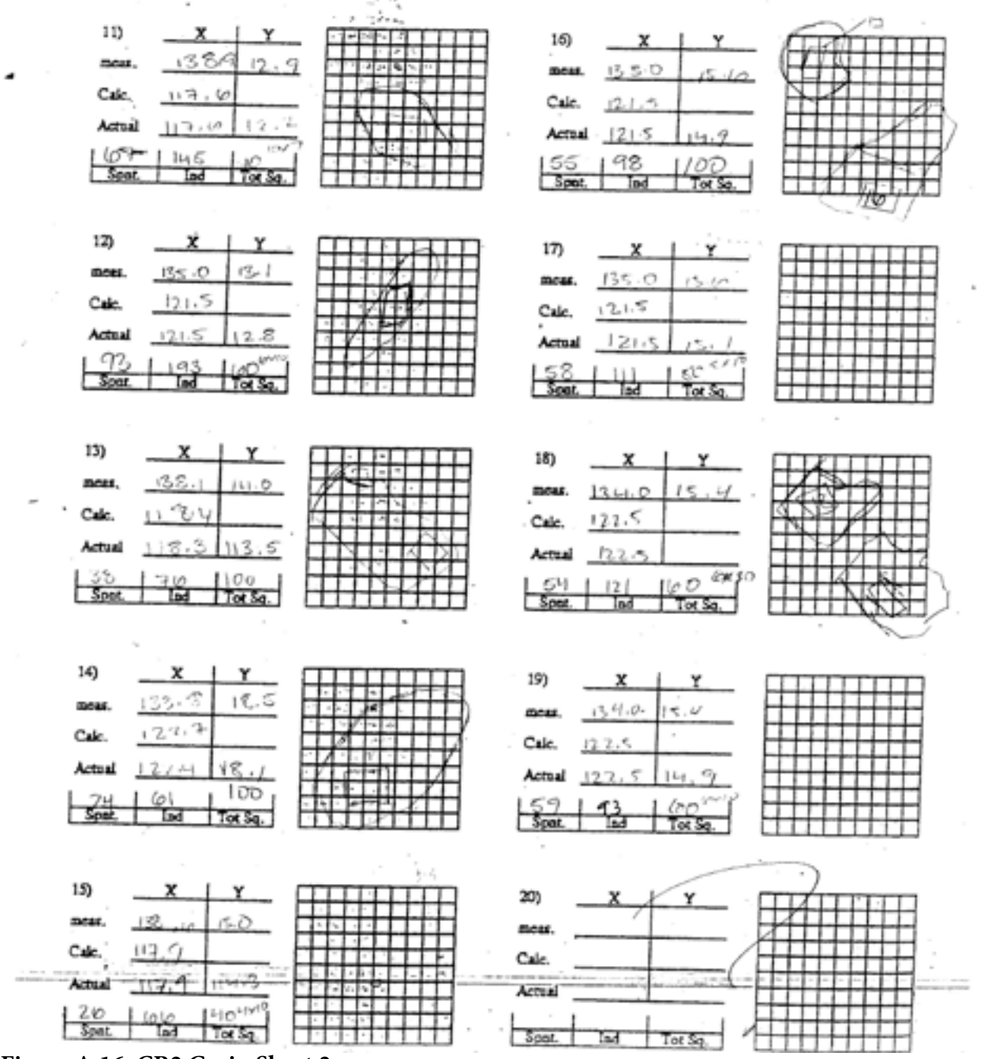


**Figure A.16: CR2 Grain Sheet 2**



```
                                    CR13A-BA
==================ZetaAge Program v. 4.7  (Brandon 4/11/97)==================
DATE/TIME: 01-18-2012/15:18:18 FILENAME: C:\FTDATA\CR13A-BA.TXT
Cr-13A Bretton Woods Granite 1770' Mt Washington PL061-10 B Anderson 1/18/12

>>NEW PARAMETERS--ZETA METHOD<<
EFFECTIVE TRACK DENSITY FOR FLUENCE MONITOR (tracks/cm^2):      3.986E+06
                                                RELATIVE ERROR (%):      2.16
                        EFFECTIVE URANIUM CONTENT OF MONITOR (ppm):     39.20
                          ZETA FACTOR AND STANDARD ERROR (yr cm^2):    101.60     7.20
                                       SIZE OF COUNTER SQUARE (cm^2):  3.600E-07
------ GRAIN AGES IN ORIGINAL ORDER ------
Grain    RhoS      (Ns)     RhoI      (Ni)  Squares  U+/-2s      Grain  Age (Ma)
 no.    (cm^-2)            (cm^-2)                              Age     --95% CI--
   1  1.00E+06 (  36) 1.44E+06 (  52)  100    14   4   138.9   88.2  215.4
   2  2.08E+06 (  60) 3.99E+06 ( 115)   80    39   8   104.9   75.3  144.4
   3  3.06E+06 (  55) 5.00E+06 (  90)   50    49  11   122.7   86.0  173.1
   4  1.90E+06 (  41) 5.05E+06 ( 109)   60    50  10    75.9   51.5  109.4
   5  1.67E+06 (  60) 4.86E+06 ( 175)  100    48   8    69.2   50.5   93.2
   6  6.94E+05 (  25) 2.22E+06 (  80)  100    22   5    63.3   38.5   99.7
   7  1.84E+06 (  53) 3.92E+06 ( 113)   80    39   7    94.4   66.7  131.8
   8  1.19E+06 (  30) 2.38E+06 (  60)   70    23   6   100.7   62.6  157.9
   9  4.17E+05 (  15) 8.61E+05 (  31)  100     8   3    97.8   48.9  184.7
  10  2.08E+06 (  45) 3.33E+06 (  72)   60    33   8   125.5   84.4  184.0
  11  9.52E+05 (  24) 3.97E+06 ( 100)   70    39   8    48.7   29.6   76.2
  12  1.28E+06 (  23) 3.00E+06 (  54)   50    30   8    86.0   50.2  141.7
  13  1.19E+06 (  43) 3.53E+06 ( 127)  100    35   6    68.4   47.0   97.1
  14  1.81E+06 (  52) 5.24E+06 ( 151)   80    52   9    69.5   49.5   95.7
  15  2.58E+06 (  65) 6.75E+06 ( 170)   70    66  11    77.1   56.8  103.1
  16  1.17E+06 (  42) 3.36E+06 ( 121)  100    33   6    70.1   48.0  100.1
  17  1.33E+06 (  48) 2.22E+06 (  80)  100    22   5   120.5   82.4  174.0
  18  1.61E+06 (  58) 3.11E+06 ( 112)  100    31   6   104.2   74.4  144.1
  19  2.50E+06 (  90) 5.06E+06 ( 182)  100    50   8    99.1   74.3  132.3
  20  1.11E+06 (  40) 2.22E+06 (  80)  100    22   5   100.7   67.0  148.5
0==================ZetaAge Program v. 4.7  (Brandon 4/11/97)==================
DATE/TIME: 01-18-2012/15:18:18 FILENAME: C:\FTDATA\CR13A-BA.TXT
Cr-13A Bretton Woods Granite 1770' Mt Washington PL061-10 B Anderson 1/18/12
Number of grains =  20
------ GRAIN AGES ORDERED WITH INCREASING AGE ------
Grain  RhoS      (Ns)     RhoI      (Ni)    Grain age (Ma)  P(X2)      Sum age (Ma)
 no.  (cm^-2)            (cm^-2)           Age  --95% CI--  (%)     Age  --95% CI--
  11  9.52E+05 (  24) 3.97E+06 ( 100)  48.7  29.6  76.2 100.0   48.7  29.6  76.2
   6  6.94E+05 (  25) 2.22E+06 (  80)  63.3  38.5  99.7  41.3   55.0  39.1  75.8
  13  1.19E+06 (  43) 3.53E+06 ( 127)  68.4  47.0  97.1  47.9   60.3  45.9  79.2
   5  1.67E+06 (  60) 4.86E+06 ( 175)  69.2  50.5  93.2  58.7   63.5  50.4  80.0
  14  1.81E+06 (  52) 5.24E+06 ( 151)  69.5  49.5  95.7  71.2   64.9  52.4  80.3
  16  1.17E+06 (  42) 3.36E+06 ( 121)  70.1  48.0 100.1  81.2   65.7  53.6  80.5
   4  1.90E+06 (  41) 5.05E+06 ( 109)  75.9  51.5 109.4  83.8   67.0  55.0  81.5
  15  2.58E+06 (  65) 6.75E+06 ( 170)  77.1  56.8 103.1  83.7   68.6  56.8  82.8
  12  1.28E+06 (  23) 3.00E+06 (  54)  86.0  50.2 141.7  83.7   69.5  57.7  83.6
   7  1.84E+06 (  53) 3.92E+06 ( 113)  94.4  66.7 131.8  61.8   71.8  59.9  86.1
   9  4.17E+05 (  15) 8.61E+05 (  31)  97.8  48.9 184.7  62.2   72.4  60.5  86.7
  19  2.50E+06 (  90) 5.06E+06 ( 182)  99.1  74.3 132.3  28.9   75.9  63.7  90.4
  20  1.11E+06 (  40) 2.22E+06 (  80) 100.7  67.0 148.5  24.4   77.2  64.9  91.8
   8  1.19E+06 (  30) 2.38E+06 (  60) 100.7  62.6 157.9  23.8   78.1  65.8  92.8
  18  1.61E+06 (  58) 3.11E+06 ( 112) 104.2  74.4 144.1  16.5   79.9  67.4  94.6
   2  2.08E+06 (  60) 3.99E+06 ( 115) 104.9  75.3 144.4  12.0   81.5  68.9  96.4
  17  1.33E+06 (  48) 2.22E+06 (  80) 120.5  82.4 174.0   5.7   83.2  70.4  98.2
   3  3.06E+06 (  55) 5.00E+06 (  90) 122.7  86.0 173.1   2.3   85.0  72.0 100.2
  10  2.08E+06 (  45) 3.33E+06 (  72) 125.5  84.4 184.0   1.1   86.4  73.3 101.9
   1  1.00E+06 (  36) 1.44E+06 (  52) 138.9  88.2 215.4   0.4   87.7  74.5 103.3

POOL 1.51E+06(  905) 3.45E+06( 2074)                       0.4   87.7  74.5 103.3
95% CI BRACKETS FOR POOLED AGE (Ma):                                    -13.3 +15.6

                                    Page 1
```

**Figure A.17: CR13 Data Sheet 1**

CR13A-BA

CENTRAL AGE (Ma): AGE DISPERSION = 0.17 88.7 73.9 106.3
95% CI BRACKETS FOR MEAN AGE (Ma): -14.7 +17.6

CHI^2 AGE (number & percentage of grains: 19, 95%) 86.4 73.3 101.9
95% CI BRACKETS FOR CHI^2 AGE (Ma): -13.1 +15.4

MEAN URANIUM CONCENTRATION +/- 2 SE (ppm): 33.9 2.1

```
▯==========ZetaAge Program v. 4.7 (Brandon 4/11/97)==========
DATE/TIME: 01-18-2012/15:18:18 FILENAME: C:\FTDATA\CR13A-BA.TXT
Cr-13A Bretton Woods Granite 1770' Mt Washington PL061-10 B Anderson 1/18/12
Kernel factor = .6 (Ratio of kernel window size to standard error)
Number of grains = 20
PEAKS IN PROBABILITY DISTRIBUTION
The modes in the distribution are found by inspecting the derivatives
of the probability density as a function of Z.
Probability distribution uses grain-only standard errors.
Total probability mass integrates to N (= number of grains).
Probability density is given as grains per delta Z=0.1.
At 50 Ma, delta Z=0.1 is equivalent to a time interval of 5 m.y.

Total range for grain ages = 49.17 to 139.25 Ma

First Search: peaks with zero first derivatives.

      AGE      PROBABILTY DENSITY AT PEAK     EST. N
      (Ma)           (grains/DZ=0.1)          (grains)

Second search: find minima in the second derivative of the Gaussian
probability density function.

      AGE      PROBABILTY DENSITY AT PEAK     EST. N
      (Ma)           (grains/DZ=0.1)          (grains)
     47.39                0.312                 1.52
     70.68                2.527                12.27
    100.66                2.848                13.83
    127.24                1.603                 7.78
▯==========ZetaAge Program v. 4.7 (Brandon 4/11/97)==========
DATE/TIME: 01-18-2012/15:18:18 FILENAME: C:\FTDATA\CR13A-BA.TXT
Cr-13A Bretton Woods Granite 1770' Mt Washington PL061-10 B Anderson 1/18/12
Kernel factor = .6 (Ratio of kernel window size to standard error)
Number of grains = 20 Barwidth (Z units) = .1
Histogram shown by asterisks and probability distribution by circles.

                PROBABILITY DENSITY (GRAINS PER DELTA Z=0.1)
                0         1         2         3         4         5         6
 AGE    COUNT|.........|.........|.........|.........|.........|.........|
  30.5 -   0 :o
  33.7 -   0 :o
  37.3 -   0 :o
  41.2 -   0 :o
  45.5 -   0 :  o
  50.3 -   1 :***o******
  55.5 -   0 :     o
  61.3 -   1 :********** o
  67.8 -   4 :**********************o****************
  74.8 -   2 :********************    o
  82.7 -   1 :**********         o
  91.3 -   1 :**********              o
 100.8 -   6 :****************************o******************************
 111.3 -   0 :                           o
 122.9 -   3 :******************o************
 135.7 -   1 :**********o
```



**Figure A.18: CR13 Data Sheet 2**



Package No. 9201-10 Sample No. CR-13A Analyst: BPA Date: 11/5/12

Sample
* X= 129.4 Y 5.7 TOP
X= 129.2 Y 13.5 BOTTOM

REPLICA
* X= 132.5 Y 5.5
X= 132.1 Y 14.2

1)
| | X | Y |
|---|---|---|
| meas. | 131.3 | 6.4 |
| Calc. | 121.60 | |
| Actual | | |

30 | 62 | 100
Spnt. | Ind | Tot Sq.

6)
| | X | Y |
|---|---|---|
| meas. | 120.2 | 7.1 |
| Calc. | 122.9 | |
| Actual | 122.1 | 7.5 |

25 | 80 | 100
Spnt. | Ind | Tot Sq.

2)
| | X | Y |
|---|---|---|
| meas. | 136.3 | 4.3 |
| Calc. | 116.10 | |
| Actual | 116.4 | 6.8 |

60 | 145 | 50 (x10)
Spnt. | Ind | Tot Sq.

7)
| | X | Y |
|---|---|---|
| meas. | 132.5 | 8.2 |
| Calc. | 120.4 | |
| Actual | 120.3 | 7.8 |

63 | 113 | 50 (x10)
Spnt. | Ind | Tot Sq.

3)
| | X | Y |
|---|---|---|
| meas. | 135.0 | 7.1 |
| Calc. | 117.60 | |
| Actual | 117.5 | 7.6 |

55 | 90 | 50
Spnt. | Ind | Tot Sq.

8)
| | X | Y |
|---|---|---|
| meas. | 133.8 | 8.3 |
| Calc. | 119.1 | |
| Actual | | |

30 | 60 | 20 (x10)
Spnt. | Ind | Tot Sq.

4)
| | X | Y |
|---|---|---|
| meas. | 124.5 | 7.6 |
| Calc. | 118.4 | |
| Actual | 113.1 | 6.0 |

41 | 109 | (x10)
Spnt. | Ind | Tot Sq.

9)
| | X | Y |
|---|---|---|
| meas. | 136.0 | 8.2 |
| Calc. | 116 | |
| Actual | | |

15 | 31 | 100
Spnt. | Ind | Tot Sq.

5)
| | X | Y |
|---|---|---|
| meas. | 136.4 | 7.1 |
| lc. | 121.5 | |
| Actual | | |

60 | 175 | 100
Spnt. | Ind | Tot Sq.

10)
| | X | Y |
|---|---|---|
| meas. | | |
| Calc. | | |
| Actual | | |

45 | 72 | 100 (x10)
Spnt. | Ind | Tot Sq.

**Figure A.19: CR13 Grain Sheet 1**

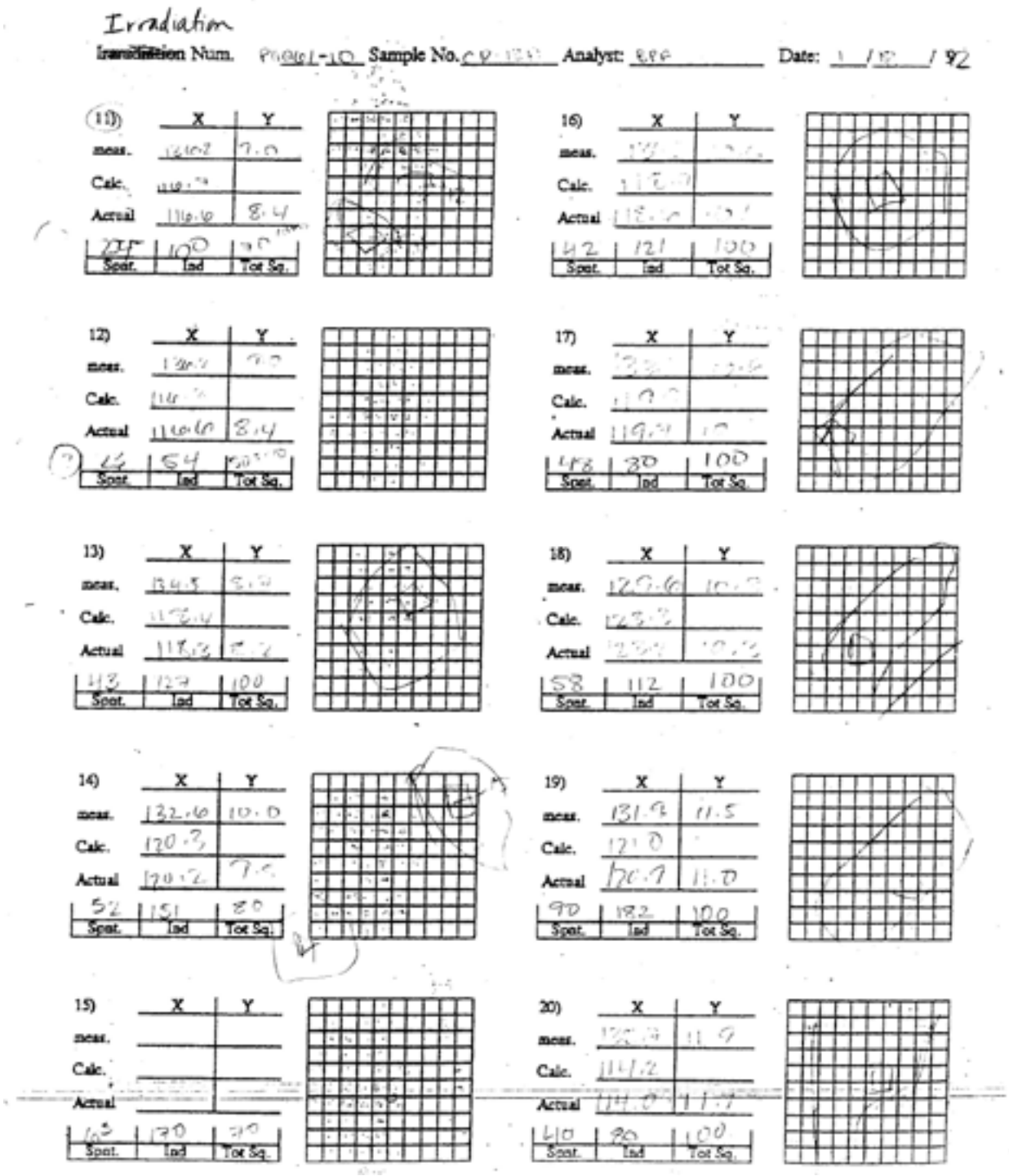


**Figure A.20: CR13 Grain Sheet 2**

## References


Bosch, F., Goresey, A.E., Martin, B., Povh, B., Nobling, R., Schwalm, D., Traxel, K., 1978, The proton microprobe: a powerful tool for nondestructive trace element analysis: Science, New Series, V. 199, N. 4330, p. 765-768.

Carlson, W.D., Donelick, R.A., Ketcham, R.A., 1999, Variability of apatite fission-track annealing kinetics: I. Experimental results; American Mineralogists, V. 84, p. 1213-1223.

Doherty, J.T., Lyons, J.B., 1980. Mesozoic erosion rates in northern New England. Geological Society of America Bulletin 91, 16–20

Eusden, J.D., 1996, Bedrock geology of the Presidential Range, New Hampshire: Harvard University : Cambridge, MA, United States, United States.

Eusden, J.D., 2010. The Presidential Range: Its Geologic History and Plate Tectonics. Durand Press, Lyme, New Hampshire. 62 pp. and 1:20,000 scale bedrock map.

Eusden, J.D., Garesche, J.M., Johnson, A.H., Maconochie, J., Peters, S.P., O'Brien, J.B., and Widmann, B.L., 1996, Stratigraphy and ductile structure of the Presidential Range, New Hampshire: Tectonic implications for the Acadian orogeny: Geological Society of America Bulletin, v. 108, no. 4, p. 417-436.

Eusden Jr., J.D., Guzofski, C.A., Robinson, A.C., Tucker, R.D., 2000. Timing of the Acadian Orogeny in Northern New Hampshire. Journal of Geology 108, 219–232

Eusden, J.D., and Lux, D.R., 1994, Slow late Paleozoic exhumation in the Presidential Range of New Hampshire as determined by the 40Ar/39Ar relief method: Geology, v. 22, no. 10, p. 909-912.

Faure, S., 2006, Paleostress analysis of Atlantic crustal extension in the Quebec Appalachians: University of Chicago Press : Chicago, IL, United States, United States.

Faure, S., Tremblay, A., and Angelier, J., 1996, State of intraplate stress and tectonism of northeastern America since Cretaceous times, with particular emphasis on the New England-Quebec igneous province: Tectonophysics, v. 255, no. 1-2, p. 111-134.

Galbraith, R.F., Laslett, G.M., Green, P.F., Duddy, I.R., 1990, Apatition fission track analysis: geological thermal history analysis based on three-dimensional random process of linear radiation damage: Philosophical Transactions: Physical Sciences and Engineering, V. 332, N. 1627, p. 419-438.

Gallagher, K., 1995, Evolving temperature histories from apatite fission-track data: Earth and Planetary Science Letters, V. 136, p 421-435.

Gallagher, K., Brown, R., Johnson, C., 1998, Fission Track Analysis and its applications to geological problems: Annual Review of Earth and Planetary Science, v. 26, p. 519-572.

Hibbard, J., van Staal, C., and Rankin, D., 2007, A comparative analysis of pre-Silurian crustal building blocks of the northern and the southern Appalachian orogen: American Journal of Science, v. 307, no. 1, p. 23-45.

Kindley, C., 2011, Paleostress Analysis of Mesozoic Extension in Fractures and Basalt Dikes, Great Gulf, NH: Bates College.

Ketcham, R.A., Donelick, R.A., Donelick, M.B., 2000, AFTSolve: A program for multi-kinetic modeling of apatite fission-track data: Geological Materials Research, V.2, N.1, p 1-31.

Kohn, M.J., Rakovan, J., Hughes, J.M., 2002, Phosphates – Geochemical, geobiological and materials importance: Reviews in Mineralogy and Geochemistry, V. 48.

Matton, G., and Jébrak, M., 2009, The Cretaceous Peri-Atlantic Alkaline Pulse (PAAP): Deep mantle plume origin or shallow lithospheric break-up?: Tectonophysics, v. 469, no. 1-4, p. 1-12.

McHone, J.G., 2000, Non-plume magmatism and rifting during the opening of the central Atlantic Ocean: Tectonophysics, v. 316, no. 3-4, p. 287-296.

McHone, J.G., 2005, Giant dikes, rifts, flood basalts, and plate tectonics; a contention of mantle models: Geological Society of America (GSA) : Boulder, CO, United 89 States, United States.

McHone, J.G., 1988, Tectonic and paleostress patterns of Mesozoic intrusions in eastern North America: Elsevier : Amsterdam, Netherlands, Netherlands.

McHone, J.G., 1995, The Christmas Cove Dike, coastal Maine; petrology and regional significance: Geological Society of America (GSA) : Boulder, CO, United States, United States.

McHone, J.G., 2003, Volatile emissions from Central Atlantic Magmatic Province basalts; mass assumptions and environmental consequences: American Geophysical Union : Washington, DC, United States, United States.

McHone, J.G., Ross, M.E., and Greenhough, J.D., 1987, Mesozoic dyke swarms of eastern North America: Geological Association of Canada : Toronto, ON, Canada, Canada.

McHone, J., and Butler, J., 1984, Mesozoic igneous provinces of New England and the opening of the North Atlantic Ocean: Geological Society of America Bulletin, v. 95, no. 7, p. 757-765.

Moench, R.H., and Aleinikoff, J.N., 2003, Stratigraphy, geochronology, and accretionary terrane settings of two Bronson Hill arc sequences, northern New England: Physics and



Chemistry of the Earth, Parts A/B/C, v. 28, no. 1-3, p. 113-160.

McHone, J., and Butler, J., 1984, Mesozoic igneous provinces of New England and the opening of the North Atlantic Ocean: Geological Society of America Bulletin, v. 95, no. 7, p. 757-765.

Nesse, W.D., 2000, Introduction to Mineralogy: Oxford University Press, New York, p. 346-349.

Reiners, P.W., Ehlers, T.D., 2005, Low Temperature Thermochonology: Techniques, Interpretations and Applications; Reviews in Mineralogy & Geochemistry, V. 58, p 19- 86.

Robinson, A.C., 1997, The Timing of Metamorphism, Deformation, and Plutonism in the Presidential Range, New Hampshire, Based on U=Pb Radiogenic Age Dating: Bates College.

Roden-Tice, M.K., and Wintsch, R.P., 2002, Early Cretaceous normal faulting in southern New England; evidence from apatite and zircon fission-track ages.: Journal of Geology, v. 110, no. 2, p. 159 - 178.

Roden-Tice, M.K., Tice, S.J., 2005. Regional-Scale mid-Jurassic to Late Cretaceous unroofing from the Adirondack Mountains through central New England based on apatite fission-track and (U-Th)/He thermochronology. Journal of Geology 113, 535–552.

Roden-Tice, M.K., Wintsch, R.P., 2002. Early Cretaceous normal faulting in southern New England: evidence from apatite and zircon fission-track ages. Journal of Geology 110, 159–178.

Roden-Tice, M.K., West Jr., D.P., Potter, J.K., Raymond, S.M., Winch, J.L., 2009. Presence of a long-term lithospheric thermal anomaly: evidence from apatite fission-track analysis in northern New England. Journal of Geology 117, 627–641.

Roden-Tice, M.K., Eusden, J.D., Wintsch, R.P., 2012. Apatite fission-track evidence for the Cretaceous development of kilometer-scale relief and steady-state Tertiary topography in New England. Geomorphology, 141, 114-120.

Rosenblum, Sam (1953) Magnetic susceptibilities of minerals in the Franz isodynamic magnetic separator. American Mineralogist, 43, 170-173.

Roulleau, E., Pinti, D.L., Stevenson, R., Takahata, N. et Sano, Y., Pitre, F., 2010. Nitrogen, helium and argon isotopes in minerals from alkaline intrusions of the Monteregian Hills, QC: Evidence for an upper mantle origin. Earth Planet. Sci. Lett.

Schlische, R.W., Withjack, M.O., and Olsen, P.E., 2003, Relative Timing of CAMP, Rifting, Continental Breakup and Basin Inversion: Tectonic Significance, in Hames, W., McHone, J.G., Renne, P., and Ruppel, C. eds., The Central Atlantic Magmatic Province: Insights from Fragments of Pangea, American Geophysical Union, Washington, DC, p. 33-59.

Schlische, R.W., 2003, Progress in understanding the structural geology, basin evolution, and tectonic history of the eastern North American rift system, in LeTourneau, P.M. and Olsen, P.E. eds., The Great Rift Valleys of Pangea in Eastern North America, Columbia University Press : New York, NY, United States, United States, p. 21-64.

VanStaal, C.R., Whalen, J.B., Valverde-Vaquero, P., Zagorevski, A., Rogers, N., 2009. Pre-Carboniferous, episodic accretion-related, orogenesis along the Laurentian margin of the northern Appalachians, 327, 271-316.

Wagner, G.A., 1968. Fission-track dating of apatites. Earth and Planetary Science Letters 4, 411–414.

Warnock, A.C., Zeitler, P.K., Wolf, R.A., Bergman, S.C., 1997. An evolution of low-temperature apatite U-Th/He thermochonometry. Geochimica et Cosmochimica Acta 61, 5371-5377.

West Jr., D.P., Roden-Tice, M.K., 2003. Late Cretaceous reactivation of the Norumbega fault zone, Maine: evidence from apatite fission-track ages. Geology 31, 649–652.

West Jr., D.P., Tomascak, P.B., Coish, R.A., Yates, M.G., Reilly, M.J., 2007. Petrogenesis of the ultrapotassic Lincoln Syenite, Maine: Late Silurian–Early Devonian melting of a source region modified by subduction driven metasomatism. American Journal of Science 307, 265–310.

West Jr., D.P., Roden-Tice, M.K., Potter, J.K., Barnard, N.Q., 2008. Assessing the role of orogen-parallel faulting in post-orogenic exhumation: low-temperature thermochronology across the Norumbega fault system, Maine. Canadian Journal of Earth Sciences 45, 287–301.